ELECTRONIC WAVEFUNCTIONS FOR SMALL MOLECULES

Thesis by

William James Hunt

In Partial Fulfillment of the Requirements

For the Degree of

Doctor of Philosophy

California Institute of Technology

Pasadena, California

1972

(Submitted September 20, 1971)

ACKNOWLEDGMENT

In my four years at Caltech, I have benefited greatly from the presence of a large and active theoretical chemistry group. All the members of this group have contributed to my education, but I especially thank Thom Dunning and Nick Winter for their part in my educational growth. I thank Jeff Hay for his creative partnership in several joint projects. The boundless enthusiasm and the keen insight of my advisor, Prof. William A. Goddard III, have been essential to my intellectual progress.

My financial support during my stay at Caltech has been provided by a National Defense Education Act fellowship. A fellowship from the Shell Companies Foundation also contributed to my support.

ABSTRACT

PART I. A simple variationally-based method for calculating electronic wavefunctions of excited states, the improved virtual orbital (IVO) method, is developed in this work. Calculations are presented for H_2O, O_2, CO, and N_2. While the IVO method gives limited accuracy in the treatment of valence excited states, the description of Rydberg states is very useful. For O_2 the theoretical prediction of 8.70 eV ($v' = 2$) for the transition from the $^3\Sigma_g^-$ ground state to the $^3\pi_g$ ($1\pi_g \rightarrow 3s\sigma_g$) Rydberg state facilitated discovery of this transition in electron impact spectra at 8.65 eV ($v' = 2$).

PART II. The N, T, and V states of ethylene have been studied with the Hartree-Fock (H-F) and configuration interaction (CI) techniques as a function of C-C bond distance and the twist angle between methylene groups. The calculated rotational barrier for the N state is 67.2 Kcal/mole, in good agreement with the experimentally derived activation energy of 65 Kcal/mole for cis-trans isomerization of 1,2di-deutero ethylene. The maximum in the N state curve lies 1.4 Kcal/mole above the minimum of the triplet state (T) curve. Both H-F and CI calculations show that the V state of planar ethylene has a more extended charge distribution than the T state. This charge distribution contracts as the methylene groups are twisted from the planar geometry.

Correlation terms included in the CI calculations contract the charge distribution considerably from its H-F size. A modified Franck-Condon principle for internal rotation suggests that the maximum absorption observed experimentally does not correspond to vertical excitation for the $N \rightarrow V$ transition.

PART III. A Generalized Valence Bond method combining the computational tractability of the usual MO-SCF approach with the conceptual advantages of a valence bond picture is proposed. The GVB method has been applied to calculation of potential curves for CH_2 in the $^3B_1$, $^1A_1$, and $^1B_1$ states. These calculations predict that the $^3B_1$ curve may cross the $^1A_1$ curve near the minimum for the $^1A_1$ state. A study of the ring opening of cyclopropane predicts a barrier height of 61 Kcal/mole for cis-trans isomerization, in good agreement with the experimentally determined activation energy of 65 Kcal/mole for 1,2 di-deutero cyclopropane. An investigation of diatomic hydrides and fluorides in the GVB picture gives a consistent view of the energy levels and one-electron energies of these molecules.

TABLE OF CONTENTS

PART I

A Simple Description of Molecular Excited States — The IVO Method

I. INTRODUCTION

In the usual closed shell Hartree-Fock approximation[1] we solve the equation

$$H^{HF}\phi_i = \epsilon_i\phi_i \qquad (1)$$

for the N/2 orbitals ϕ_i corresponding to the N/2 lowest eigenvalues ϵ_i. These occupied orbitals are used to form a Slater determinant wavefunction for the electronic ground state of an N-electron molecule. This approximation usually gives a good description of one-electron properties[2,3,4] such as dipole moments and of equilibrium geometries.[5] Equation (1) also gives a complete set of orbitals orthogonal to the occupied orbitals. These unoccupied or virtual orbitals, called regular virtual orbital (RVO) in this work, are often used to construct excited state wavefunctions in which an occupied orbital is replaced by a virtual orbital.[1] As is well known,[6] such wavefunctions often lead to poor approximations for excited state wavefunctions. However, the computational convenience and ease of interpretation offered by this approach are very attractive features. This paper presents an improved virtual orbital (IVO) method in which the Hartree-Fock operator in (1) is modified to give variationally correct virtual orbitals for excited state wavefunctions.[7] Calculations by this method are no more time consuming than the usual RVO calculations. We investigate the excited states of H_2O, O_2, N_2 and CO.

II. APPROXIMATE EXCITED STATE WAVEFUNCTIONS

The Hartree-Fock (H-F) approximation[8] is the basis for many useful concepts in quantum chemistry. The Hartree-Fock-Roothaan (HFR) equations[1] have extended the application of the H-F method to quantitative calculations on polyatomic molecules. One-electron properties are accurately predicted by the H-F description.[2-4] In addition the H–F wavefunction is a convenient starting point for more accurate treatments of molecular electronic structure. For these reasons the H-F wavefunction for the ground state of a molecule provides a good standard for comparison for an excited state wavefunction.

For a closed shell system with N electrons the H-F wavefunction is

$$\Psi^{HF} = A[\psi_1(1)\psi_2(2)\cdots\psi_i(i)\cdots\psi_N(N)] \qquad (1)$$

where A is the antisymmetrizer and ψ_i is a one-electron spin orbital involving spin and space coordinates of electron (i). The spin orbitals ψ_i in (1) are eigenfunctions of the operator H^{HF}

$$H^{HF}\psi_i = \epsilon_{ii}\psi_i \qquad (2)$$

with eigenvalues ϵ_{ii}, where

$$H^{HF} = h + \sum_{j=1}^{N} (J_j - K_j) \qquad (3)$$

The operator h is equal to the kinetic energy ($-\frac{1}{2}\nabla^2$) plus nuclear attraction terms (V_N). The coulomb and exchange operators are defined by

$$J_j\psi_i = \int \psi_j^*(1)\ 1/r_{12}\ \psi_j(1)d\tau_1\psi_i(2) \qquad (4)$$

and

$$K_j\psi_i = \int \psi_j^*(1)\ 1/r_{12}\ \psi_i(1)d\tau_1\psi_j(2) \qquad (5)$$

The Hamiltonian operator (H) for the many-electron system has been taken as containing kinetic energy, nuclear attraction and electron-electron coulomb repulsion terms. The nuclei are assumed to be fixed. Atomic units are used in the kinetic energy operator defined above.

Equation (2) has not only the N solutions present in (1) but other unoccupied or virtual solutions. The solutions of (2) form a complete set of one-electron spin orbitals and the wavefunctions of the form of (1) constructed using these solutions form a complete set of functions for description of the wavefunction of an N-electron system. The functions like (1) will be described as $\Psi_{ij\cdots}^{ab\cdots}$ where orbitals $ij\cdots$ have been replaced by $ab\cdots$ in (1).

We now give two pertinent theorems for closed shell H-F wavefunctions. For an (N-1) electron system we make the approximation that orbitals ψ_i for i = 1 to (N-1) in the wavefunction Ψ(N-1) are unchanged from Ψ^{HF} (for N electrons). The function Ψ(N-1) is of the same form as (1) but involves one less orbital ψ_N. The total energy $E_{(N-1)}$ of $\Psi_{(N-1)}$ is related to the energy E^{HF} of Ψ^{HF} by

$$E_{(N-1)} = E^{HF} - \epsilon_{NN} \tag{6}$$

where ϵ_{NN} is the eigenvalue of the orbital ψ_N removed to form $\Psi_{(N-1)}$. This is Koopmans' Theorem.[9]

Brillouin's theorem[10] states that

$$\langle \Psi_i^a | H-E | \Psi^{HF} \rangle = \int \Psi_i^{a*} H \Psi^{HF} d\tau_1 d\tau_2 \cdots d\tau_i \cdots d\tau_N = 0 \tag{7}$$

for all functions Ψ_i^a. Now we make a perturbation expansion of the Hamiltonian H as

$$H = H_N^{HF} + (H - H_N^{HF}) = H^{(0)} + H^{(1)} \tag{8}$$

$$H = \sum_i H^{HF}(i) + (H - \sum_i H^{HF}(i))$$

where $H_N^{HF}(i)$ is the H-F Hamiltonian acting on electron i. Then the exact wavefunction for the system Ψ becomes

$$\Psi = \Psi^{HF} + \Psi^{(1)} + \cdots + \Psi^{(I)} + \cdots \tag{9}$$

If we expand $\Psi^{(1)}$ as

$$\Psi^{(1)} = \sum_{i,a} \Psi_i^a C_i^a + \sum_{i>j,a,b} C_{ij}^{ab} \Psi_{ij}^{ab} + \cdots \tag{10}$$

only the C_{ij}^{ab} coefficients are non-zero. This is because only one and two-electron operators are present in H and $H^{(1)}$ and because of (7). One consequence of this theorem is that Hartree-Fock wavefunctions for closed shell systems predict one-electron properties accurately through first order.

The spin orbital ψ_i may be expressed as a product of a space orbital ϕ_j and a spin function $\sigma_i = \alpha$ or β. Requiring double occupation of the orbitals ϕ_j leads to the Restricted Hartree-Fock method (RHF). For open shells we imply the RHF method when we refer to H-F.

Koopmans' Theorem suggests that the excited state wavefunction Ψ_{EX} might be constructed by replacing spin orbital ψ_i by ψ_a or

$$\Psi_{EX} = \Psi_i^a \tag{11}$$

This is called the virtual orbital method.[1] In order to avoid confusion we will refer to this method as the regular virtual orbital (RVO) method. The advantage of this method is that it requires very little effort beyond obtaining the ground state wavefunction. In Ψ_i^a one space orbital $\phi_j(\psi_i = \phi_j\sigma_i)$ from Ψ^{HF} is singly occupied. Then, if Ψ_i^a has spin projection Ms = O a linear combination of functions Ψ_i^a and $\Psi_i^{a'}$ must be used to give a pure singlet (with plus sign) or triplet state:

$$\Psi_{EX} = \Psi_i^a \pm \Psi_i^{a'} \tag{12}$$

where Ψ_i^a contains $\psi_\ell = \phi_j\alpha$ and $\psi_a = \phi_b\beta$ and $\Psi_i^{a'}$ contains

$$\psi_{\ell'} = \phi_j\beta \text{ and } \psi_{a'} = \phi_b\alpha.$$

The energies of the singlet E_S and triplet E_T excited states relative to ground state energy $E_{G.S.}$ are

$$E_T = E_{GS} - \epsilon_{ii} + \epsilon_{aa} - J_{ia}$$

$$E_S = E_T + 2\ K_{ia} \tag{13}$$

where

$$J_{ia} = \langle \psi_a | J_i | \psi_a \rangle = \int \psi_a^*\, J_i\, \psi_a\, d\tau$$

$$K_{ia} = \langle \psi_a | K_i | \psi_a \rangle = \int \psi_a^*\, K_i\, \psi_a\, d\tau$$

The RVO method is discussed in Section II of Appendix A.

The excited state wavefunction may be represented as a sum of terms Ψ_i^a with coefficients C_i^a:

$$\Psi_{EX} = \sum_{i,a} \Psi_i^a\, C_i^a \tag{14}$$

The optimum coefficients C_i^a are determined by equations derived from application of the variational principle. This approach has been used by Pariser and Parr[11] in pi electron treatments of the spectra of aromatic molecules. We shall refer to this approach as the single excitation configuration interaction method (SECI).

We may add more terms to the expansion in (14) to produce an extensive configuration interaction (CI) wavefunction. For consistency a CI calculation is then necessary for the ground state. This approach has recently been used by several authors[12, 13] with good results. However, the CI procedure is rather time-consuming and complicated for general use.

Another approach would be to calculate a H-F wavefunction for each excited state separately. This approach is also rather expensive if a number of states are to be examined. We expect that the orbitals occupied in the ground state will be only slightly altered in an excited state wavefunction. The main effect of the SCF procedure should be to optimize the new orbital ϕ_a. This suggests that we might keep all the orbitals from the ground state H-F wavefunction fixed and solve a variational equation for ϕ_a.

The orbital ϕ_a would satisfy the equation

$$H^{IVO}\phi_a = [h + \sum_{j\neq i} (2J_j - K_j) + J_i \pm K_i]\phi_a = \epsilon_a\phi_a \qquad (15)$$

with the restriction that ϕ_a be orthogonal to all occupied H-F orbitals. The sign before K_i is determined by the spin of the excited state, plus for a singlet and minus for a triplet. Since H^{IVO} does not depend on ϕ_a we solve this equation once and obtain the wavefunctions Ψ_i^a. These IVO wavefunctions satisfy the conditions.

$$\begin{aligned} \langle \Psi_i^a | H | \Psi_i^b \rangle &= 0 \\ \langle \Psi_i^a | H | \Psi^{HF} \rangle &= 0 \end{aligned} \qquad (16)$$

The energy of the ground state was divided in (6) into a part ϵ_i dependent on ϕ_i and a part independent of orbital ϕ_i. Similarly the eigenvalue ϵ_a contains all parts of the energy expression for the excited state involving ϕ_a. The total energy of the excited state Ψ_i^a is

$$E_i^a = E^{HF} - \epsilon_i + \epsilon_a \tag{17}$$

and the excitation energy for this state relative to the ground state at the same nuclear geometry is

$$\Delta E = \epsilon_a = \epsilon_i \tag{18}$$

Using the Hylleraas-Undheim-MacDonald separation theorem,[14] we may show that the Nth IVO solution Ψ_i^a gives an energy which is an upper bound to the exact energy of the Nth state. This insures that IVO wavefunctions can provide proper representations of excited states.[15]

Equation (16) suggests that we could view the IVO method as a restricted form of the SECI method in which all replacements Ψ_i^b of only one orbital are allowed. If the CI wavefunction is

$$\Psi_{IVO} = \sum_b C_i^b \Psi_i^b$$

then the IVO orbital is

$$\phi_{IVO} = \sum_b C_i^b \phi_b$$

Lefebvre-Brion and Moser[16] carried out CI calculations on Rydberg levels in diatomic molecules which were equivalent to the IVO method. Most of these calculations used a minimum basis set of Slater orbitals. The one-electron equation (15) provides a more efficient computational method, however.

In actual calculations a finite basis set is used. The OCBSE method[17] is used to produce solutions of (15) which are orthogonal to the occupied orbitals. The matrix equation to be solved has the form

$$\underset{\sim}{H}^{IVO}\,\underset{\sim}{C}^{IVO} = \underset{\sim}{S}\,\underset{\sim}{C}^{IVO}\,\underset{\sim}{E} \tag{19}$$

where

$$H_{\mu\nu} = \langle \chi_\mu | H^{IVO} | \chi_\nu \rangle$$

and

$$S_{\mu\nu} = \langle \chi_\mu | \chi_\nu \rangle$$

are respectively the IVO Hamiltonian matrix and the overlap matrix over the basis functions used. The virtual orbitals from the solution of equation (1) in our basis set form a complete set of functions orthogonal to the occupied orbitals and to each other. Then we transform equation (19) so that it is in terms of the RVO basis. We diagonalize the transformed Hamiltonian to get the IVO solutions and transform them back to the original basis. The equations for this procedure are

$$H'_{ab} = \sum_{\mu\nu} C^{RVO}_{\mu a} H^{IVO}_{\mu\nu} C^{RVO}_{\nu b}$$

$$\underset{\sim}{H'}\,\underset{\sim}{C'} = \epsilon\,\underset{\sim}{C'}$$

$$C^{IVO}_{\nu\epsilon} = \sum_{a} C^{RVO}_{\nu a}\, C'_{ac}$$

where indices μ and ν refer to the original basis and indices a and b refer to the RVO used.

III. IONIZATION POTENTIALS FOR IVO

Two methods of calculating excitation energies have been used in our calculations. The excitation energy is

$$\Delta E = \epsilon_a - \epsilon_i \tag{20}$$

for a transition from orbital ϕ_i to IVO orbital ϕ_a. The eigenvalues ϵ_a and ϵ_i come from the IVO and ground state SCF calculations respectively. However ϵ_i, the Koopmans' Theorem estimate of the ionization potential, is often in error. For Rydberg states which resemble the positive ion with an extra electron at a large distance, this error would be transferred to the excitation energy. We may simply correct the excitation energies by using the experimental value for the ionization potential for ϵ_i. The method with the Koopmans' Theorem value for ϵ_i(KIP) will be used for valence states.

Experimental ionization potentials (EIP) will be employed for Rydberg states. In using an experimental ionization potential we must choose between adiabatic and vertical measurements. For our purposes the vertical transition values are correct since the excited state calculations are carried out at the equilibrium geometry for the ground state. In addition, our purpose is to locate the maximum intensity of transitions. The vertical,[18, 19] adiabatic and calculated ionization potentials needed for our calculations

are listed in Table I. Since Rydberg states involve an ion-like core, we investigated construction of the IVO Hamiltonian with orbitals from the SCF wavefunction for the corresponding positive ion. Results for Rydberg states were little affected by this change but valence states were raised in energy since the ion orbitals are inappropriate for valence excited states. We use ground state orbitals in all calculations reported in this work.

Several points should be clarified before describing the results of calculations. The IVO method can be extended easily to cases where the ground state wavefunction is an open shell HF wavefunction. In O_2 the excitations $1\pi_g \rightarrow \sigma$ require no modifications in the procedure. The expressions for H^{IVO} and ΔE are unchanged. For the excitations $1\pi_\mu \rightarrow \sigma$ several ionization limits are possible so that ϵ_i must be replaced by a correctly computed value for the particular ionization potential to be used. For $1\pi \rightarrow \pi$ transitions in all diatomics several different states result; a different operator H^{IVO} is used for each of these states.

IV. CALCULATIONAL DETAILS

A number of calculations on various molecules have shown that the contracted Gaussian basis set denoted [4s3p1d/2s1p] developed by Dunning[20] gives very good results for molecular equilibrium geometries and one-electron properties. This basis uses four s, three p and one d function on each first row atom (Li-Ne). Two s and one p function are used on each hydrogen atom. For this work our main interest centered on Rydberg states; since polarization functions (d on first row atoms and p on hydrogen with large exponents) are not important for Rydberg orbitals, we did not use them in our calculation.

A good description of Rydberg orbitals does require basis functions with low exponents having appreciable amplitude far from the molecule. Tests on the oxygen atom indicated a simple procedure for choosing basis functions well enough so that optimization of orbital exponents could be avoided. From knowledge of typical quantum defects ~ 1 for ns and 0.5-0.7 for np, we pick an effective 3s, 3p and 3d Slater orbital exponent. The 2 term d Gaussian function set was taken to fit[21] a 3d function of exponent $\zeta = 1.0$ since a quantum defect of 0.10-0.0 is typical for d Rydberg levels. Since s and p functions were already present in the basis set, only the low exponent functions from an expansion of a 3s or 3p Slater orbital were needed.

The requirement that $n = 4$ Rydberg orbitals be moderately well described complicated the selection of basis functions. The exponents of the set of four s and three p functions are given in Table II. The

energies for the ground state SCF wavefunctions for all molecules considered are given in Table III. The low exponent basis functions were not included for the ground state calculations.

This set of diffuse basis functions was added on each first row atom. For this reason the basis set is effectively much larger for N_2, CO, and O_2 than for H_2O. The main result is that more Rydberg states are adequately described for the diatomic molecules. However, even for H_2O the 3s, 4s, 5s, 3p, 4p and 3d orbitals appear to be adequately described.

V. RESULTS FOR H_2O

All known[22] excited states of H_2O are probably Rydberg states; for this reason we expect good agreement with experimental results. In the following discussion experimental numbers appear in parentheses following the theoretical result. Information on low-lying (below 11.5 eV) states is summarized in Table IV. A typical electron impact spectrum[23] is given in Figure I.

The lowest singlet excited state is $^1B_1$ ($1b_1 \rightarrow 3sa_1$) at 7.30 (7.50) eV. The spectrum shows a broad continuous absorption peaking at 7.50 eV. As expected SCF potential curves calculated by Miller et al.[25] for this state go smoothly downhill to $H(^2S) + OH(^2\Pi)$.

The next observed singlet state is the $^1A_1(3a_1 \rightarrow 3sa_1)$ state at 9.59 (9.75) eV. A long series of bands corresponding to bending in the upper state are observed.

Walsh's rules[26] predict the equilibrium geometry for the upper state will be linear or nearly linear. Calculations by Horsley and Fink[27] also predict a linear geometry.

Two singlet states involving 3p orbitals are found near 10 eV. Both the $^1B_1$ ($1b_1 \rightarrow 3pa_1$) state at 10.04 (10.00) eV and the $^1A_1(1b_1 \rightarrow 3pb_1)$ state at 10.16 (10.17) eV produce sharp peaks in the optical absorption and electron impact spectra. The equilibrium geometries for these states are probably quite close to that of the ground state.[28] The $^1A_2(1b_1 \rightarrow 3pb_2)$ state at 9.04 eV has not been observed experimentally.

Results for higher states are given in Table V. We note that the 4s and 3d orbitals are ordered correctly but the excitation energy of the $1b_1 \rightarrow 4s$ state is underestimated by 0.36 eV.

Since triplet states are more difficult to observe experimentally, calculations may supply important new information about these states. First we discuss the $(1b_1 \rightarrow 3p)$ triplet states. The $^3A_1(1b_1 \rightarrow 3pb_1)$ state is predicted to be at 9.71 eV while the $^3B_1(1b_1 \rightarrow 3pa_1)$ state is found at 9.97 eV. This ordering is reversed from the singlet state because of the larger exchange integral of the $1b_1$ orbital with the $3pb_1$ orbital than with $3pa_1$. Recent electron impact studies by Trajmar, Williams, and Kuppermann[23] have identified a triplet state producing a single sharp peak at 9.81 eV similar to the singlet peaks at 10.00 and 10.17 eV. From our result we conclude that this peak may have contributions from both the $^3B_1$ and $^3A_1$ states. The $^3A_2$ $(1b_1 \rightarrow 3pa_2)$ state is located much lower in energy at 8.68 eV. No experimental information about this state has been found.

The $^3A_1(3a_1 \rightarrow 3sa_1)$ state at 8.69 eV would be difficult to observe due to the presence of bands from the corresponding singlet state. SCF calculations on this state[27] show that its equilibrium geometry is linear.

The lowest triplet state is calculated to be the $^3B_1(1b_1 \rightarrow 3sa_1)$ state at 6.65 eV. The continuous absorption from the corresponding singlet state would probably prevent observation of this state. SCF calculations[25] suggest that the potential curve goes smoothly downhill toward $H(^2S) + OH(^2\Pi)$. This dissociation limit lies 5.5 eV above

the ground state. The limit $H_2(^1\Sigma_g^+) + O(^3P)$ is 5.03 eV above the ground state of H_2O. Recent experimental evidence[23, 29, 30] clearly shows a broad weak absorption peaking at 4.5 eV (onset at 3.8 eV) with characteristics of a triplet state. No state calculated in this work is close to this energy region. Further, the state must be bound with respect to both dissociation limits mentioned. The experimental procedure eliminates any negative ion as the state responsible.

Goddard[31] has speculated that transitions of the dimer may be responsible. Strong hydrogen bonding in the H_2O H_2O^+ core might lower the energy of the $(1b_1 \rightarrow 3sa_1)$ Rydberg state sufficiently to produce the 4.5 eV triplet state. Several previous theoretical calculations have been carried out on water. Harada and Murrell[32] used the excited states of the neon atom as a starting point for a perturbation treatment. La Paglia[33] used the oxygen atom as the basis for a perturbation calculation. In both cases the success of the calculations was limited. Lin and Duncan[34] used a one-center model in a very approximate calculation. As mentioned above, SCF calculations have been carried out on the $^1B_1(1b_1 \rightarrow 3sa_1)$ state by Miller et al[25] and on the $^3A_1$ and $^1A_1$ states from the $(3a_1 \rightarrow 3sa_1)$ transition by Horsley and Fink.[27]

VI. RESULTS FOR O_2

A short list of low-lying states of O_2 is given in Table VI and the electron impact spectrum[35,36] is given in Figure 2. The ground state of O_2 is $^3\Sigma_g^-$ with the H-F configuration

$$(1\sigma_g)^2(1\sigma_u)^2(2\sigma_g)^2(2\sigma_u)^2(3\sigma_g)^2(1\pi_u)^4(1\pi_g)^2$$

The $^1\Delta_g$ state at 0.97 eV[35] and the $^1\Sigma_g^+$ state at 1.67 eV[35] have the same H-F configuration. The configuration

$$\cdots (1\pi_u)^3(1\pi_g)^3$$

gives rise to the $^3\Sigma_u^+$, $^3\Delta_u$ and $^1\Sigma_u^-$ states near 6 eV.[35,36] The $^3\Sigma_u^-$ state from this configuration is responsible for the Schuman-Runge bands and for part of the broad continuum extending from 7 to 9 eV and peaking near 8.6 eV.[35,36]

The valence states $^3\pi_g$ and $^1\pi_g$ correspond to the $3\sigma_g \rightarrow 1\pi_g$ transition and are expected to have repulsive potential curves.[37]

Since no orbitals unoccupied in the ground state wavefunction are involved, the IVO method is not appropriate for these valence states. In the present study we focus on Rydbert states.

The first ionization potential for O_2 at 12.54 eV involves removal of an electron from the π_g orbital. Removal of the π_u orbital gives several ionization potentials, the lowest of which is at 16.93 eV for the $^4\pi_u$ state of O_2^+. We consider only Rydberg states corresponding to transitions from the $1\pi_g$ orbital. The lowest of these

states is the $^3\pi_g(1\pi_g \rightarrow 3s\sigma_g)$ state at 8.70 eV (8.62).[38] Transition to this state is not allowed by dipole selection rules, but the electron impact spectrum in Figure 2 shows several sharp peaks superimposed on the 7 to 9 eV continuum. The vibrational spacing and Franck-Condon factors obtained from analysis of the spectra agree with those of the positive ion.

The $3\sigma_u$ orbital calculated for the $(1\pi_g \rightarrow 3\sigma_u)$ transition is a valence orbital. Its excitation energy, 10.85 eV, is calculated using the theoretical value for the ionization potential (KIP). CI calculation by Schaefer and Miller[39] and SCF calculations by the author indicate that the H-F approximation is poor for this state.

Several states arise from the $(1\pi_g \rightarrow 3p\pi)$ transition. The $^3\Sigma_u^-$ state at 9.91 eV is responsible for the sharp peak seen at 9.97 eV. The $^3\Sigma_u^+$ state at 9.88 eV is not dipole-allowed but may contribute to the electron-impact spectra. The $^3\Delta_u$ state at 9.81 eV is probably responsible for the very weak feature recently observed near 9.8 eV in electron impact spectra.[39] The other states $^1\Sigma_u^-$ at 9.73 eV, $^1\Delta_u$ at 10.01 eV and $^1\Sigma_u^+$ at 10.10 eV probably have not been observed. The $^3\pi$ $(1\pi_g \rightarrow 3p\sigma_u)$ state at 10.45 eV produces the sharp peak at 10.29 eV. The corresponding singlet state $^1\pi_u$ is calculated to lie at 10.93 eV.

In Figures 3 and 4 the behavior of the differential cross-section as a function of scattering angle from electron impact studies[36] is shown for several transitions. The 9.97 eV feature behaves in a more complicated way than does the 10.29 peak. Contributions to

the differential cross section of the 9.97 peak from the $^3\Sigma_u^+$ state could explain this difference. Lindholm[40] has suggested that the 9.97 eV and 10.29 eV peaks might both belong to a vibrational progression for the $^3\Sigma_u^-$ state. If that were the case the differential cross sections for the two peaks should behave in a similar way.

A listing of results for higher states is given in Table VII. We will not discuss these states in detail.

Calculations using model potentials have been carried out on O_2 by Betts and McKoy.[41] A discussion of their work on O_2, N_2, and CO is deferred until Section VIII.

VII. RESULTS FOR CO

For CO we examined excitations from the 5σ and 1π orbitals to both valence and Rydberg orbitals. Results for low-lying states are shown in Table VIII. Figure 5 is the electron impact spectrum of Trajmar et al.[42]

The valence states of CO are not located as well as the Rydberg states are. This illustrates the limitations of the simple IVO method. The largest error is 0.63 eV for the $^3\Sigma^-$ state. The result of these errors is incorrect ordering of the $^1\pi$, $^3\Sigma^-$, and $^3\Delta$ states. In a CI calculation Lefebvre-Brion et al.[43] obtained better results for valence states, but results for Rydberg states were not as good. In a later calculation Lefebvre-Brion and Moser[44] used a CI method to get IVO orbitals in a successful study of the $5\sigma \rightarrow n\sigma$ and $5\sigma \rightarrow n\pi$ Rydberg states. They concluded that the state at 11.52 eV (exptl) called $E^1\Sigma^+$ was actually the $^1\pi\,(5\sigma \rightarrow 3p\pi)$ state. Our results are in agreement with this assignment as is the interpretation of experimental results given by Lindholm.[45]

Their suggestion that the $F^1\pi\,(5\sigma \rightarrow 3d\pi)$ state at 12.37 eV might be a $(5\sigma \rightarrow 4s\sigma)$ transition is not in agreement with Lindholm's findings[45] or our results.

We note that the position of the $(5\sigma \rightarrow 3d)$ and $(5\sigma \rightarrow 4s)$ states are reversed in our calculations. This is an example of the general tendency for states involving s orbitals to have excitation energies below the experimental value and for those states involving d orbitals to be overestimated.

Lindholm[45] has suggested that the ($1\pi \rightarrow 3p\sigma$) and ($1\pi \rightarrow 3p\pi$) transitions have an irregular intensity distribution in which the first band is the strongest. This behavior is ascribed to pre-ionization. In recording these experimental results in Tables VIII and IX, we have corrected the adiabatic value in the usual way as though the $\nu' = 2$ band were really the strongest.

The full listing of results is in Table IX.

VIII. RESULTS FOR N_2

The nitrogen molecule is the largest component of the earth's atmosphere; its electronically excited states play a major role in the chemistry and physics of the upper atmosphere.[46,48] Our main concern here is to provide information on the position of Rydberg singlet and triplet states. In Figure 6 we show an electron impact spectrum for N_2 taken by Trajmar and Brinkman.[49] A short table of IVO results for low-lying states appears in Table X while Table XI contains a complete listing.

For the valence states the IVO method does not work especially well. The errors made for these states by the IVO description are not systematic. This result shows the need for a more sophisticated approach for both N_2 and CO. However, for Rydberg states the accuracy of the IVO method is more satisfactory. In comparison to the similar calculations of Lefebvre-Brion and Moser[50] (LM) the present work gives about the same results for n = 3 or n = 4 Rydberg states, but in contrast to the earlier work higher states seem to be adequately described in our calculations. The ν_{00} values of LM have been modified by adding 0.23 eV for states involving $1\pi_\mu$ excitations to give vertical excitation energies. This permits comparison with our results.

Carroll and Yoshino[52] suggested that several features (the r', k', s', and h states) are actually vibrational levels of the $p'\,^1\Sigma^+$ state. From Gilmore's work[53] we see that the potential curve for the valence state $b'\,^1\Sigma_\mu^+$ from the excitation $(1\pi_\mu - 1\pi_g)$ probably crosses the

$3\sigma_g \rightarrow 3p$ curve[54] at $\nu' = 2$. This perturbation changes the Franck-Condon factors so that more levels are seen here than were predicted from the Franck-Condon factors for the ion.

The $3\sigma_g \rightarrow 3p$ states have been discussed recently by Lindholm.[51] The state designated p' $^1\Sigma_\mu^+$ is usually assigned to the band at 12.94 eV. This would then be the first member of the Rydberg series ($1\pi_\mu \rightarrow np\sigma_\mu$). The corresponding experimentally observed bands are the Worley-Jenkins series. Recently a peak at 13.21 eV has been identified as a $^1\pi_\mu$ state[52] (from a $3\sigma_g \rightarrow 3p\pi_\mu$ transition). Lindholm notes that this assignment is consistent with his interpretation of CO Rydberg states. In addition peaks with an intensity of about 10% of the $\nu' = 0$ peaks may be found for the $\nu' = 1$ vibrational levels of both states as would be expected from the Franck-Condon factors for the $^2\Sigma_g^+$ state of N_2^+.

Dressler[55] has recently made a deperturbation study of energy levels in this region of the spectrum. He concludes that both the $^1\Sigma_\mu^+(3\sigma_g \rightarrow 3p\sigma_\mu)$ and $^1\pi_\mu(3\sigma_g \rightarrow 3p\pi_\mu)$ states are perturbed by valence states of the same symmetry. Geiger and Schröder[56] have observed that the intensity distribution within the vibrational progression of the valence b' $^1\Sigma_\mu^+$ $(1\pi_\mu \rightarrow 1\pi_g)$ state is also irregular. This is shown to result from homogeneous perturbation by the $^1\Sigma_u^+(3\sigma_g \rightarrow 3p\sigma_u)$ and by the $^1\Sigma_u^+$ $(3\sigma_g \rightarrow 4p\sigma_u)$ states.

The final result is that the $\nu'=0$ levels for these states from IVO calculations are predicted to be at 13.04 eV(12.91 eV) for the $^1\pi_\mu$ $(3\sigma_g \rightarrow ep\pi)$ and at 13.17 eV (12.935) for the $^1\Sigma_g \rightarrow 3p\sigma_g \rightarrow 3p\sigma_\mu$) state.

Thus the theoretical ordering is correct but the splitting is overestimated. The $^1\pi_u$ ($1\pi_u \rightarrow 3s\sigma_g$) state is correctly placed well above these states at 13.5 eV(13.345 eV).

Because of the higher ionization potential of the $1\pi_u$ orbital, only the $1\pi_u \rightarrow 3s$ and $1\pi_u \rightarrow 3p$ states are below 15 eV in our calculation. The states arising from the $1\pi_u \rightarrow 3p$ transition are not seen in absorption from the ground state but have been studied in emission. Our results are not in conflict with the assignments[51,47] for the $^1\Delta_g$, $^1\Sigma_g^-$, or $^1\pi_g$ although differences between calculated excitation energies and experimental values are somewhat larger than usual.

Mulliken[47] has suggested that the h $^1\Sigma_u^+$ state at 14.21 eV corresponds to a ($1\pi_u \rightarrow 4d\sigma_g$) transition. Betts and McKoy[41] find the first $d\sigma_u$ orbital to be bound by 2.70 eV for an excitation energy of 14.22 eV. However, this corresponds to a quantum defect of 1.75 for a 4d orbital or 0.75 for a 3d orbital. Such quantum defects seem quite unreasonable in comparison to the usual values of 0.1-0.0 encountered. Our calculations and those of Lefebvre-Brion and Moser[50] predict values of 15.41 eV and 15.53 eV for the excitation energy ($\nu'=1$) of this state (i.e., a quantum defect of about 0.0, a more reasonable value). We note also the suggestion of Carroll and Yoshino[52] discussed above that the h $^1\Sigma_u^+$ state was a vibrational level of the $^1\Sigma_u^+$ ($3\sigma_g \rightarrow 3p\sigma_u$) state. We conclude that the result of Betts and McKoy[41] was an artifact of the simple method employed.

IX. CONCLUSION

From the discussion above we conclude that the IVO method can provide useful information about excited states. For O_2 the results provided a guide for interpreting several features of the electron impact spectrum. For CO and N_2 general agreement was found with the similar calculations of Lefebvre-Brion and Moser.[43, 50]

The model calculations of Betts and McKoy[41] appear to give some useful information about molecular Rydberg states but splittings between $p\sigma$ and $p\pi$ orbitals are much smaller than those calculated here or those observed experimentally. Their result that for N_2 the $4d\sigma_g$ orbital is more bound than the $4p\sigma_g$ orbital is more bound than the $4p\sigma_u$ orbital is probably due to the presence of valence character in $4d\sigma_g$.

The articles of Lindholm[40, 45, 57] present an interpretation of experimental information about Rydberg states based only on a few concepts about Rydberg states. Since these concepts are similar to the ideas used in the IVO method, it is not surprising that the results are usually in agreement with his conclusions. We feel that Lindholm's interpretations would be enhanced by simple IVO calculations.

Our assessment of the IVO method is that used in conjunction with experimental evidence, it can be a useful tool in understanding Rydberg excited states of atoms and molecules.

REFERENCES

1. C. C. J. Roothaan, Rev. Mod. Phys., 23, 69 (1951).
2. D. B. N. Neumann and J. W. Moscowitz, J. Chem. Phys., 49, 2056 (1968).
3. D. B. Neumann and J. W. Moskowitz, J. Chem. Phys., 50, 2216 (1969).
4. S. Aung., R. M. Pitzer, S. I. Chan, J. Chem. Phys., 49, 2071 (1968).
5. W. A. Lathan, W. J. Hehre and J. A. Pople, J. Amer. Chem. Soc., 93, 808 (1971).
6. M. B. Robin, H. Basch, N. A. Kuebler, B. E. Kaplan and J. Meinwald, J. Chem. Phys., 48, 5037 (1968).
7. A short discussion of the IVO method and preliminary results on H_2O are contained in W. J. Hunt and W. A. Goddard III, Chem. Phys. Lett., 3, 414 (1969). (Appendix I).
8. Reference 1 discusses the Hartree-Fock approximation thoroughly.
9. T. Koopmans, Physica 1, 104 (1934).
10. L. Brillouin, Actualites Sci. et Ind., No. 71 (1933).
11. R. Pariser and R. G. Parr, J. Chem. Phys., 21, 466 (1953).
12. J. L. Whitten and M. Hackmeyer, J. Chem. Phys., 51, 5584 (1969).
13. R. J. Buenker and S. D. Peyerimhoff, J. Chem. Phys., 53, 1368 (1970).
14. (a) E.A.Hylleraas and B. Undheim, Z. Phys., 65, 759 (1930).
    (b) J. K. L. MacDonald, Phys. Rev., 43, 830 (1933).

15. Sometimes we get only an upper bound on the energy of the Nth state when we want, say, the (N + K)th state. The theorem is of little use in these cases.

16. H. Lefebvre-Brion and G. M. Moser, J. Mol. Spectroscopy., 15, 211 (1965).

17. W. J. Hunt, T. H. Dunning Jr., and W. A. Goddard III, Chem. Phys. Lett., 3, 606 (1969).

18. D. W. Turner and D. P. May, J. Chem. Phys., 45, 471 (1966).

19. D. C. Frost and C. A. McDowell, Can. J. Chem., 36, 39 (1958).

20. T. H. Dunning, J. Chem. Phys., 53, 3385 (1970); T. H. Dunning, unpublished work. The hydrogen s basis set is scaled for a Slater exponent of 1.2.

21. S. Huzinaga, J. Chem. Phys., 42, 1293 (1965).

22. Reference 24 contains a compilation of data for singlet states. Reference 23 reports recent studies of triplet states of water.

23. S. Trajmar, W. Williams, and A. Kuppermann, J. Chem. Phys., 54, 2274 (1971).

24. G. Herzberg, Electronic Spectra of Polyatomic Molecules, (D. Van Nostrand Company, Princeton, 1967).

25. K. J. Miller, S. R. Mielczarek, and M. Krauss, J. Chem. Phys., 51, 26 (1969).

26. A. D. Walsh, J. Chem. Soc., 2260 (1953). The similar state $^1A_1 - {}^1\Delta_g$ in NH_2 probably has a bond angle of 145° (see Ref. 24).

27. J. A. Horsley and W. H. Fink, J. Chem. Phys., 50, 750 (1969).

28. J. W. C. Johns, Can J. Phys., 41, 209 (1963). A detailed analysis of rotational structure for the 10.00 eV band gave an equilibrium geometry close to that for the ground state.

29. G. J. Schulz, J. Chem. Phys., 33, 1661 (1960).

30. R. N. Compton, R. H. Heubner, P. W. Reinhardt and L. G. Christophorou, J. Chem. Phys., 38, 901 (1968).

31. W. A. Goddard III, private communication.

32. Y. Harada and J. N. Murrell, Mol. Phys., 14, 153 (1968).

33. S. R. LaPaglia, J. Chem. Phys., 41, 1427 (1964).

34. T. F. Lin and A. B. F. Duncan, J. Chem. Phys., 48, 866 (1968).

35. S. Trajmar, D. C. Cartwright and W. Williams, "Differential and Integral Cross Sections for the Electron Impact Excitation of the $^1\Delta_g$ and b $^1\Sigma_g^+$ States of O_2," Phys. Rev., A3, Oct. 1971.

36. S. Trajmar, W. Williams and A. Kuppermann, "The Angular Dependence of Electron Impact Excitation Cross Sections of O_2," J. Chem. Phys., to be published.

37. H. F. Schaefer and F. E. Harris, J. Chem. Phys., 48, 4946 (1968).

38. a. D. C. Cartwright, private communication.
b. J. Geiger and B. Schröder, J. Chem. Phys.,.

39. H. F. Schaefer and W. H. Miller, to be published.

40. E. Lindholm, Arkiv, För Fysik, 40, 117 (1969).

41. T. Betts and V. McKoy, J. Chem. Phys., 54, 113 (1971).

42. S. Trajmar, W. Williams and D. C. Cartwright, "The Excitation of Electronic States of CO by Electron Impact," I. C. P. E. A. C. Conference Proceedings, Amsterdam, 1971, p. 1066.

43. H. Lefebvre-Brion, C. Moser and R. K. Nesbet, J. Chem. Phys., 35, 1702 (1961).

44. H. Lefebvre-Brion and C. M. Moser, J. Mol. Spectroscopy, 13, 418 (1964).

45. E. Lindholm, Arkiv för Fysik, 40, 103 (1969).

46. D. C. Cartwright, Phys. Rev., 3, 1331 (1970).

47. R. S. Mulliken, in The Threshold of Space, edited by M. Zelikoff, Pergamon Press, New York, 1957, p. 169.

48. A. Omholt, In Aurora and Airglow, Reinhold, New York, 1967, p. 59.

49. S. Trajmar and R. T. Brinkman, Annals of Geophysics, p. 201 (1970).

50. H. Lefebvre-Brion and C. M. Moser J. Chem. Phys., 43, 1394 (1965).

51. E. Lindholm, Arkiv för Fysik, 40, 111 (1969).

52. P.K. Carroll and K. Yoshino, J. Chem. Phys., 47, 3073 (1967).

53. F. R. Gilmore, J. Quant. Spectrsc. Radiat. Transfer, 5, 369 (1965).

54. Since the matrix element causing the two curves to avoid each other will be rather small, we will discuss the problem using the natural or diabatic curves which do cross.

55. K. Dressler, Proc. Intern. Conf. Spectry. Bombay, 1, 104 (1967).

56. J. Geiger and B. Schröder, J. Chem. Phys, 50, 7 (1969).

57. E. Lindholm, Arkiv, för Fysik, 40, 97 (1969).

58. A. Skerbele, V. D. Meyer and E. N. Lassettre, J. Chem. Phys., 43, 817 (1965).

59. G. Herzberg, Molecular Spectra and Molecular Structure; Spectra of Diatomic Molecules, D. Van Nostrand Company, Inc., Princeton, 1950.

60. Y. Tanaka, A. S. Jarsa and F. LeBlance, J. Chem. Phys., 26, 862 (1957).

Table 1. Ionization Potentials for H_2O, O_2, N_2 and CO

State	Exptl. (eV)[a] 0-0	Vertical	Calculated (eV)[d] KT		
$H_2O^+(^2B_1)$	12.62	12.62	13.78	$1b_1$	1.16
$H_2O^+(^2A_1)$	b	14.35[c]	15.43	$3a_1$	1.08
$O_2^+(^2\pi_g)$	12.08	12.54(n=2)[e]	14.93	$1\pi_g$	2.39
$O_2^+(^4\pi_u)$	16.12	16.93(v=6)	16.05	$1\pi_u$	
$N_2^+(^2\Sigma_g^+)$	15.59	15.59	17.05	$3\sigma_g$	1.46
$N_2^+(^2\pi_u)$	16.73	16.96(ν=1)	16.97	$1\pi_u$	.01
$N_2^+(^2\Sigma_u^+)$	18.78	18.78	21.02	$2\sigma_u$	2.24
$CO^+(^2\Sigma^+)$	14.00	14.00	15.18	5σ	1.18
$CO^+(^2\pi^+)$	16.54	16.91(ν=2)	17.60	1π	.69
$CO^+(^2\Sigma^+)$	19.65	19.65	21.72	4σ	2.07

[a] All experimental data from D. W. Turner and D. P. May, J. Chem. Phys., 45, 471 (1966), Ref. 18, except for H_2O^+.

[b] Not observed.

[c] D. C. Frost and C. A. McDowell, Can. J. Chem., 36, 39(1958)Ref. 19.

[d] From the present work (using Koopmans Theorem).

[e] Vibrational Level of ion used.

Table II. Basis Set for IVO Calculations

Symmetry	Exponent		
	Carbon	Nitrogen	Oxygen
s	0.0408	0.059	0.08
	0.0102	0.015	0.02
	0.00255	0.0037	0.005
	0.0006375	0.00092	0.00125
x, y, z	0.0255	0.037	0.05
	0.006375	0.0092	0.0125
	0.00159	0.0023	0.003125
$x^2, y^2, z^2,$	0.036358	0.036358	0.036358
xy, xz, yz	0.010769	0.010769	0.010769

Table III. Ground State SCF Energies

MOLECULE		ENERGY
H_2O	$^1A_1$	-76.0105
O_2	$^3\Sigma_g^-$	-149.5756
N_2	$^1\Sigma_g^+$	-108.8877
CO	$^1\Sigma^+$	-112.6969

Table IV. Low-Lying Excited States of H_2O

State	Transition	Dipole Allowed	Excitation Energy(eV) Calc	Exptl[a]
$^3B_1$	$1b_1 \rightarrow 4a_1$ (3s)		6.68	
$^1B_1$	$1b_1 \rightarrow 4a_1$ (3s)	Yes	7.30	7.50
$^3A_2$	$1b_1 \rightarrow 2b_2$ (3p)		8.68	
$^3A_1$	$3a_1 \rightarrow 4a_1$ (3s)		8.69	
$^1A_2$	$1b_1 \rightarrow 2b_2$ (3p)		9.04	
$^1A_1$	$3a_1 \rightarrow 4a_1$ (3s)	Yes	9.59	9.75
$^3A_1$	$1b_1 \rightarrow 2b_1$ (3p)		9.70	9.81[b]
$^3B_1$	$1b_1 \rightarrow 5a_1$ (3p)		9.96	
$^1B_1$	$1b_1 \rightarrow 5a_1$ (3p)	Yes	10.04	10.00
$^1A_1$	$1b_1 \rightarrow 2b_1$ (3p)	Yes	10.16	10.17
$^3B_2$	$3a_1 \rightarrow 2b_2$ (3p)		10.48	
$^3B_1$	$1b_1 \rightarrow 6a_1$ (4s)		10.51	
$^1B_1$	$1b_1 \rightarrow 6a_1$ (4s)	Yes	10.64	11.00
$^3A_2$	$1b_1 \rightarrow 2b_2$ (3d)		10.79	
$^1A_2$	$1b_1 \rightarrow 3b_2$ (3d)		10.87	
$^3B_1$	$1b_1 \rightarrow 7a_1$ (3d)		11.05	
$^1B_1$	$1b_1 \rightarrow 7a_1$ (3d)	Yes	11.07	11.11
$^1B_2$	$3a_1 \rightarrow 2b_2$ (3p)	Yes	11.13	
$^3A_1$	$1b_1 \rightarrow 3b_1$ (3d)		11.16	
$^3B_1$	$1b_1 \rightarrow 8a_1$ (3d)		11.16	

$^1B_1$	$1b_1 \rightarrow 8a_1$ (3d)	Yes	11.17	11.11
$^1A_1$	$1b_1 \rightarrow 3b_1$ (ed)	Yes	11.17	11.11
$^3A_2$	$1b_1 \rightarrow 4b_2$ (4p)		11.18	
$^1A_2$	$1b_1 \rightarrow 4b_2$ (4p)		11.21	
$^3A_1$	$1b_1 \rightarrow 4b_1$ (4p)		11.32	
$^3B_1$	$1b_1 \rightarrow 9a_1$ (4p)		11.40	
$^1B_1$	$1b_1 \rightarrow 9a_1$ (4p)	Yes	11.42	
$^1A_1$	$1b_1 \rightarrow 4b_1$ (4p)	Yes	11.48	

---

[a] Reference 58 except for the 9.81 eV triplet state.

[b] Reference 23.

Table V. Complete IVO Results for H_2O

State	Trans	KIP	EIP	Explt
$^3B_1$ (T)	$1b_1 \rightarrow 4a_1$	7.84	6.68	
	$1b_1 \rightarrow 5a_1$	11.12	9.96	
	$1b_1 \rightarrow 6a_1$	11.67	10.51	
	$1b_1 \rightarrow 7a_1$	12.21	11.05	
	$1b_1 \rightarrow 8a_1$	12.32	11.16	
	$1b_1 \rightarrow 9a_1$	12.56	11.40	
	$1b_1 \rightarrow 10a_1$	12.78	11.62	
	$1b_1 \rightarrow 11a_1$	13.10	11.94	
	$1b_1 \rightarrow 12a_1$	13.33	12.17	
	$1b_1 \rightarrow 13a_1$	13.70	12.54	
$^1B_1$ (S)	$1b_1 \rightarrow 4a_1$ (4s)	8.46	7.30	7.50
	$1b_1 \rightarrow 5a_1$ (3p)	11.20	10.04	10.00
	$1b_1 \rightarrow 6a_1$ (4s)	11.80	10.64	11.00
	$1b_1 \rightarrow 7a_1$ (3d)	12.23	11.07	11.11
	$1b_1 \rightarrow 9a_1$ (4p)	12.58	11.42	11.37
	$1b_1 \rightarrow 10a_1$ (5s)	12.82	11.66	11.75
	$1b_1 \rightarrow 11a_1$	13.16	13.00	
	$1b_1 \rightarrow 12a_1$	13.39	12.23	
	$1b_1 \rightarrow 13a_1$	13.77	12.61	
$^3A_1$ (T)	$3a_1 \rightarrow 4a_1$	9.77	8.69	
	$3a_1 \rightarrow 5a_1$	12.60	11.52	

	$3a_1 \rightarrow 6a_1$	13.40	12.32	
	$3a_1 \rightarrow 7a_1$	13.88	12.80	
	$3a_1 \rightarrow 8a_1$	13.97	12.89	
	$3a_1 \rightarrow 9a_1$	14.16	13.08	
	$3a_1 \rightarrow 10a$	14.46	13.38	
	$3a_1 \rightarrow 11a$	14.75	13.67	
	$3a_1 \rightarrow 12a_1$	15.01	13.93	
	$3a_1 \rightarrow 13a_1$	15.34	14.26	
$^1A_1(S)$	$3a_1 \rightarrow 4a_1$	10.67	9.59	9.75
	$3a_1 \rightarrow 5a_1$	13.00	11.92	
	$3a_1 \rightarrow 6a_1$	13.59	12.51	
	$3a_1 \rightarrow 7a_1$	13.89	12.81	
	$3a_1 \rightarrow 8a_1$	13.97	12.89	
	$3a_1 \rightarrow 9a_1$	14.30	13.22	
	$3a_1 \rightarrow 10a_1$	14.54	13.46	
	$3a_1 \rightarrow 11a_1$	15.05	13.97	
	$3a_1 \rightarrow 12a_1$	15.15	14.07	
$^3A_2$	$1b_1 \rightarrow 2b_2$	9.84	8.68	
	$1b_1 \rightarrow 3b_2$	11.95	10.79	
	$1b_1 \rightarrow 4b_2$	12.34	11.18	
	$1b_1 \rightarrow 5b_2$	12.80	11.64	
	$1b_1 \rightarrow 6b_2$	13.61	12.45	
$^1A_2$	$1b_1 \rightarrow 2b_2$	10.20	9.04	
	$1b_1 \rightarrow 3b_2$	12.03	10.87	
	$1b_1 \rightarrow 4b_2$	12.37	11.21	

	$1b_1 \rightarrow 5b_2$	12.83	11.67	
	$1b_1 \rightarrow 6b_2$	13.64	12.48	
$^3B_2$	$3a_1 \rightarrow 2b_2$	11.56	10.48	
	$3a_1 \rightarrow 3b_2$	13.54	12.46	
	$3a_1 \rightarrow 4b_2$	14.00	12,92	
	$3a_1 \rightarrow 5b_2$	14.44	13.36	
	$3a_1 \rightarrow 6b_2$	15.19	14.11	
$^1B_2$	$3a_1 \rightarrow 2b_2$	12.21	11.13	
	$3a_1 \rightarrow 3b_2$	13.80	12.72	
	$3a_1 \rightarrow 4b_2$	14.07	12.99	
	$3a_1 \rightarrow 5b_2$	14.60	13.52	
	$3a_1 \rightarrow 6b_2$	15.25	14.17	
$^3A_1$	$1b_1 \rightarrow 2b_1$	10.86	9.70	
	$1b_1 \rightarrow 3b_1$	12.32	11.16	
	$1b_1 \rightarrow 4b_1$	12.48	11.32	
	$1b_1 \rightarrow 5b_1$	13.18	12.02	
	$1b_1 \rightarrow 6b_1$	13.72	12.56	
$^1A_1$	$1b_1 \rightarrow 2b_1$ (3p)	11.32	12.56	10.17
	$1b_1 \rightarrow 3b_1$ (3d)	12.33	11.17	11.11
	$1b_1 \rightarrow 4b_1$ (4p)	12.64	11.48	11.49
	$1b_1 \rightarrow 5b_1$	13.52	12.36	
$^3B_1$	$3a_1 \rightarrow 2b_1$	12.76	11.68	
	$3a_1 \rightarrow 3b_1$	13.97	12.89	
	$3a_1 \rightarrow 4b_1$	14.21	13.13	
	$3a_1 \rightarrow 5b_1$	14.99	13.89	

	$3a_1 \rightarrow 6b_1$	15.39	14.31
$^1B_1$	$3a_1 \rightarrow 2b_1$	12.82	11.74
	$3a_1 \rightarrow 3b_1$	13.98	12.90
	$3a_1 \rightarrow 4b_1$	14.24	13.16
	$3a_1 \rightarrow 5b_1$	15.06	13.98

---

[a] Reference 58.

Table VI. Low-lying Rydberg States of O_2

State	Transition	Dipole Allowed	Excitation Energy Calc	Exptl[a]
$^3\pi_g$	$1\pi_g \rightarrow 4\sigma_g$ (3s)		8.70	
$^1\pi_g$	$1\pi_g \rightarrow 5\sigma_g$ (3s)		8.81	
$^1\Sigma_u^-$	$1\pi_g \rightarrow 2\pi_u$ (3p)		9.73	
$^3\Delta_u$	$1\pi_g \rightarrow 2\pi_u$ (3p)		9.81	
$^3\Sigma_u^+$	$1\pi_g \rightarrow 2\pi_u$ (3p)		9.88	
$^3\Sigma_u^-$	$1\pi_g \rightarrow 2\pi_u$ (3p)	Yes	9.91	9.97
$^1\Delta_u$	$1\pi_g \rightarrow 2\pi_u$ (3p)		10.01	
$^1\Sigma_u^+$	$1\pi_g \rightarrow 2\pi_u$ (3p)		10.10	
$^3\pi_u$	$1\pi_g \rightarrow 4\sigma_u$ (3p)	Yes	10.45	10.29
$^3\pi_u$	$1\pi_g \rightarrow 3\sigma_u$(valence)	Yes	10.85	
$^3\pi_g$	$1\pi_g \rightarrow 5\sigma_g$ (3d)		10.86	
$^1\pi_g$	$1\pi_g \rightarrow 5\sigma_g$ (3d)		10.88	
$^1\pi_u$	$1\pi_g \rightarrow 4\sigma_u$		10.93	
$^1\Sigma_g^-$	$1\pi_g \rightarrow 2\pi_g$		11.04	
$^3\Delta_g$	$1\pi_g \rightarrow 2\pi_g$		11.05	
$^3\Sigma_u^+$	$1\pi_g \rightarrow 2\pi_g$		11.07	
$^3\Sigma_g^-$	$1\pi_g \rightarrow 2\pi_u$ (3p)		11.07	
$^3\pi_g$	$1\pi_g \rightarrow 6\sigma_g$		11.08	
$^1\pi_g$	$1\pi_g \rightarrow 6\sigma_g$		11.09	
$^1\Delta_g$	$1\pi_g \rightarrow 2\pi_g$		11.09	
$^1\Sigma_g^+$	$1\pi_g \rightarrow 2\pi_g$		11.11	

$^3\pi_g$	$1\pi_g \rightarrow 8\sigma_g$		11.74
$^3\Sigma_u^-$	$1\pi_g \rightarrow 4\pi_u$ (5p)	Yes	11.79
$^3\Delta_u$	$1\pi_g \rightarrow 4\pi_u$		11.79
$^1\Sigma_u^-$	$1\pi_g \rightarrow 4\pi_u$		11.79
$^3\pi_u$	$1\pi_g \rightarrow 6\sigma_u$	Yes	11.79
$^1\pi_u$	$1\pi_g \rightarrow 6\sigma_u$		11.79
$^3\Sigma_u^+$	$1\pi_g \rightarrow 4\pi_u$		11.80
$^1\Sigma_u^+$	$1\pi_g \rightarrow 4\pi_u$		11.80
$^1\Delta_u$	$1\pi_g \rightarrow 4\pi_u$		11.80
$^3\pi_u$	$1\pi \rightarrow 7\sigma_u$ (4d)	Yes	11.87
$^3\pi_g$	$1\pi \rightarrow 7\delta_u$		11.92
$^1\pi_u$	$1\pi \rightarrow 3\pi_u$ (valence)		11.96

Reference 40.

Table VII. Complete IVO Results for O_2

State	Trans	Excit KIP	EIP	Exptl[a]
$^1\pi_g$ (S)	$1\pi_g \rightarrow 4\sigma_g$	11.20	8.81	
	$1\pi_g \rightarrow 5\sigma_g$	13.27	10.88	
	$1\pi_g \rightarrow 6\sigma_g$	13.48	11.09	
	$1\pi_g \rightarrow 7\sigma_g$	14.04	11.65	
	$1\pi_g \rightarrow 8\sigma_g$	14.13	11.74	
	$1\pi_g \rightarrow 9\sigma_g$	14.51	12.12	
$^1\pi_u$	$1\pi_g \rightarrow 3\sigma_u$ (valence)	11.96	9.57	
	$1\pi_g \rightarrow 4\sigma_u$	13.32	10.93	
	$1\pi_g \rightarrow 5\sigma_u$	13.96	11.57	
	$1\pi_g \rightarrow 6\sigma_u$	14.18	11.79	
	$1\pi_g \rightarrow 7\sigma_u$	14.31	11.92	
	$1\pi_g \rightarrow 8\sigma_u$	14.56	12.17	
$^3\pi_g$	$1\pi_g \rightarrow 4\sigma_g$	11.09	8.70	
	$1\pi_g \rightarrow 5\sigma_g$	13.25	10.86	
	$1\pi_g \rightarrow 6\sigma_g$	13.47	11.08	
	$1\pi_g \rightarrow 7\sigma_g$	14.03	11.64	
	$1\pi_g \rightarrow 8\sigma_g$	14.13	11.74	
	$1\pi_g \rightarrow 9\sigma_g$	14.51	12.12	
$^3\pi_u$	$1\pi_g \rightarrow 3\sigma_u$ (valence)	10.85	8.46	
	$1\pi_g \rightarrow 4\sigma_u$ (3p)	12.84	10.45	10.29
	$1\pi_g \rightarrow 5\sigma_u$ (3d)	13.82	11.43	

	$1\pi_g \rightarrow 6\sigma_u$ (4p)	14.18	11.79
	$1\pi_g \rightarrow 7\sigma_u$ (4d)	14.26	11.87
	$1\pi_g \rightarrow 8\sigma_u$ (5p)	14.51	12.12
$^3\Sigma_u^+$	$1\pi_g \rightarrow 2\pi_u$	12.27	9.88
	$1\pi_g \rightarrow 3\pi_u$	13.72	11.33
	$1\pi_g \rightarrow 4\pi_u$	14.19	11.80
	$1\pi_g \rightarrow 5\pi_u$	14.58	12.19
$^3\Sigma_g^+$	$1\pi_g \rightarrow 2\pi_g$	13.46	11.07
	$1\pi_g \rightarrow 3\pi_g$	14.10	11.71
	$1\pi_g \rightarrow 4\pi_g$	14.62	12.23
$^1\Sigma_u^+$	$1\pi_g \rightarrow 2\pi_u$	12.49	10.10
	$1\pi_g \rightarrow 3\pi_u$	13.79	11.40
	$1\pi_g \rightarrow 4\pi_u$	14.19	11.80
	$1\pi_g \rightarrow 5\pi_u$	14.90	12.51
$^1\Sigma_g^+$	$1\pi_g \rightarrow 2\pi_g$	13.50	11.11
	$1\pi_g \rightarrow 3\pi_g$	14.12	11.73
	$1\pi_g \rightarrow 4\pi_g$	14.67	12.28
$^1\Sigma_u^-$	$1\pi_g \rightarrow 2\pi_u$	12.12	9.73
	$1\pi_g \rightarrow 3\pi_u$	13.68	11.29
	$1\pi_g \rightarrow 4\pi_u$	14.18	11.79
	$1\pi_g \rightarrow 5\pi_u$	14.48	12.09
$^1\Sigma_g^-$	$1\pi_g \rightarrow 2\pi_g$	13.43	11.04
	$1\pi_g \rightarrow 3\pi_g$	14.09	11.70
	$1\pi_g \rightarrow 4\pi_g$	14.60	12.21
$^3\Delta_u$	$1\pi_g \rightarrow 2\pi_u$	12.20	9.81

	$1\pi_g \rightarrow 3\pi_u$	13.70	11.31	
	$1\pi_g \rightarrow 4\pi_u$	14.18	11.79	
	$1\pi_g \rightarrow 5\pi_u$	14.53	12.14	
$^3\Delta_g$	$1\pi_g \rightarrow 2\pi_g$	13.44	11.05	
	$1\pi_g \rightarrow 3\pi_g$	14.09	11.70	
	$1\pi_g \rightarrow 4\pi_g$	14.61	12.22	
$^1\Delta_u$	$1\pi_g \rightarrow 2\pi_u$	12.40	10.01	
	$1\pi_g \rightarrow 3\pi_u$	13.77	11.38	
	$1\pi_g \rightarrow 4\pi_u$	14.19	11.80	
	$1\pi_g \rightarrow 5\pi_u$	14.78	12.39	
$^1\Delta_g$	$1\pi_g \rightarrow 2\pi_g$	13.48	11.09	
	$1\pi_g \rightarrow 3\pi_g$	14.11	11.72	
	$1\pi_g \rightarrow 4\pi_g$	14.65	12.26	
$^3\Sigma_u^-$	$1\pi_g \rightarrow 2\pi_u$ (3p)	12.30	9.91	9.97
	$1\pi_g \rightarrow 3\pi_u$ (4p)	13.73	11.34	
	$1\pi_g \rightarrow 4\pi_u$ (5p)	14.18	11.79	
	$1\pi_g \rightarrow 5\pi_u$	14.66	12.27	
$^3\Sigma_g^-$	$1\pi_g \rightarrow 2\pi_g$ (3d)	13.46	11.07	
	$1\pi_g \rightarrow 3\pi_g$ (4d)	14.10	11.71	
	$1\pi_g \rightarrow 4\pi_g$ (5d)	14.63	12.24	

Reference 40

Table VIII. Low-Lying States of CO

State	Transition	Calc. Ref. 44	Excitation Energy Calc	Exptl[a]
$^3\pi$	$5\sigma \rightarrow 2\pi$ (v)	6.20	5.76	6.22
$^3\Sigma^+$	$\pi \rightarrow 2\pi$ (v)	7.87	7.64	8.25
$^3\Delta$	$\pi \rightarrow 2\pi$ (v)	8.77	8.54	8.96
$^1\pi$	$5\sigma \rightarrow 2\pi$ (v)	9.37	9.04	8.74
$^3\Sigma^-$	$\pi \rightarrow 2\pi$ (v)	9.67	9.43	8.80
$^1\Delta$	$\pi \rightarrow 2\pi$ (v)		9.92	
$^3\Sigma^+$	$5\sigma \rightarrow 6\sigma$ (3s)	10.3	10.11	10.39
$^1\Sigma^+$	$5\sigma \rightarrow 6\sigma$ (3s)	11.0	10.85	10.78
$^3\Sigma^+$	$5\sigma \rightarrow 6\sigma$ (3p)	11.4	11.30	11.42
$^3\pi$	$5\sigma \rightarrow 3\pi$ (3p)	11.4	11.37	
$^1\pi$	$5\sigma \rightarrow 3\pi$ (3p)	11.5	11.49	11.52
$^1\Sigma^+$	$5\sigma \rightarrow 7\sigma$ (3p)	11.5	11.51	11.40
$^3\Sigma^+$	$5\sigma \rightarrow 8\sigma$ (4s)	12.4	12.35	
$^1\Sigma^+$	$5\sigma \rightarrow 8\sigma$ (4s)	12.6	12.52	12.58
$^3\Sigma^+$	$5\sigma \rightarrow 9\Sigma$ (3d)	12.5	12.55	
$^3\pi$	$5\sigma \rightarrow 4\pi$ (3d)	12.6	12.56	
1π	$5\sigma \rightarrow 4\pi$ (3d)	12.6	12.56	12.37
$^1\Sigma^+$	$5\sigma \rightarrow 9\sigma$ (3d)	12.5	12.61	
$^3\pi$	$5\sigma \rightarrow 5\pi$ (4p)	12.8	12.75	
$^3\Sigma^+$	$5\sigma \rightarrow 10\sigma$	12.8	12.75	
$^1\pi$	$5\sigma \rightarrow 5\pi$ (4p)	12.8	12.79	12.81

$^1\Sigma^+$	$5\sigma \rightarrow 10\sigma$ (4p)	12.8	12.81	12.81
$^3\Sigma^+$	$5\sigma \rightarrow 11\sigma$		13.13	
$^3\pi$	$1\pi \rightarrow 6\sigma$		13.15	
$^3\Sigma^+$	$\pi \rightarrow 3\pi$		13.16	
$^1\Sigma^+$	$5\sigma \rightarrow 11\sigma$ (4d)		13.18	
$^3\Sigma^+$	$5\sigma \rightarrow 12\sigma$		13.20	
$^1\Sigma^+$	$5\sigma \rightarrow 12\sigma$ (5s)		13.25	13.19
$^3\pi$	$5\sigma \rightarrow 6\pi$		13.26	
$^1\pi$	$5\sigma \rightarrow 6\pi$ (4d)		13.27	13.10
$^3\pi$	$5\sigma \rightarrow 7\pi$		13.28	
$^1\pi$	$5\sigma \rightarrow 7\pi$ (5p)		13.29	13.31
$^1\Sigma^+$	$5\sigma \rightarrow 13\sigma$ (5p)		13.29	13.29
$^3\Sigma^+$	$5\sigma \rightarrow 13\sigma$		13.29	
$^1\pi$	$1\pi \rightarrow 6\sigma$ (3s)		13.36	13.48
$^3\Sigma^+$	$5\sigma \rightarrow 14\sigma$		13.41	
$^1\Sigma^+$	$5\sigma \rightarrow 14\sigma$		13.42	
$^3\Sigma^+$	$5\sigma \rightarrow 15\sigma$		13.43	
$^3\pi$	$5\sigma \rightarrow 8\pi$		13.46	
$^1\pi$	$5\sigma \rightarrow 8\pi$ (5d)		13.47	13.44
$^1\Sigma^+$	$5\sigma \rightarrow 15\sigma$		13.47	
$^3\Sigma^+$	$5\sigma \rightarrow 16\sigma$		13.60	
$^1\Sigma^+$	$5\sigma \rightarrow 16\sigma$		13.63	
$^3\Sigma^+$	$5\sigma \rightarrow 17\sigma$		13.85	
$^3\Sigma^+$	$5\sigma \rightarrow 18\sigma$		13.95	
$^1\Sigma^-$	$1\pi \rightarrow 2\pi$		14.17	

$^3\Delta$	$\pi \rightarrow 3\pi$	14.28	
$^1\Delta$	$\pi \rightarrow 3\pi$	14.34	
$^3\Sigma^-$	$\pi \rightarrow 3\pi$	14.39	
$^1\Sigma^+$	$1\pi \rightarrow 2\pi$ (3p)	14.47	14.44
$^3\pi$	$1\pi \rightarrow 7\sigma$	14.55	
$^1\pi$	$1\pi \rightarrow 7\sigma$ (3p)	14.59	14.40
$^1\Sigma^-$	$1\pi \rightarrow 3\pi$	14.68	
$^1\Sigma^+$	$5\sigma \rightarrow 17\sigma$	14.92	

---

[a] References 45,49 and 60.

Table IX. Complete IVO Results for CO

State	Transition	Excitation Energy (eV) KIP	EIP	Exptl.
$^1\pi$	$5\sigma \rightarrow 2\pi$ (v)	9.04	7.86	8.74
	$5\sigma \rightarrow 3\pi$ (3p)	12.67	11.49	11.52
	$5\sigma \rightarrow 4\pi$ (3d)	13.74	12.56	12.37
	$5\sigma \rightarrow 5\pi$ (4p)	13.97	12.79	12.81
	$5\sigma \rightarrow 6\pi$ (4d)	14.45	13.27	13.10
	$5\sigma \rightarrow 7\pi$ (5p)	14.47	13.29	13.31
	$5\sigma \rightarrow 8\pi$ (5d)	14.65	13.47	13.44
$^3\pi$	$5\sigma \rightarrow 2\pi$ (v)	5.76	4.58	6.22
	$5\sigma \rightarrow 3\pi$	12.55	11.37	
	$5\sigma \rightarrow 4\pi$	13.74	12.56	
	$5\sigma \rightarrow 5\pi$	13.93	12.75	
	$5\sigma \rightarrow 6\pi$	14.44	13.26	
	$5\sigma \rightarrow 7\pi$	14.46	13.28	
	$5\sigma \rightarrow 8\pi$	14.64	13.46	
$^1\Sigma^-$	$1\pi \rightarrow 2\pi$	14.86	14.17	
	$1\pi \rightarrow 3\pi$	15.37	14.68	
	$1\pi \rightarrow 4\pi$	16.33	15.64	
	$1\pi \rightarrow 5\pi$	16.47	15.78	
	$1\pi \rightarrow 6\pi$	16.86	16.17	
	$1\pi \rightarrow 7\pi$	16.91	16.22	
	$1\pi \rightarrow 8\pi$	17.13	16.44	

$^1\Sigma^+$	$1\pi \rightarrow 2\pi$ (3p)	15.16	14.47	14.44
	$1\pi \rightarrow 3\pi$ (3d)	15.97	15.28	15.20
	$1\pi \rightarrow 4\pi$ (4p)	16.42	15.73	15.66
	$1\pi \rightarrow 5\pi$ (4d)	16.85	16.16	15.99
	$1\pi \rightarrow 6\pi$ (5p)	16.89	16.20	16.17
	$1\pi \rightarrow 7\pi$ (4f)	16.93	16.24	
	$1\pi \rightarrow 8\pi$ (5d)	17.23	16.54	16.33
$^1\Delta$	$\pi \rightarrow 2\pi$ (v)	9.92	9.23	
	$\pi \rightarrow 3\pi$	15.03	14.34	
	$\pi \rightarrow 4\pi$	16.17	15.48	
	$\pi \rightarrow 5\pi$	16.37	15.68	
	$\pi \rightarrow 6\pi$	16.85	16.16	
	$\pi \rightarrow 7\pi$	16.87	16.18	
	$\pi \rightarrow 8\pi$	17.09	16.40	
	$\pi \rightarrow 9\pi$	17.49	16.80	
$^3\Delta$	$\pi \rightarrow 2\pi$ (v)	8.54	7.85	8.96
	$\pi \rightarrow 3\pi$	14.97	14.28	
	$\pi \rightarrow 4\pi$	16.15	15.46	
	$\pi \rightarrow 5\pi$	16.36	15.67	
	$\pi \rightarrow 6\pi$	16.85	16.16	
	$\pi \rightarrow 7\pi$	16.87	16.18	
	$\pi \rightarrow 8\pi$	17.08	16.39	
	$\pi \rightarrow 9\pi$	17.44	16.75	
$^3\Sigma^-$	$\pi \rightarrow 2\pi$ (v)	9.43	8.74	8.80
	$\pi \rightarrow 3\pi$	15.08	14.39	

	$\pi \rightarrow 4\pi$	16.18	15.49	
	$\pi \rightarrow 5\pi$	16.39	15.70	
	$\pi \rightarrow 6\pi$	16.86	16.17	
	$\pi \rightarrow 7\pi$	16.88	16.19	
	$\pi \rightarrow 8\pi$	17.09	16.40	
	$\pi \rightarrow 9\pi$	17.51	16.82	
	$\pi \rightarrow 2\pi$ (v)	7.64	6.95	8.25
	$\pi \rightarrow 3\pi$	14.85	13.16	
	$\pi \rightarrow 4\pi$	16.13	15.44	
	$\pi \rightarrow 5\pi$	16.32	15.63	
	$\pi \rightarrow 6\pi$	16.85	16.16	
	$\pi \rightarrow 7\pi$	16.85	16.16	
	$\pi \rightarrow 8\pi$	17.07	16.38	
	$\pi \rightarrow 9\pi$	17.38	16.69	
$^1\pi$	$1\pi \rightarrow 6\sigma$ (3s)	14.05	13.36	13.48
	$1\pi \rightarrow 7\sigma$ (3p)	15.28	14.59	14.00
	$1\pi \rightarrow 8\sigma$ (4s)	15.94	15.25	15.35
	$1\pi \rightarrow 9\sigma$ (3d)	16.19	15.50	---
	$1\pi \rightarrow 10\sigma$ (4p)	16.46	15.77	15.66
	$1\pi \rightarrow 11\sigma$ (5s)	16.70	16.01	16.09
	$1\pi \rightarrow 12\sigma$ (4d)	16.86	16.17	---
	$1\pi \rightarrow 13\sigma$ (5p)	16.92	16.23	16.17
	$1\pi \rightarrow 14\sigma$	16.99	16.30	
	$1\pi \rightarrow 15\sigma$	17.11	16.42	
	$1\pi \rightarrow 16\sigma$	17.21	16.52	

	$1\pi \rightarrow 16\sigma$	17.21	16.52	
	$1\pi \rightarrow 17\sigma$	17.38	16.69	
$^3\pi$	$1\pi \rightarrow 6\sigma$	13.84	13.15	
	$1\pi \rightarrow 7\sigma$	15.24	14.55	
	$1\pi \rightarrow 8\sigma$	15.86	15.17	
	$1\pi \rightarrow 9\sigma$	16.18	15.49	
	$1\pi \rightarrow 10\sigma$	16.44	15.75	
	$1\pi \rightarrow 11\sigma$	16.67	15.98	
	$1\pi \rightarrow 12\sigma$	16.86	16.17	
	$1\pi \rightarrow 13\sigma$	16.91	16.22	
	$1\pi \rightarrow 14\sigma$	16.97	16.28	
	$1\pi \rightarrow 15\sigma$	17.10	16.41	
	$1\pi \rightarrow 16\sigma$	17.20	16.51	
	$1\pi \rightarrow 17\sigma$	17.35	16.66	
	$1\pi \rightarrow 18\sigma$	17.58	16.89	
$^1\Sigma^+$	$5\sigma \rightarrow 6\sigma$ (3s)	12.03	10.85	10.78
	$5\sigma \rightarrow 7\sigma$ (3p)	12.69	11.51	11.40
	$5\sigma \rightarrow 8\sigma$ (3d)	13.70	12.52	---
$^1\Sigma^+$	$5\sigma \rightarrow 9\sigma$ (4s)	13.79	12.61	12.58
	$5\sigma \rightarrow 10\sigma$ (4p)	13.99	12.81	12.81
	$5\sigma \rightarrow 11\sigma$ (4d)	14.36	13.18	
	$5\sigma \rightarrow 12\sigma$ (5s)	14.43	13.25	13.19
	$5\sigma \rightarrow 13\sigma$ (5p)	14.47	13.29	13.29
	$5\sigma \rightarrow 14\sigma$	14.60	13.42	
	$5\sigma \rightarrow 15\sigma$	14.65	13.47	

	$5\sigma \rightarrow 16\sigma$	14.81	13.63
	$5\sigma \rightarrow 17\sigma$	15.10	14.92
$^3\Sigma^+$	$5\sigma \rightarrow 6\sigma$	11.29	10.11
	$5\sigma \rightarrow 7\sigma$	12.48	11.30
	$5\sigma \rightarrow 8\sigma$	13.53	12.35
	$5\sigma \rightarrow 9\sigma$	13.73	12.55
	$5\sigma \rightarrow 10\sigma$	13.93	12.75
	$5\sigma \rightarrow 11\sigma$	14.28	13.13
	$5\sigma \rightarrow 12\sigma$	14.38	13.20
	$5\sigma \rightarrow 13\sigma$	14.47	13.29
	$5\sigma \rightarrow 14\sigma$	14.59	13.41
	$5\sigma \rightarrow 15\sigma$	14.61	13.43
	$5\sigma \rightarrow 16\sigma$	14.78	13.60
	$5\sigma \rightarrow 17\sigma$	15.03	13.85
	$5\sigma \rightarrow 18\sigma$	15.13	13.95

[a] References 45, 59 and 60.

Table X. Low-lying States of N_2.

State	Transition	Excitation Energy Calc. Ref. 50	Calc.	Exptl[a]
$^3\Sigma_u^+$	$\pi_u \rightarrow 1\pi_g$ (v)		6.22	7.6[b]
$^3\Delta_u$	$\pi_u \rightarrow 2\pi_g$ (v)		7.31	8.08
$^3\pi_g$	$3\sigma_g \rightarrow 1\pi_g$ (v)		7.78	7.9
$^3\Sigma_u^-$	$\pi_u \rightarrow 1\pi_g$ (v)		8.38	9.4
$^1\Delta_u$	$\pi_u \rightarrow 1\pi_g$ (v)		9.04	10.4
$^1\pi_g$	$3\sigma_g \rightarrow 1\pi_g$ (v)		9.70	9.2
$^3\Sigma_g^+$	$3\sigma_g \rightarrow 4\sigma_g$ (3s)	11.9	12.04	11.88
$^1\Sigma_g^+$	$3\sigma_g \rightarrow 4\sigma_g$ (3s)	12.5	12.35	12.26
$^3\pi_u$	$3\delta_g \rightarrow 2\pi_u$ (3p)	13.0	13.00	---
$^1\pi_u$	$3\sigma_g \rightarrow 2\pi_u$ (3p)	13.1	13.04	12.910
$^3\Sigma_u^+$	$3\sigma_g \rightarrow 3\sigma_u$ (3p)	13.0	13.07	12.84
$^1\Sigma_u^+$	$3\sigma_g \rightarrow 3\sigma_u$ (3p)	13.1	13.17	12.935
$^3\pi_u$	$\pi_u \rightarrow 4\sigma_g$ (3s)	13.23	13.23	---
$^1\pi_u$	$\pi_u \rightarrow 4\sigma_g$ (3s)	13.43	13.50	13.345
$^3\Sigma_g^+$	$3\sigma_g \rightarrow 5\sigma_g$ (3d)	13.9	13.94	---
$^1\Sigma_g^+$	$3\sigma_u \rightarrow 5\sigma_g$ (3d)	14.0	13.98	---
$^3\Sigma_g^+$	$\pi_u \rightarrow 2\pi_u$ (3p)		14.10	
$^3\Sigma_g^+$	$3\sigma_g \rightarrow 6\sigma_g$ (4s)		14.14	
$^3\pi_g$	$3\sigma_g \rightarrow 2\pi_g$ (3d)	14.9	14.15	
$^1\pi_g$	$3\sigma_g \rightarrow 2\pi_g$ (3d)	15.0	14.16	

$^1\Sigma_g^+$	$3\sigma_g \rightarrow 6\sigma_g$ (4s)		14.21	
$^3\Delta_g$	$\pi_u \rightarrow 2\pi_u$ (3p)		14.25	
$^1\Delta_g$	$\pi_u \rightarrow 2\pi_u$ (3p)	14.33	14.31	14.57
$^3\Sigma_g^-$	$\pi_u \rightarrow 2\pi_u$ (3p)		14.38	
$^3\Sigma_u^+$	$3\sigma_g \rightarrow 4\sigma_u$ (4p)	14.4	14.39	
$^3\pi_u$	$3\sigma_g \rightarrow 3\pi_u$ (4p)	14.4	14.39	
$^1\pi_u$	$3\sigma_g \rightarrow 3\pi_u$ (4p)	14.5	14.41	14.41
$^1\Sigma_u^+$	$3\sigma_g \rightarrow 4\sigma_u$ (4p)	14.5	14.42	14.33
$^3\pi_g$	$\pi_u \rightarrow 3\sigma_u$ (3p)		14.55	
$^1\Sigma_g^+$	$\pi_u \rightarrow 2\pi_u$ (3p)		14.59	
$^1\Sigma_g^-$	$\pi_u \rightarrow 2\pi_u$ (3p)	14.43	14.60	14.27*
$^1\pi_g$	$\pi_u \rightarrow 3\sigma_u$ (3p)	14.55	14.60	14.38
$^3\Sigma_g^+$	$3\sigma_g \rightarrow 7\sigma_g$ (4d)	14.72		
$^1\Sigma_g^+$	$3\sigma_g \rightarrow 7\sigma_g$ (4d)		14.74	
$^3\pi_g$	$3\sigma_g \rightarrow 3\pi_g$ (4d)		14.78	
$^3\Sigma_g^+$	$3\sigma_g \rightarrow 8\sigma_g$ (5s)		14.79	
$^1\pi_g$	$3\sigma_g \rightarrow 3\pi_g$ (4d)		14.79	
$^1\Sigma_g^+$	$3\sigma_g \rightarrow 8\sigma_g$ (5c)		14.82	
$^3\Sigma_u^+$	$3\sigma_g \rightarrow 5\sigma_u$ (5p)	14.9	14.83	
$^1\Sigma_u^+$	$3\sigma_g \rightarrow 5\sigma_u$ (5p)	14.9	14.84	14.85
$^3\pi_u$	$3\sigma_g \rightarrow 4\pi_u$ (5p)	14.9	14.85	
$^1\pi_u$	$3\sigma_g \rightarrow 4\pi_u$ (5p)	15.0	14.86	14.88
$^3\Sigma_u^+$	$3\sigma_g \rightarrow 6\sigma_u$ (4f)		14.88	
$^1\Sigma_u^+$	$3\sigma_g \rightarrow 6\sigma_u$ (4f)		14.90	

$^3\pi_u$	$3\sigma_g \rightarrow 5\pi_u$ (5d)	14.98
$^1\Sigma_u^-$	$\pi_u \rightarrow 1\pi_g$ (3d)	15.00
$^1\pi_u$	$3\sigma_g \rightarrow 5\pi_u$ (5d)	15.00

---

[a] Experimental values are taken References 46, 47, 56 and 57.

Table XI. Complete Results for N_2

State	Trans	Excitation Energy (eV) KIP	EIP	Exptl
$^3\Delta_g$	$\pi_u \rightarrow 2\pi_u$	14.26	14.25	
	$\pi_u \rightarrow 3\pi_u$	15.73	15.72	
	$\pi_u \rightarrow 4\pi_u$	16.23	16.22	
	$\pi_u \rightarrow 5\pi_u$	16.33	16.32	
$^3\Delta_u$	$\pi_u \rightarrow 1\pi_h$ (v)	7.31	7.30	
	$\pi_u \rightarrow 2\pi_g$	15.53	15.52	
	$\pi_u \rightarrow 3\pi_g$	16.16	16.15	
	$\pi_u \rightarrow 4\pi_g$	16.56	16.55	
$^1\Delta_g$	$\pi_u \rightarrow 2\pi_u$	14.32	14.31	14.57
	$\pi_u \rightarrow 3\pi_u$	15.76	15.75	
	$\pi_u \rightarrow 4\pi_u$	16.24	16.23	
	$\pi_u \rightarrow 5\pi_u$	16.36	16.35	
$^1\Delta_u$	$\pi_u \rightarrow 1\pi_g$ (v)	9.04	9.03	
	$\pi_u \rightarrow 2\pi_g$	15.55	15.54	
	$\pi_u \rightarrow 3\pi_g$	16.17	16.16	
	$\pi_u \rightarrow 4\pi_g$	16.57	16.56	
$^1\Sigma_g^+$	$\pi_u \rightarrow 2\pi_u$ (3p)	14.60	14.59	
	$\pi_u \rightarrow 3\pi_u$ (4p)	15.87	15.86	
	$\pi_u \rightarrow 4\pi_u$	16.24	16.23	
	$\pi_u \rightarrow 5\pi_u$	16.55	16.54	

$^1\Sigma_u^+$	$\pi_u \rightarrow 1\pi_g$	15.42	15.41	
	$\pi_u \rightarrow 2\pi_g$	16.10	16.09	
	$\pi_u \rightarrow 3\pi_g$	16.47	16.46	
	$\pi_u \rightarrow 4\pi_g$	17.47	17.46	
$^1\Sigma_g^-$	$\pi_u \rightarrow 2\pi_u$	14.61	14.60	14.27
	$\pi_u \rightarrow 3\pi_u$	15.86	15.85	
	$\pi_u \rightarrow 4\pi_u$	16.25	16.24	
	$\pi_u \rightarrow 5\pi_u$	16.52	16.51	
$^1\Sigma_u^-$	$\pi_u \rightarrow 1\pi_g$	15.01	15.00	
	$\pi_u \rightarrow 2\pi_g$	15.83	15.82	
	$\pi_u \rightarrow 3\pi_g$	16.27	16.26	
	$\pi_u \rightarrow 4\pi_g$	16.77	16.76	
$^3\Sigma_g^-$	$\pi_u \rightarrow 2\pi_u$	14.39	14.38	
	$\pi_u \rightarrow 3\pi_u$	15.77	15.76	
	$\pi_u \rightarrow 4\pi_u$	16.24	16.23	
	$\pi_u \rightarrow 5\pi_u$	16.37	16.36	
$^3\Sigma_u^-$	$\pi_u \rightarrow 1\pi_g$ (v)	8.38	8.37	
	$\pi_u \rightarrow 2\pi_g$	15.56	15.55	
	$\pi_u \rightarrow 3\pi_g$	16.17	16.16	
	$\pi_u \rightarrow 4\pi_g$	16.58	16.57	
$^3\Sigma_g^+$	$\pi_u \rightarrow 2\pi_u$	14.11	14.10	
	$\pi_u \rightarrow 3\pi_u$	15.69	15.68	
	$\pi_u \rightarrow 4\pi_u$	16.22	16.21	
	$\pi_u \rightarrow 5\pi_u$	16.30	16.29	
$^3\Sigma_u^+$	$\pi_u \rightarrow 1\pi_g$ (v)	6.22	6.21	

	$\pi_u \rightarrow 2\pi_g$	15.51	15.50	
	$\pi_u \rightarrow 3\pi_g$	16.15	16.14	
	$\pi_u \rightarrow 4\pi_g$	16.55	16.54	
$^1\pi_u$	$\pi_u \rightarrow 4\sigma_g$ (3s)	13.51	13.50	13.345
	$\pi_u \rightarrow 5\sigma_g$ (3d)	15.36	15.35	15.24
	$\pi_u \rightarrow 6\sigma_g$ (4s)	15.57	15.56	15.38
	$\pi_u \rightarrow 7\sigma_g$ (4d)	16.11	16.10	16.01
	$\pi_u \rightarrow 8\sigma_g$ (5s)	16.19	16.18	16.06
	$\pi_u \rightarrow 9\sigma_g$ (5d)	16.45	16.44	16.35
	$\pi_u \rightarrow 10\sigma_g$	16.62	16.61	
$^1\pi$	$\pi_u \rightarrow 3\sigma_u$	14.61	14.60	14.38
	$\pi_u \rightarrow 4\sigma_u$	15.81	15.80	
	$\pi_u \rightarrow 5\sigma_u$	16.23	16.22	
	$\pi_u \rightarrow 6\sigma_u$	16.28	16.27	
	$\pi_u \rightarrow 7\sigma_u$	16.51	16.50	
	$\pi_u \rightarrow 8\sigma_u$	16.83	16.82	
$^3\pi_u$	$\pi_u \rightarrow 4\sigma_g$	13.33	13.32	
	$\pi_u \rightarrow 6\sigma_g$	15.56	15.55	
	$\pi_u \rightarrow 7\sigma_g$	16.08	16.07	
	$\pi_u \rightarrow 8\sigma_g$	16.18	16.17	
	$\pi_u \rightarrow 9\sigma_g$	16.42	16.41	
	$\pi_u \rightarrow 10\sigma_g$	16.60	16.59	
$^3\pi_g$	$\pi_u \rightarrow 3\sigma_u$	14.56	14.55	
	$\pi_u \rightarrow 4\sigma_u$	15.80	15.79	
	$\pi_u \rightarrow 5\sigma_u$	16.23	16.22	

	$\pi_u \rightarrow 6\sigma_u$	16.27	16.26	
	$\pi_u \rightarrow 7\sigma_u$	16.51	16.50	
	$\pi_u \rightarrow 8\sigma_u$	16.81	16.80	
$^1\Sigma_g^+$	$3\sigma_g \rightarrow 4\sigma_g$ (3s)	13.81	12.35	12.26
	$3\sigma_g \rightarrow 5\sigma_g$ (3d)	15.44	13.98	
	$3\sigma_g \rightarrow 6\sigma_g$ (4s)	15.67	14.21	
	$3\sigma_g \rightarrow 7\sigma_g$ (4d)	16.20	14.74	
	$3\sigma_g \rightarrow 8\sigma_g$ (5s)	16.28	14.82	
	$3\sigma_g \rightarrow 9\sigma_g$ (5d)	16.56	15.10	
	$3\sigma_g \rightarrow 10\sigma_g$	16.69	15.23	
$^1\Sigma_u^+$	$3\sigma_g \rightarrow 3\sigma_u$ (3p)	14.63	13.17	12.94
	$3\sigma_g \rightarrow 4\sigma_u$ (4p)	15.88	14.42	14.33
	$3\sigma_g \rightarrow 5\sigma_u$ (5p)	16.30	14.84	14.85
	$3\sigma_g \rightarrow 6\sigma_u$	16.36	14.90	
	$3\sigma_g \rightarrow 7\sigma_u$	16.59	15.13	
	$3\sigma_g \rightarrow 8\sigma_u$	16.90	15.44	
$^3\Sigma_g^+$	$3\sigma_g \rightarrow 4\sigma_g$	13.50	12.04	
	$3\sigma_g \rightarrow 5\sigma_g$	15.40	13.94	
	$3\sigma_g \rightarrow 6\sigma_g$	15.60	14.14	
	$3\sigma_g \rightarrow 7\sigma_g$	16.18	14.72	
	$3\sigma_g \rightarrow 8\sigma_g$	16.25	14.79	
	$3\sigma_g \rightarrow 9\sigma_g$	16.52	15.06	
	$3\sigma_g \rightarrow 10\sigma_g$	16.65	15.19	
$^3\Sigma_u^+$	$3\sigma_g \rightarrow 3\sigma_u$	14.53	13.07	
	$3\sigma_g \rightarrow 4\sigma_u$	15.85	14.39	

	$3\sigma_g \rightarrow 5\sigma_u$	16.29	14.83	
	$3\sigma_g \rightarrow 6\sigma_u$	16.34	14.88	
	$3\sigma_g \rightarrow 7\sigma_u$	16.58	15.12	
	$3\sigma_g \rightarrow 8\sigma_u$	16.81	15.35	
$^1\pi_u$	$3\sigma_g \rightarrow 2\pi_u$ (3p)	14.50	13.04	13.21
	$3\sigma_g \rightarrow 3\pi_u$ (4p)	15.87	14.41	14.41
	$3\sigma_g \rightarrow 4\pi_u$ (5p)	16.32	14.86	14.88
	$3\sigma_g \rightarrow 5\pi_u$	16.46	15.00	
$^1\pi_g$	$3\sigma_g \rightarrow 1\pi_g$ (v)	9.70	8.24	
	$3\sigma_g \rightarrow 2\pi_g$	15.62	14.16	
	$3\sigma_g \rightarrow 3\pi_g$	16.25	14.79	
	$3\sigma_g \rightarrow 4\pi_g$	16.65	15.19	
$^3\pi_u$	$3\sigma_g \rightarrow 2\pi_u$	14.46	13.00	
	$3\sigma_g \rightarrow 3\pi_u$	15.85	14.39	
	$3\sigma_g \rightarrow 4\pi_u$	16.31	14.85	
	$3\sigma_g \rightarrow 5\pi_u$	16.44	14.98	
$^3\pi_g$	$3\sigma_g \rightarrow 1\pi_g$(v)	7.78	6.32	
	$3\sigma_g \rightarrow 2\pi_g$	15.61	14.15	
	$3\sigma_g \rightarrow 3\pi_g$	16.24	14.78	
	$3\sigma_g \rightarrow 4\pi_g$	16.64	15.18	

---

[a] Experimental data is taken from References 46, 47, 56 and 57.

FIGURE CAPTIONS

Fig. 1 — Electron impact energy loss spectrum of H_2O at 53 eV incident energy at a scattering angle of 20°. Ref. 23.

Fig. 2 — Electron impact energy loss spectrum of O_2. Refs. 35, 36, 38a.

Fig. 3 — Differential cross section of O_2 as a function of scattering angle for impact of 20 eV electrons. Ref. 36.

Fig. 4 — Differential cross section of O_2 as a function of scattering angle for impact of 45 eV electrons. Ref. 36.

Fig. 5 — Electron impact energy loss spectrum for CO at 20 eV with a 20° scattering angle. Ref. 42.

Fig. 6 — Electron impact energy loss spectrum for N_2 at 40 eV with a 10° scattering angle. Ref. 49.

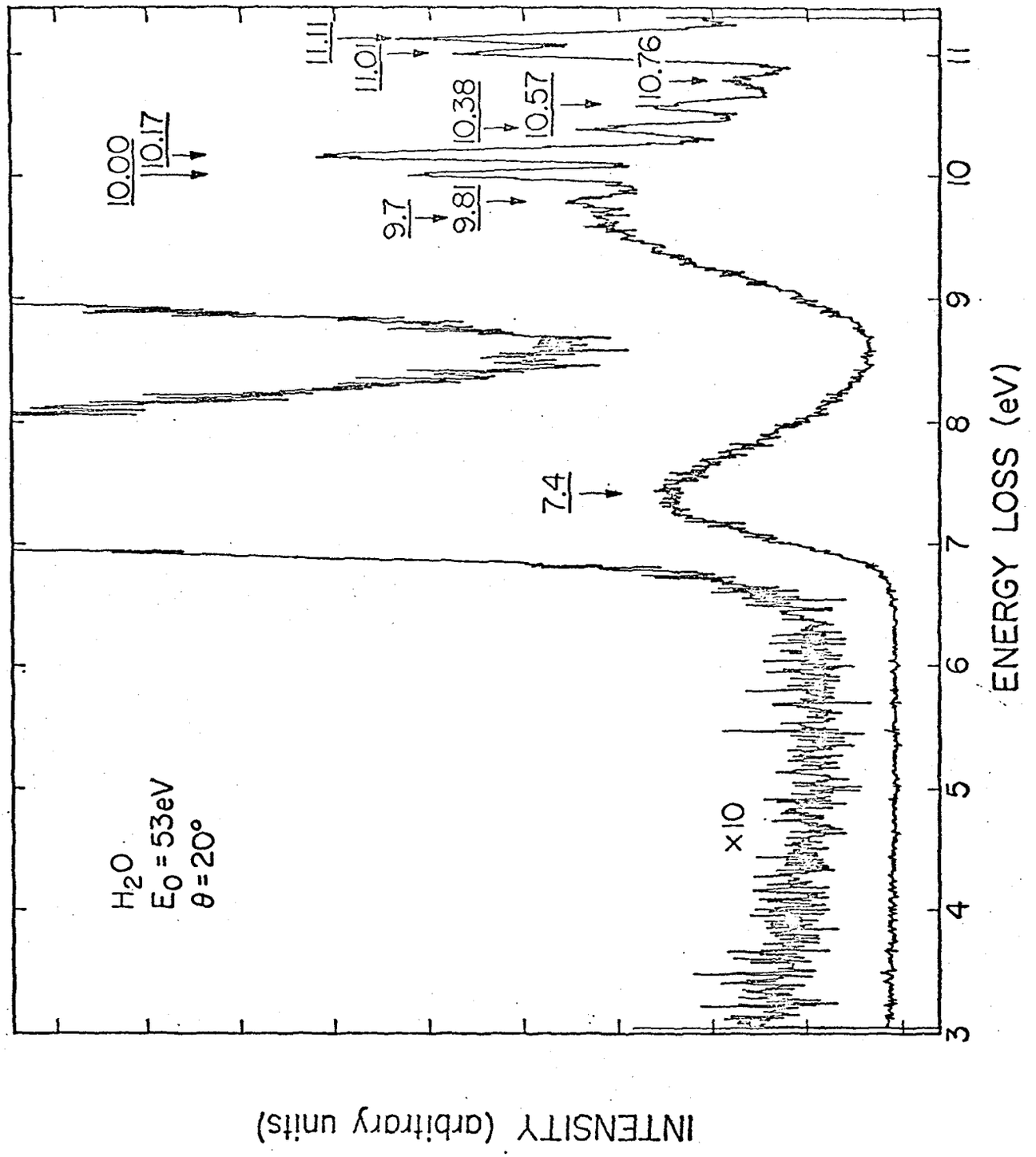
INTENSITY (arbitrary units)
ENERGY LOSS (eV)
3
4
5
6
7
8
9
10
11
H_2O
$E_0 = 53eV$
$\theta = 20°$
×10
7.4
9.7
9.81
10.00
10.17
10.38
10.57
10.76
11.01
11.11

ELECTRON IMPACT SPECTRUM OF O_2

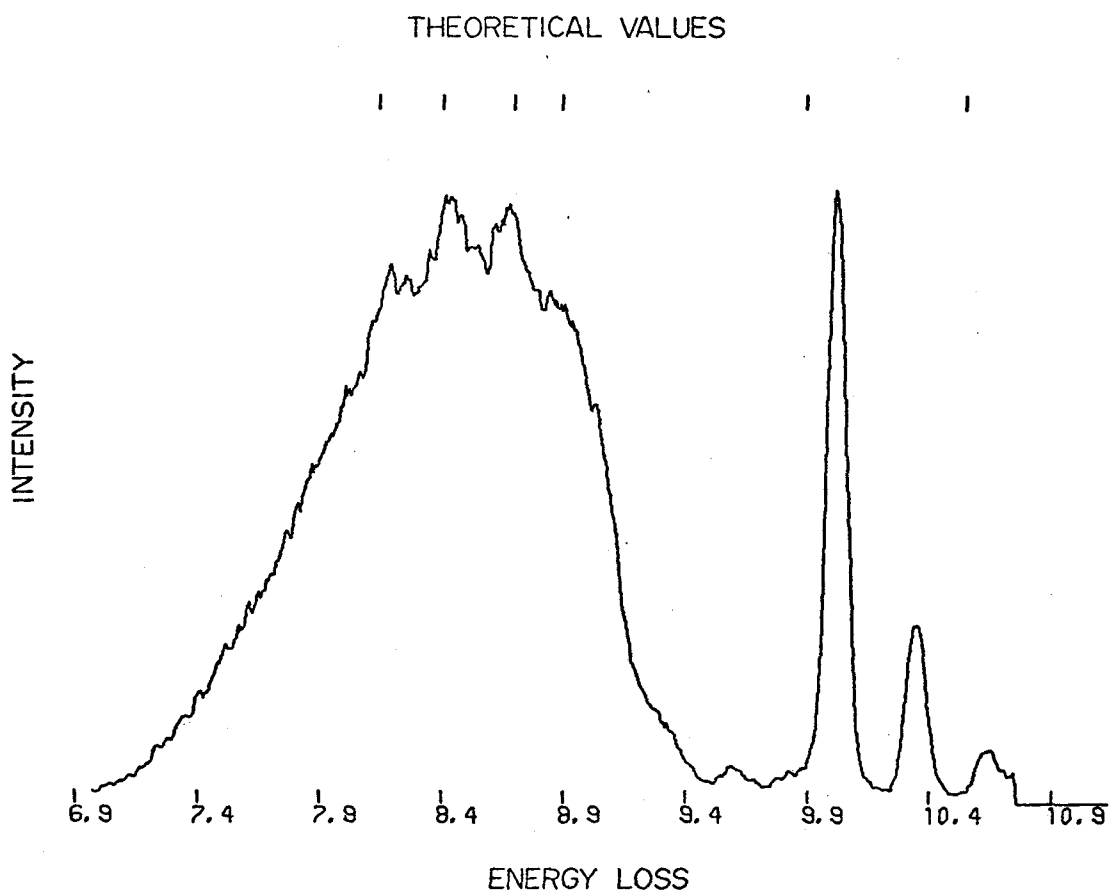

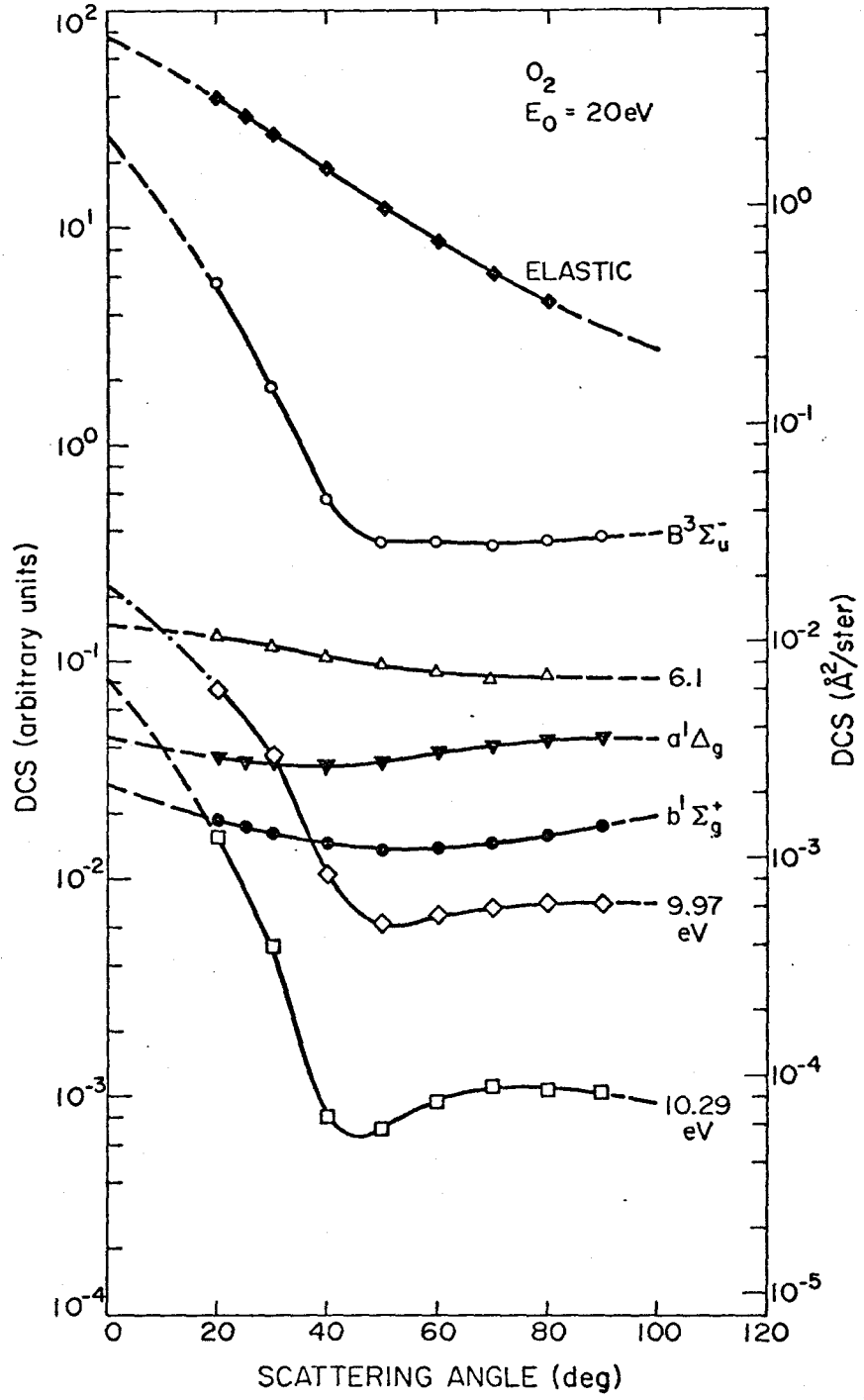
O_2
E_0 = 20eV
ELASTIC
$B^3\Sigma_u^-$
6.1
$a^1\Delta_g$
$b^1\Sigma_g^+$
9.97 eV
10.29 eV
DCS (arbitrary units)
DCS (Å²/ster)
SCATTERING ANGLE (deg)
0
20
40
60
80
100
120
10^2
10^1
10^0
10^{-1}
10^{-2}
10^{-3}
10^{-4}
10^0
10^{-1}
10^{-2}
10^{-3}
10^{-4}
10^{-5}

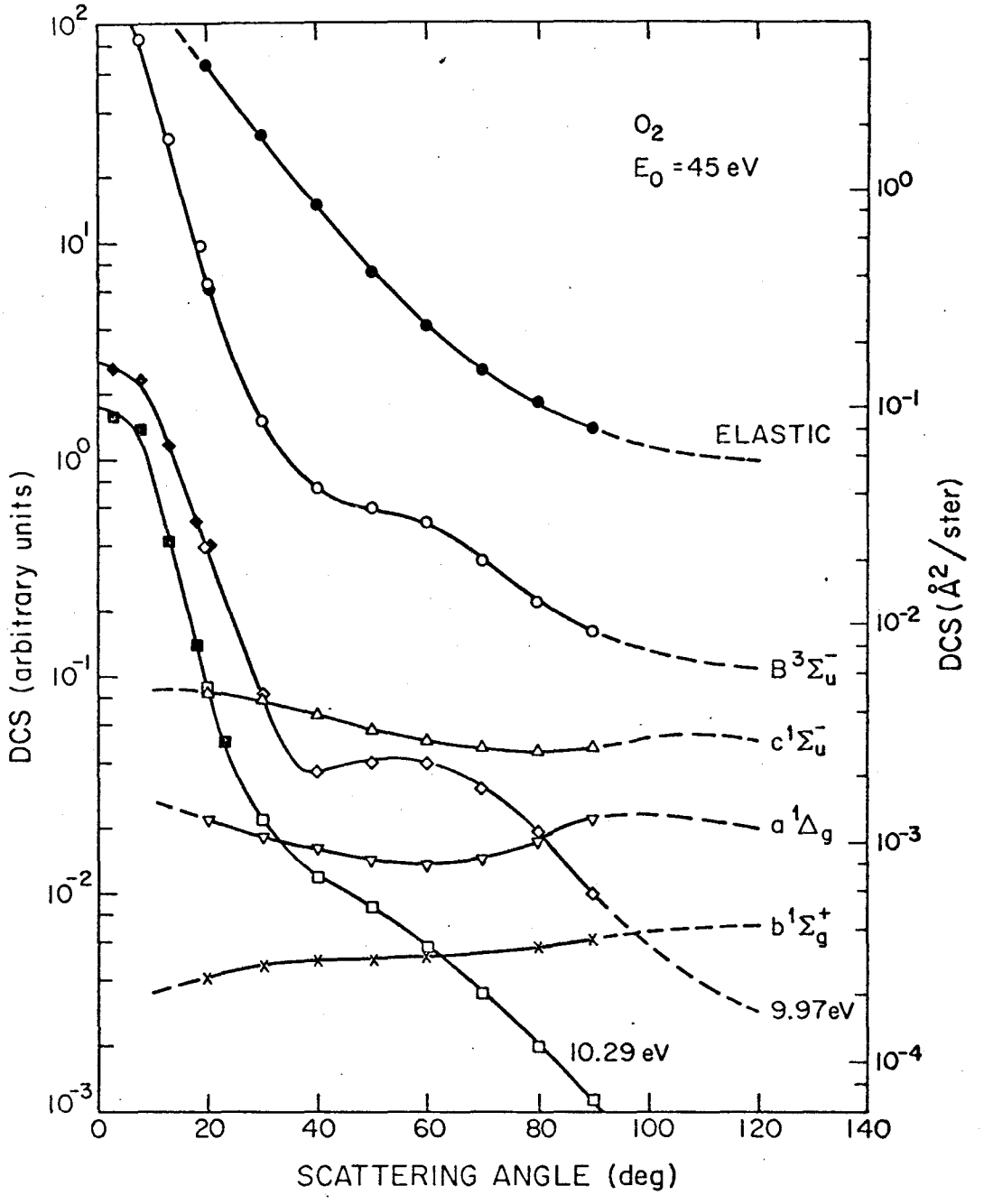
O_2
E_0 = 45 eV
ELASTIC
$B^3\Sigma_u^-$
$c^1\Sigma_u^-$
$a^1\Delta_g$
$b^1\Sigma_g^+$
9.97eV
10.29 eV
DCS (arbitrary units)
DCS (Å²/ster)
SCATTERING ANGLE (deg)
10^2
10^1
10^0
10^{-1}
10^{-2}
10^{-3}
10^0
10^{-1}
10^{-2}
10^{-3}
10^{-4}
0
20
40
60
80
100
120
140

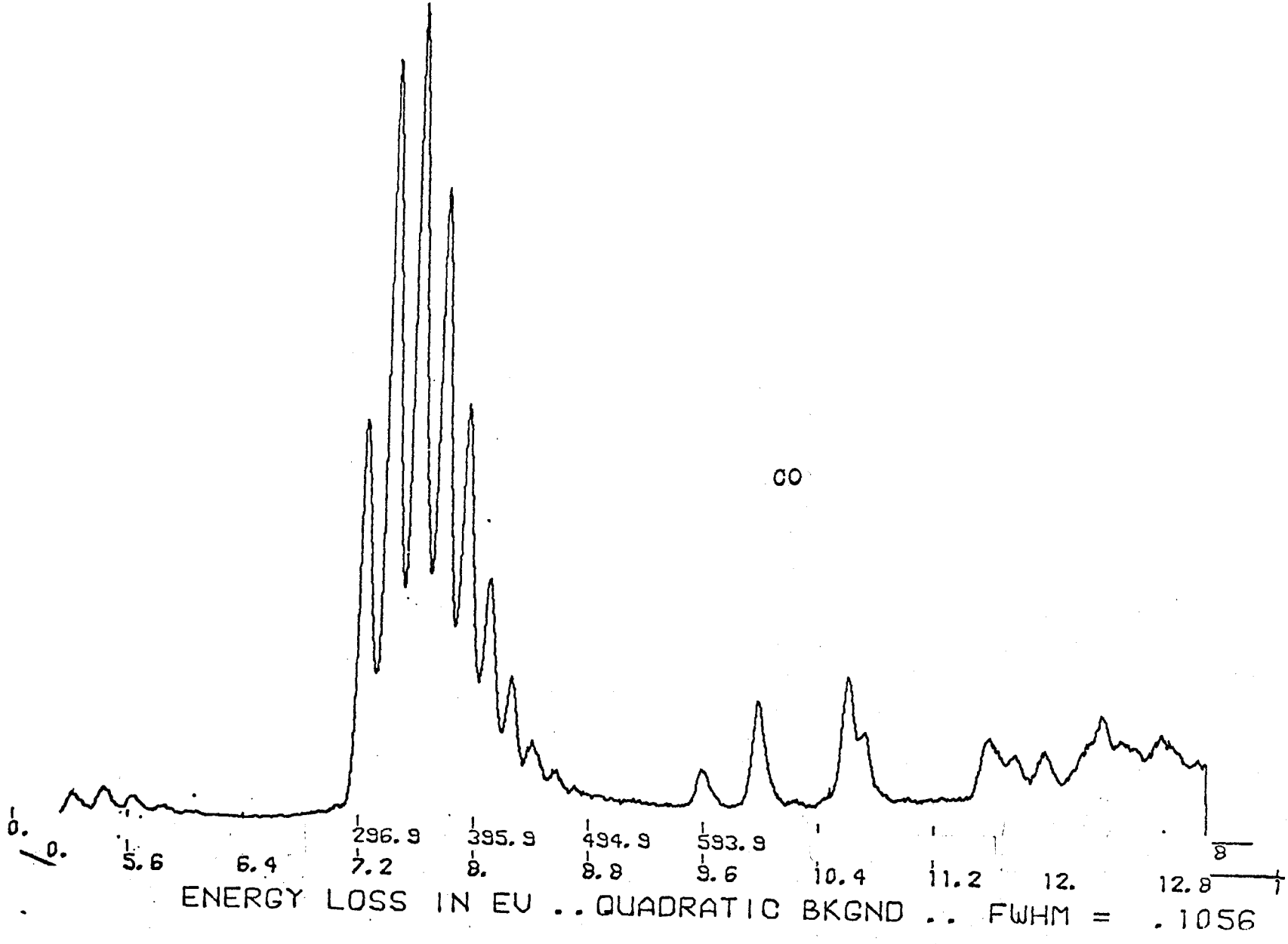
CO
0.
0.
5.6
6.4
7.2
8.
8.8
9.6
10.4
11.2
12.
12.8
296.9
395.9
494.9
593.9
8
ENERGY LOSS IN EV .. QUADRATIC BKGND .. FWHM = .1056

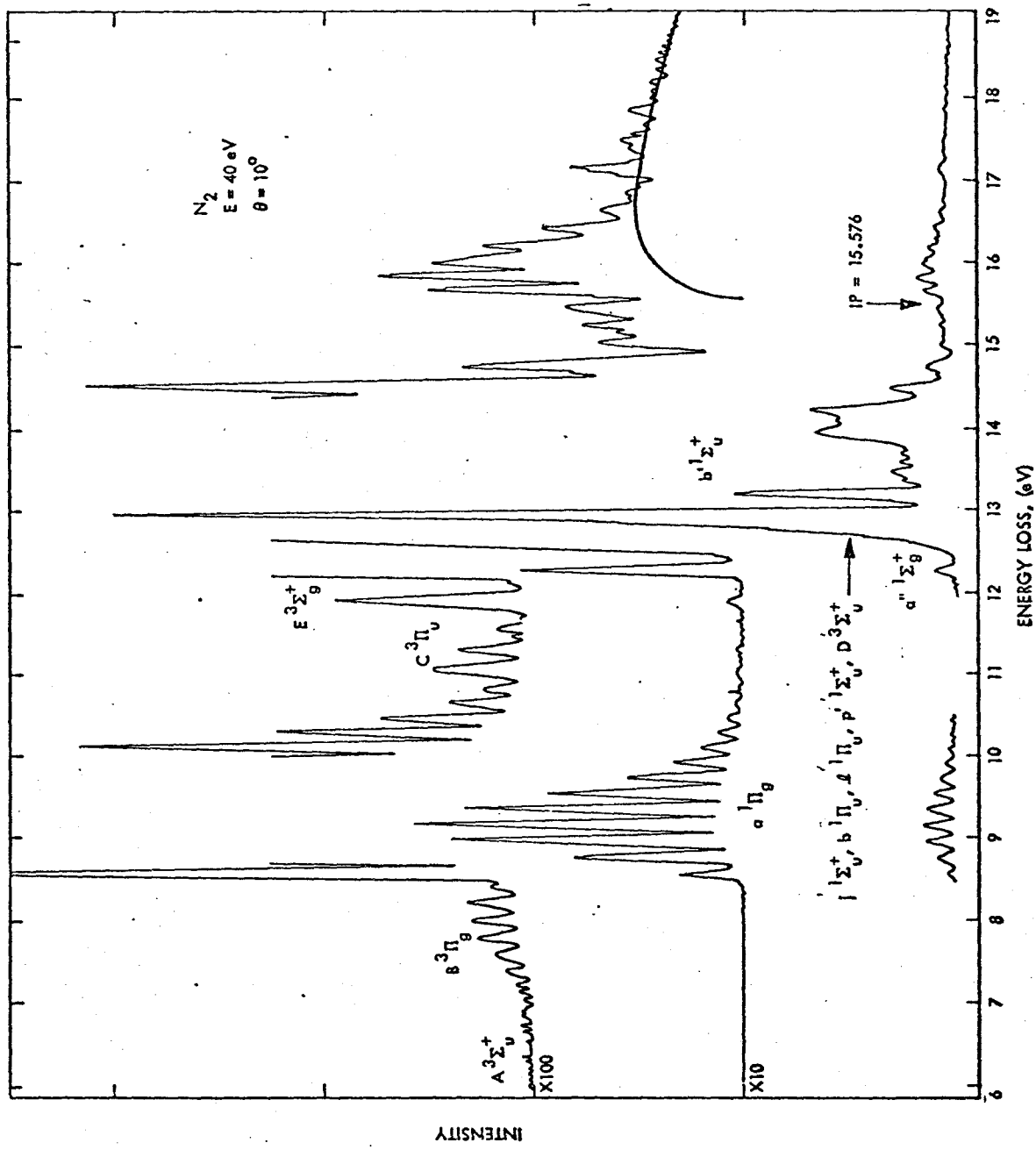
N_2
E = 40 eV
θ = 10°
IP = 15.576
$A^3\Sigma_u^+$
$B^3\Pi_g$
$E^3\Sigma_g^+$
$C^3\Pi_u$
$a\,^1\Pi_g$
$b'^1\Sigma_u^+$
$i\,^1\Sigma_u^+, b\,^1\Pi_u, A'^1\Pi_u, p'^1\Sigma_u^+, D^3\Sigma_u^+$
$a''^1\Sigma_g^+$
X100
X10
INTENSITY
ENERGY LOSS, (eV)

PART II

An Investigation of the N, T, and V States of Ethylene

I. INTRODUCTION

The ethylene molecule has traditionally served as a model for larger conjugated and aromatic hydrocarbons. Its absorption spectrum has provided a test case for many theoretical approaches.[1] Most of the interest in ethylene has centered on the triplet state, denoted T,[2] and the singlet state, denoted V. These states have been described as involving a $\pi \rightarrow \pi^*$ orbital excitation from the ground state, denoted N. The energy relationship between these three states provides the basic empirical information for most semi-empirical π-electron theories.[1]

However, ab initio calculations[2-9] have performed poorly in accounting for the observed absorption maxima in the spectrum. The usual result is that the excitation energy for the V state is overestimated by several eV. For example, the minimum basis set calculation by Kaldor and Shavitt[8] gives 13.2 eV for the vertical excitation energy of the N → V transition in contrast to the experimental value[1] of 7.6 eV.[10] The calculated value of 4.5 eV for the N → T transition agrees well with the experimental value of 4.6 eV.[11, 12] A calculation by Schulman et al.[6] using a larger basis set predicted values of 4.2 eV and 9.3 eV in better agreement with experiment. Even this calculation left much to be desired, however.

An earlier calculation by Huzinaga[13] predicted values of 4.4 and 7.3 eV, in excellent agreement with experiment. This calculation optimized the size of the π^* orbital, a feature not included in previous calculations. The result of this optimization was that the π^* orbital for the V state was much larger in extent than the

π^* orbital for the T state. The calculated ionization potential was, however, 2 eV below the experimental value. The calculation by Huzinaga was apparently ignored by other workers, since it involved only the π electrons. All electron Hartree-Fock calculations by Dunning, Hunt, and Goddard[14] later demonstrated a similar result. In this work the π^* orbitals for the T and V states were very different, having expectation values of $\langle X^2 \rangle$ of 2.7 and 42.1 atomic units. The conclusion reached in this work was that the Hartree-Fock description of C_2H_4 required a more expanded basis set than formerly used; previous predictions of much higher excitation energies for the V state were primarily a result of restrictions in the basis set used. Employing a flexible basis set led to a prediction of 4.22 eV and 8.28 eV for the T and V state excitation energies.

Traditional ideas[1] about the V state had suggested that it did not involve an expanded or Rydberg orbital. Experiments[4,5,15] on the absorption spectrum of C_2H_4 in liquid or solid rare gases or in nitrogen gas at high pressure suggested that the V state was not an expanded or Rydberg state. Under these experimental conditions the N $\rightarrow$ V transition was little affected (as valence states usually behaved[16]) rather than shifted to much higher energy as is the case for Rydberg states.[16] A later theoretical study by Basch and McKoy[17] asserted that the extended π^* orbital was an artifact of the H-F method.

Recently Buenker, Peyerimhoff and Kammer[18] made a study of excited states of C_2H_4 in which they suggested that the vertical transition energy may not correspond to the experimental absorption maximum. They noted that a strong dependence of the electronic transition moment on molecular geometry would cause this deviation from the Franck-Condon principle. A more recent paper by Buenker, Peyerimhoff and Hsu[19] suggests that a transition to a 3p Rydberg state which is not dipole allowed for planar C_2H_4 plays an important role for transitions to non-planar ethylene.

The present work was undertaken to achieve several goals. First the value of the rotational barrier for the ground state N and the relative position of the T state potential were needed for a better understanding of cis-trans isomerization processes.[20]

The second goal was a improved description of the V state and its potential surface. We wished to explain not just the vertical excitation energy and the form of the V state wavefunction for the planar molecule but to show what vibrational modes were important in the observed spectra.

II. COORDINATE SYSTEM AND NOTATION

For planar ethylene we adopt the convention of Merer and Mulliken[3] that the z axis passes through both carbon atoms and that the x axis is perpendicular to the molecular plane. The π orbital ϕ_π has the form

$$\phi_\pi \approx p_{xA} + p_{xB}$$

where p_{xA} is a p function on carbon A and belongs to the symmetry type b_{3u}. The symmetries of various orbitals and states of planar ethylene are shown in Table I.

When the CH_2 groups are twisted with respect to each other, the inversion symmetry is lost and b_{2u} and b_{2g} belong to the same symmetry type b_2. At a twist angle of 90° (perpendicular CH_2 groups) the symmetry types b_2 and b_3 merge to form an e two-dimensional irreducible representation of the point group D_{2d}. In the following we discuss three orbitals, π, π^*, and 3pCH. As shown above, the π orbital for planar ethylene is a plus combination of p functions on each center. For twisted ethylene we designate π orbitals to be plus combinations of two p functions, each perpendicular to the CH_2 group on which it is centered. The π^* orbital involves a minus combination of the same p orbitals. The 3pCH orbital is a plus combination of p orbitals in the CH_2 planes. The notation 3pCH indicates that this orbital is actually a 3p Rydberg orbital, while CH indicates that the orbital extends beyond the CH bonds in the CH_2 plane.

The geometry of the CH_2 groups was kept fixed with the HCH angle at 120° and the C-H distance at 1.07 Å. For the ground state equilibrium geometry a C-C distance of 1.35 Å was used. These values were used in several previous calculations.[6,7] Three kinds of geometry changes were explored: C-C stretching, twisting the CH_2 groups relative to each other, and wagging one

or both CH_2 groups. In the latter motion the hydrogen atoms on one end are rotated about an axis which is parallel to the H-H line and passes through the carbon atom.

III. EXPERIMENTAL INFORMATION

The observed optical absorption from both the N → T and N → V states shows a long progression of bands.[3, 11, 12] Since the N → T transition is spin forbidden, less information has been obtained about these bands. However, the intervals between the N → T bands, about 990 cm^{-1}, are now generally accepted to be due to internal rotation of the CH_2 groups about the C-C bond.[3] The minimum for the T state curve occurs for perpendicular CH_2 groups. A recent estimate[3] places this minimum about 57 kcal/mole above the planar N state energy. Since the N and T states both have a H-F configuration $\cdots(2e)^2$ at the perpendicular geometry, Hund's rule suggests that the T state will lie below the N state. The distance between the two curves at this geometry may determine the role of the T state in photosensitized isomerization reactions.[20]

The progression of bands for the N → V transitions has been shown by McDiarmid and Charney[21] to be about 800 cm^{-1} for C_2H_4 and 550 cm^{-1} for C_2D_4. This isotope ratio, about 1.45, is very close to the ratio $\sqrt{2}$ expected for a twisting frequency. Using a simple harmonic potential for each state, McDiarmid and Charney[21] achieve a good description of the overall band structure in terms

of only a twisting motion. The differences between the spectra of C_2H_4 and C_2D_4 are not adequately reproduced by this simple model.

Wilkinson and Mulliken,[23] using the resemblance between the N → V bands and the $^3\Sigma_g^- \rightarrow {}^3\Sigma_u^-$ Schumann-Runge bands of O_2, explained the C_2H_4 bands in terms of C-C bond stretching. A later discussion by Merer and Mulliken[3] revises the model to one involving coupled twisting and C-C bond stretching. In both papers the relation[24] for bond stretching modes was used to estimate the

$$r_0^{2.88}\omega_0 = \text{constant}$$

optimum C-C bond length, $r_0 = 1.80$ Å, for the planar V state, although the vibrational frequency ω_0 certainly involves some twisting motion. The fact that O_2 is isoelectronic with C_2H_4 is also employed.[3] The H-F configuration for the planar V state is shown to correspond formally to the configuration $(1\pi_u)^3(1\pi_g)^3$ of the $^3\Sigma_u^-$ state of O_2.[25] However, the analogy between the two molecules is not close, since the ground states have different spin multiplicities. Very simple calculations on the perpendicular V state made by Mulliken[26] were used to estimate a value of 1.44 Å for the C-C bond length in the perpendicular V state.

The estimates discussed above suggested that the twisting motion would be coupled to a C-C stretching motion.[3] Calculations were made by Merer and Mulliken[3] using a model potential surface. The resulting Franck-Condon factors lead to qualitative agreement with experiment. The difference between the C_2H_4 and

C_2D_4 spectra is accounted for adequately. However, the calculations did not check the assumption that C-C bond stretch was important.

Ogilvie[27] proposed that wagging of the CH_2 groups was responsible for the entire vibrational structure. Merer and Mulliken[3] emphasized that this explanation is quite unsatisfactory. However, wagging might play a minor role in the spectra. For example, a combination of wagging and twisting might satisfactorily explain the observed vibrational structure. We conclude that the interpretation of the experimental information is at present not settled. It appears likely that several plausible models might be proposed.

IV. CALCULATIONS

The calculations all used a double zeta basis of contracted Gaussian functions augmented by two low exponent Gaussian p functions with exponents of 0.027 and 0.0084. For planar ethylene these p functions were added to each atom in the x direction. For all other geometries both p_y and p_x functions were added on each atom. The double zeta basis was constructed by contracting the 7 s function Gaussian basis of Whitman and Hornback[28] to give four s-type basis functions on each carbon. The 3 p function set was used to construct 2 p functions in each direction. The 3 s function expansion of Huzinaga[29] for hydrogen was scaled with an effective Slater exponent of 1.2 and

contracted to give 2 s basis functions. The ideas discussed by Dunning[30] were used in producing the contracted basis set.

The vertical excitation energies for the T and V states calculated using H-F wavefunctions for N, T and V states in this basis differed from the value reported previously with a larger basis set by less than 0.1 eV. The calculated difference between the V state energies for planar and perpendicular ethylenes was equally close in the two basis sets. This justifies using the smaller basis set even though considerably higher total energies are calculated. Calculations were run using the integral evaluation routines from the Polyatom system of programs, as modified by Basch et al.[31] All SCF calculations were made with programs developed by the author. A configuration interaction (CI) program written by P. J. Hay was used in the CI calculations.

V. CALCULATIONS ON THE N AND T STATES

One objective of the present work was an accurate calculation of the rotational barrier for the N state. Previous studies[7-9] have shown that a two configuration wavefunction involving the H-F term (SIGMA)$(\pi)^2$ and the additional term (SIGMA)$(\pi^*)^2$ is necessary to give a consistent description of the ground state for this process. In fact the two terms become equally important for a twist angle of 90°. In these earlier calculations[7-9] a 2 × 2 configuration interaction calculation was carried out using the occupied π and unoccupied π^* orbitals from a Hartree-Fock calculation of the usual

type. Using a minimum basis set of Slater functions, Kaldor and Shavitt[8] calculated a rotational barrier of 83 kcal/mole with the two configuration wavefunction. Buenker,[9] using the fixed group Gaussian lobe basis of Whitten,[32] calculated barrier heights of 126 and 83 kcal/mole for the Hartree-Fock and two configuration wavefunctions. The agreement of the two calculations is reasonable in that the basis set used by Buenker[9] is only slightly more flexible than the minimum basis set of Kaldor and Shavitt.[8] In our calculation the orbitals in the two configuration wavefunction were optimized at each geometry. This more consistent procedure plus the use of a more flexible basis gave an improved value of 67.3 kcal/mole for the barrier height. This is in good agreement with the experimental activation energy of 65 kcal/mole found for cis-trans isomerization of 1, 2 dideutero ethylene.[33] The optimum C-C bond length at the saddle point is found to be 1.43 Å.

A large number of calculations[4-9, 13, 14, 17-19] have been reported for the T state. In most cases the calculated vertical excitation energies are in good agreement with experiment if the two-term N state wavefunction is used with the H-F wavefunction for the T state. For example, in our study using the H-F energy for each state gives an N → T excitation energy of 3.44 eV, while using the two-term N state energy gives 4.24 eV in good agreement with the experimental value of 4.6 eV. The energy for the perpendicular ethylene geometry has a minimum 65.9 kcal/mole above the planar ethylene N state for a bond length of 1.43 Å. Thus

for perpendicular ethylene only 1.4 kcal/mole separates the N and T states.

In Table II we give the calculated energy for the N and T states as a function of twist angle. The 0° angle corresponds to a C-C bond length of 1.35 Å, while the other points refer to a bond length of 1.41 Å. The 0° point is to be used as the equilibrium geometry for the N state. Table III contains the N and T state energies as a function of C-C distance for a twist angle of 90°. Finally in Table IV we summarize results from several references for the rotational barrier in the N state and for the vertical and adiabatic excitation energies of the T state.

VI. SCF CALCULATIONS ON THE V STATE

Several groups of calculations have been run for the V state of C_2H_4. In the first set the energy of the open shell H-F wavefunction for this state was calculated as a function of C-C distance for a planar molecule. These results are given in Table V. The optimum distance is 1.41 Å, which is in agreement with the results of larger basis set calculations by Basch and McKoy.[17] Next with a bond distance of 1.41 Å open shell H-F calculations were carried out for twisted C_2H_4 with angles (θ) of 30°, 60°, and 90°. These results are listed in Table III. As expected, the energy of the V state is lowest at 90°. As pointed out recently by Buenker et al.,[19] the state R(3pCH) from the (sigma)(π)(3pCH) configuration is of the same symmetry, $^1B_1$, as the (sigma)(π)(π^*) configuration for twisted

ethylene. For planar ethylene the 3pCH orbital is $2b_{2u}$ and the state R(3pCH) is $^1B_{1g}$. Thus the transition moment for the dipole operator is zero for 0°. For twisted ethylene at 30° we find that the lowest $^1B_1$ SCF solution involves the 3pCH orbital. The second state uses the π^* orbital. We show contour plots of these orbitals and the π orbital[34] in Fig. 2. The plane used for these plots passes through the two hydrogen atoms in a CH_2 group and is perpendicular to the C-C axis. The in-plane hydrogen atoms are marked with crosses, while the position of the hydrogen atoms below the plane at the other end of the molecule are indicated by circled crosses. The π and π^* orbitals are perpendicular to the CH_2 plane, while the 3pCH orbital is in the CH_2 plane. At θ = 60° the lowest solution involves the π^* orbital, while the second solution R(3pCH) involves the 3pCH orbital. Contour plots of these orbitals are also shown in Fig. 2. From these plots we see that the π^* orbital is quite Rydberg-like at 30° but is much more valence-like at 60°. The eigenvalue of the π^* orbital changes correspondingly from -0.06 hartree at 30° to -0.12 hartree at 60°.

In the next stage of calculations the optimum C-C bond distance for the V state at 90° was calculated to be 1.35 Å. This series of calculations is reported in Table III under the name V state (D_{2d}). Each H-F orbital was required to transform according to a particular irreducible representation of the point group D_{2d}.

Another series of calculations investigated geometries involving wagging one or both CH_2 groups. The twist angle was

fixed at 90° and the C-C bond length at 1.35 Å. Since a geometry which involved wagging both ends by 30° produced a higher energy for the V state, this mode was abandoned. Wagging only one end increased the N and T state energies but lowered the V state energy.[35] The optimum wagging angle was found to be beyond 30°. The energies obtained in this set of calculations are given in Table IV. We note that these energies are much lower than those for the V state (D_{2d}) energies of Table III. Extrapolation of these energies back to a wagging angle of 0° produces a much lower energy than the V state (D_{2d}) energy at 1.35 Å. In fact if the calculation for 0° wagging angle does not require the orbitals to transform as irreducible representations of the group D_{2d}, a solution is found with an energy of -77.73080. In this solution a doubly occupied $p\pi$ orbital is localized on the "wagged" end of the molecule. This orbital has a dipole moment (measured from the midpoint of the C-C bond) of 1.25 a.u. This would predict a molecular dipole moment of 2.5 a.u., since the orbital is doubly occupied, but polarization of the sigma orbitals reduces the total dipole moment to 1.5 a.u. The normal V state (D_{2d}) wavefunction involved a sum of C^-–C^+ and C^+–C^- terms. But since the sigma orbitals experienced only a symmetric average potential from the pi orbitals, they were unable to polarize in the opposite direction to reduce the ionic character. In terms of the D_{2d} symmetry functions this back polarization by sigma orbitals is a correlation effect involving double replacement configurations of the form $\sigma^2\pi\pi^* \rightarrow \sigma\sigma^*\pi^2$ and $\sigma\sigma^*\pi^{*2}$.

Using the low symmetry type solution, the behavior of the energy as a function of C-C bond length was investigated. A minimum was found at 1.41 Å using the energies shown in Table III under the title V(low-sym).

VII. CI CALCULATIONS ON THE V STATE

The results of these H-F calculations suggested that σ-π correlation terms might be important in the description of ionic states such as the V state. The inclusion of such terms might lead to a significant contraction of the π^* orbital. Several configuration interaction (CI) calculations were made to investigate the importance of these terms. Because of limitations in the capabilities of the CI program, the calculations had to be fairly small in size. From the arguments below and from the results of a few more extensive test cases,[37] we concluded that a four electron CI calculation on the two electrons from the sigma bond and the two pi electrons would best answer the current need. The justification for this type of calculation and the procedure used in the calculation are described below.

The C-C bond orbital may polarize without removing charge from the bond region. In contrast, polarization of the CH bonds requires charge transfer from one bond to another and is expected to be less important. Further, we felt that polarization of the C-C bond could be adequately described by use of one additional basis function in a CI calculation, an anti-bonding C-C orbital

localized in the bond region. In order to find a suitable C-C antibonding orbital we carried out a generalized valence bond (GVB) calculation[37] on C_2H_4. In this calculation the C-C bond is described by a two-electron wavefunction $\Omega(1, 2)$ of the form

$$\Omega_i(1, 2) = [C_1\phi_1(1)\phi_1(2) - C_2\phi_2(1)\phi_2(2)] \times$$

$$[\alpha(1)\beta(2) - \beta(1)\alpha(2)]$$

where $\phi_1(1)$ and $\phi_2(1)$ are bonding and anti-bonding orbitals and $\alpha(1)$ and $\beta(1)$ are the usual spin functions. This two-electron function replaces the doubly occupied orbital ϕ_i in the H-F wavefunction. The coefficients C_1 and C_2 are optimized in the calculation.

Since we were seeking a valence-like V state wavefunction, we used an SCF calculation[38] on a valence state as the starting point. Calculations were carried out for twist angles of 0°, 30°, 60°, and 90°. The 0° calculation involved a C-C bond length of 1.35 Å, while a bond length of 1.41 Å was used for calculations at the other twist angles. The GVB orbitals σ_{CC}, σ^*_{CC}, π and π^* were calculated for the triplet (T) state at 0°, 30°, and 60°. Since the π^* for the singlet is different from that for the triplet, we also used the unoccupied orbitals of the same symmetry as the π^* orbital in the CI calculation to permit optimum adjustment of this orbital in the CI calculation. Thus for the V state the CI calculation included the configurations

TYPE I. $\sigma^2\pi\pi^*$

II. $\sigma^2\pi V$

III. $\sigma\sigma^*\pi^2$

IV. $\sigma\sigma^*\pi^{*2}$

where V is a virtual orbital of the same symmetry as the π^* orbital. The type II terms change the shape of the π^* orbital, while terms of type III and IV permit polarization of the sigma orbitals. For consistency a calculation was run on the N state using terms of the form

$\sigma^2\pi^2$

$\sigma^2\pi^{*2}$

$\sigma^{*2}\pi^2$

$\sigma^{*2}\pi^{*2}$

$\sigma\sigma^*\pi\pi^*$

For the 90° twist angle the orbitals for the CI calculation were taken from a GVB calculation on the V state, since the V state is valence-like at this geometry. Since the π and π^* orbitals were optimized for the V state, inclusion of virtual orbitals of π or π^* was not considered to be important.

Results from the CI calculations are shown in Table VI. The total energy of the N, T and V states is given as well as the height (in eV) above the energy obtained for the N state at 0°. We note first that the energy obtained for the CI wavefunction is higher at 0° than the H-F energy (Table II). This indicates that SCF

rearrangement effects on the sigma orbitals are about as important as the correlation effects included in the CI wavefunction. A calculation was also run using only terms of types I and II as an approximation to the H-F wavefunction for the V state. From the two CI calculations we see that the energy is lowered 0.66 eV by the inclusion of correlation terms. In addition, as shown in Table VII, the expectation values of x^2, y^2 and z^2 for the four-electron wavefunction are considerably smaller when correlation terms are present. Another interesting point is that the transition moment for the N → V transition is increased by addition of correlation terms as shown in Table VIII.

Careful examination of the CI solutions for 30° shows that the lowest solution (of $^1B_1$ symmetry) involves a π^* orbital, while the second involves a 3pCH orbital. The wavefunction $(SIGMA)^2(\pi)$-(3pCH) is $^1B_{1g}$ at 0° and has a zero dipole transition moment with the N state. Thus at 30° and 60° the second solution has a small transition moment with the N state as expected. The inversion of the two solutions at 30° relative to the H-F results is caused by two factors. The correlation terms are far more important for the π^* orbital state than for the 3pCH* orbital state. In addition, the sigma orbitals from the triplet state are probably more nearly optimum for the $\pi\pi^*$ state than for the R(3pCH) state. However, from both calculations it is clear that an avoided crossing between the R(3pCH) state with a small transition moment for all twist

angles and the π^* orbital state with a large transition moment takes place between 0° and 60°.

For 90° the CI energy is slightly below the energy from the low-symmetry H-F wavefunction. Thus the CI calculation is probably including the polarization of the sigma orbitals.

In summary, the CI calculations predict a vertical excitation energy of 8.9 eV and an energy for the V state at 90° about 6.8 eV above the 0° N state. Expectation values of x^2, y^2 and z^2 for the V state at 0° indicate that the CI wavefunction is still significantly more expanded in space than either the N or T state wavefunctions. The transition moment for the $\pi \rightarrow$ 3pCH state is quite small, while the moment for the $\pi \rightarrow \pi^*$ state is slowly varying over the range θ = 0 to 60°.

VIII. DISCUSSION

Basch and McKoy[17] have asserted that the results produced by the Hartree-Fock calculation are artifactual and that a valence-like solution is produced by the RPA[40] approach. However, later calculations using improved RPA methods[41] give 9.3 eV for the vertical excitation energy rather than 7.6-8.5 eV as reported by Basch and McKoy.[17]

Buenker et al.[18] have recently studied the excited states of C_2H_4 using SCF calculations followed by limited CI calculations. However, for the $^1B_{1u}$ V state, their calculation actually included only correlation between the two pi electrons. Earlier work by

Dunning et al.[14] showed these terms to be unimportant for the V state. For the ground state the effect of CI for the pi electrons is equivalent to using the two-configuration wavefunction described above in Section IV. In a later paper Buenker, Peyerimhoff and Hsu[19] interpret the spectra in terms of the R(3pCH) state producing a strong dependence of the transition moment on twist angle. With this view the maximum in the absorption spectrum might correspond to non-vertical transitions. However, we find the transition moment of the R(3pCH) state to be so weak that this state is not important in the absorption spectra. The transition moment for the $\pi \rightarrow \pi^*$ state is a relatively constant function of the twist angle until θ is greater than 60°.

Although the arguments presented by Buenker et al.[19] are unconvincing, the idea that the maximum in the absorption spectra corresponds to a non-vertical excitation is very attractive. The CI calculations performed gave a vertical excitation energy of 8.9 eV. Earlier calculations indicated that SCF readjustment of the sigma core was responsible for an energy gain of about 0.6 eV. Using these figures we estimate that a CI calculation starting from the V state SCF orbitals would give a vertical excitation energy of 8.3 eV. Our conclusion is that no appropriate excited state will be found with a vertical excitation energy of 7.6 eV.

There is an alternate explanation for the maximum absorption corresponding to a non-vertical transition. The usual application of the Franck-Condon principle[42] is to curves such as that

shown in Fig. 2. The vertical excitation energy is the vertical distance from the bottom of the ground state curve to the upper curve. The upper state vibrational wavefunction with the largest overlap with the ground state's lowest vibrational level ($\nu'' = 0$) is the one with a classical turning point near R_e for the ground state. This vibrational function decays smoothly near R_e so that no cancellations occur in the overlap with the $\nu'' = 0$ function. Upper state vibrational functions above the vertical excitational energy oscillate near R_e and suffer cancellations in their overlap with the lower state vibrational function.

However, for a twisting motion the curves shown in Fig. 3 are quite different. The vertical excitation energy corresponds to the top of the upper state curve. Since the vibrational wavefunction at the vertical excitational energy does not have a classical turning point, it would resemble a free rotor wavefunction with high energy. In order to get a smoothly decaying vibrational function, we must go some distance below the top of the barrier. If we are too close to the top of the curve, the vibrational function is energetic enough to oscillate all the way through the barrier. If we are too far below the top, the function decays so fast that no overlap with the lower vibrational function is produced. The distance below the top of the curve which produces the largest Franck-Condon factor is dependent on the details of the two potential curves.

This explanation would be pleasing in several respects. First the inability of ab initio theoretical calculations to predict a vertical excitation energy near 7.6 eV is explained. A value of 8.0 eV might be reasonable with the modified Franck-Condon argument presented here. Also the experiments showing that the V state behaved as a valence state would be compatible with a moderately diffuse or extended electron distribution calculated for the planar V state. The experiments would be showing the valence-like character of a twisted ethylene.

No theoretical evidence has been found in this work for a large change in the optimum C-C bond length between planar and perpendicular ethylene V state, and thus we find no support for the coupled stretching and twisting model of Merer and Mulliken.[3] Some evidence is found for participation in the observed vibrational structure by a wagging mode. This may account for the observed differences between the C_2H_4 and C_2D_4 spectra.

IX. CONCLUSIONS

We have presented several sets of calculations for the N, T, and V states of C_2H_4. From these calculations we obtained a simple explanation of the importance of σ-π correlation terms as polarization of the sigma core by the ionic pi electron system. The CI calculations also suggested that a substantial contraction of the electron distribution results from the σ-π correlation, but that

the V state is still more spatially extended than the N or T states.

The role of a R(3pCH) state in the absorption spectrum was shown to be small. In addition the electronic transition moment for the V state was shown to be nearly constant so that the use of Franck-Condon overlap integrals is appropriate. However, an examination of the Franck-Condon principle for internal rotation potential curves suggests that the maximum absorption intensity may correspond to a non-vertical excitation. This explains several contradictions between theory and experiment.

The explanation of the N → V absorption spectrum we present is rather complex. The vibrational modes responsible for the complex structure observed appear to be twisting and wagging of the CH_2 groups. In addition, the vertical transition energy is probably near 8 eV. The V state wavefunction at the planar geometry is likely to be moderately expanded in comparison to that for the T state. This explanation does rationalize many experimental and theoretical findings, but it suggests that similar states for other unsaturated hydrocarbons may also be difficult to explain in terms of simple models.

REFERENCES

[1]R. G. Parr, Quantum Theory of Molecular Electronic Structure (W. A. Benjamin, Inc., New York, 1964).

[2]The notation of states of ethylene as N, T or V is taken from Reference 3.

[3]A. J. Merer and R. S. Mulliken, Chem. Rev. 69, 639 (1969).

[4]M. B. Robin, R. R. Hart, and N. A. Kuebler, J. Chem. Phys. 44, 1803 (1966).

[5]M. B. Robin, H. Basch, N. A. Kuebler, B. E. Kaplan and J. Meinwald, J. Chem. Phys. 48, 5037 (1968).

[6]J. M. Schulman, J. W Moskowitz and C. Hollister, J. Chem. Phys. 46, 2759 (1967).

[7]J. W. Moskowitz and M. C. Harrison, J. Chem. Phys. 42, 1726 (1964).

[8]U. Kaldor and I. Shavitt, J. Chem. Phys. 48, 191 (1968).

[9]R. Buenker, J. Chem. Phys. 48, 1368 (1968).

[10]M. Zelikoff and K. Watanabe, J. Opt. Soc. Am. 43, 756 (1953).

[11]C. Reid, J. Chem. Phys. 18, 1299 (1950).

[12]D. F. Evans, J. Chem. Soc., p. 1735 (1960).

[13]S. Huzinaga, J. Chem. Phys. 36; 453 (1962).

[14]T. H. Dunning, W. J. Hunt, and W. A. Goddard III, Chem. Phys. Lett. 4, 147 (1969).

[15]E. Miron, B. Raz and J. Jortner, Chem. Phys. Lett. 6, 563 (1970).

[16]S. A. Rice and J. Jortner, J. Chem. Phys. 44, 4470 (1966).

[17]H. Basch and V. McKoy, J. Chem. Phys. 53, 1628 (1970).

[18]R. J. Buenker, S. D. Peyerimhoff and W. E. Kammer, J. Chem. Phys. 53, 814 (1971).

[19]R. J. Buenker, S. D. Peyerimhoff, and H. Hsu, "A New Interpretation for the Structure of the V-N Bands of Ethylene," to be published.

[20]See Reference 3 for a discussion of the role of the triplet state T in isomerization reactions.

[21]R. McDiarmid and E. Charney, J. Chem. Phys. 47, 1517 (1967). Reference 22 contains a further development of the ideas in this paper.

[22]R. McDiarmid, J. Chem. Phys. 50, 1794 (1969).

[23]P. G. Wilkinson and R. S. Mulliken, J. Chem. Phys. 23, 1895 (1955).

[24]This rule has been used to relate the bond length and vibrational frequency in diatomic molecules. The value of 2.88 gives good agreement for O_2 $^3\Sigma_g^-$ and $^3\Sigma_u^-$. This relation was first used by R. M. Badger [Phys. Rev. 35, 1038 (1930)].

[25]In order to get the correspondence we associate two CH bonding orbitals with the π_{uy} and π_{gy} orbitals of O_2.

[26]R. S. Mulliken, Tetrahedron 5, 253 (1959).

[27]J. F. Ogilvie, J. Chem. Phys. 49, 474 (1968).

[28]D. R. Whitman and C. J. Hornback, J. Chem. Phys. 51, 398 (1969).

[29]S. Huzinaga, J. Chem. Phys. 42, 1293 (1965).

[30]T. H. Dunning, J. Chem. Phys. 53, 2823 (1970).

[31](a) "Program Set for Non-empirical Molecular Calculations, POLYATOM," Program QCPE 47.1 of the Quantum Chemistry Program Exchange (QCPE), Indiana University, Bloomington, Ind. (b) H. Basch, M. B. Robin, and N. A. Kuebler, J. Chem. Phys. 47, 1201 (1967).

[32]J. L. Whitten, J. Chem. Phys. 44, 359 (1966).

[33]A. Lifshitz, S. H. Bauer, and E. L. Resler, Jr., J. Chem. Phys. 38, 2056 (1963).

[34]The π orbital was taken from the SCF calculation for the V state $(\pi)(\pi^*)$.

[35]Earlier calculations[36] have arrived at the conclusion that wagging both the CH_2 groups was important for the T and not the V state. This may have been the result of using very small basis sets and approximate methods.

[36](a) L. Burnelle, J. Chem. Phys. 43, 529 (1965). (b) J. Burnelle and C. Litt, Mol. Phys. 9, 433 (1965).

[37]In the test calculations an antibonding orbital was obtained for each bond. All terms, involving any σ and any π^* orbital, of the form $\sigma\sigma^*\pi\pi$ and $\sigma\sigma^*\pi^*\pi^*$ were included. Results were similar to those reported here. The C-C sigma bond orbitals bonding and antibonding played the largest role.

[38]Generalized valence bond wavefunctions are thorougly discussed in Part III of this thesis.

[39]The SCF calculation of GVB orbitals was accomplished with the general SCF program written by the author and P. J. Hay.

[40]T. Shibuya and V. McKoy, Phys. Rev. A2, 2208 (1970).

[41]T. Shibuya and V. McKoy, "Application of the RPA and Higher RPA to the V and T states of Ethylene," to be published.

[42]For an adequate discussion of the Franck-Condon principle for diatomic molecules, see G. Hertzberg, Molecular Spectra and Molecular Structure; Spectra of Diatomic Molecules, (D. Van Nostrand Company, Inc., Princeton, 1950).

TABLE I. Symmetry information for C_2H_4.

Orbital or State	Form[a] ($\theta = 0°$)	Planar (D_{2h})	Twisted $\theta = 45°$ (D_2)	Perpendicular[b] D_{2d}
π	$p_x + p_x$	b_{3u}	b_3	e[c]
π^*	$p_x - p_x$	b_{2g}	b_2	e[c]
3pCH*	$p_y + p_y$	b_{2u}	b_2	e
N	$\cdots(\pi)^2$	$^1A_{1g}$	$^1A_1$	$^1B_2$
T	$\cdots(\pi)(\pi^*)$	$^3B_{1u}$	$^3B_1$	$^3A_2$
V	$\cdots(\pi)(\pi^*)$	$^1B_{1u}$	$^1B_1$	$^1B_1$
	$\cdots(\pi)(3pCH^*)$	$^1B_{1g}$	$^1B_1$	d

[a]As the molecule is twisted, the p_x orbital becomes a P_Q orbital where $Q = x \cos \theta + y \sin \theta$.

[b]The usual notation for D_{2d} is discarded for one consistent with the D_2 and D_{2h} forms.

[c]The π and π^* orbitals become degenerate.

[d]The configuration is (1e)(2e) so that several states result.

TABLE II. Energy of C_2H_4 states as a function of twist angle.

State[a]	Twist Angle 0°[b]	30°[c]	60°[c]	90°[c]
N (2 configuration)	-77.96898[d]	-77.94836	-77.90195	-77.86173
	0.0[e]			
T	-77.81300	-77.83906	-77.85615	-77.86398
	4.24[e]	3.54	3.07	2.86
V	-77.66536	-77.66702	-77.69347	-77.706765
	8.26[e]	8.22	7.50	7.14
R (3pCH)	—	-77.68936	—	—

[a]SCF wavefunctions were used in these calculations.

[b]C-C distance is 1.35 Å.

[c]C-C distance is 1.41 Å.

[d]Total energy in atomic units.

[e]Energy in eV relative to N state energy at 0°.

TABLE III. Energy of ethylene state as a function of C-C bond length

State	Geometry		C-C Distance 1.35	1.38	1.41	1.44	1.50
V	planar	a.u.	-77.66218	-77.66472	-77.66538	-77.66455	——
		eV	8.26 [c]	8.28	8.26	8.28	
V^{a} (D_{2d})	perpendicular		-77.70852	-77.70847	-77.70676	-77.70372	——
			7.09 [c]	7.09	7.14	7.22	
V^{b} (low sym)	perpendicular		-77.73080	-77.73327	-77.73306	-77.73216	——
			6.48 [c]	6.41	6.42	6.44	
N	perpendicular		-77.85299	——	-77.86173	-77.86376	-77.86299
T	perpendicular		-77.8556	——	-77.86398	-77.86587	-77.86505

[a] The orbitals are required to transform according to the point group D_{2d}.

[b] The orbitals are not restricted to be symmetry functions.

[c] Energy relative to the N state 2-configuration energy for planar geometry.

TABLE IV. Results of previous calculations

	Ref. 7[a]	Ref. 8[b]	Ref. 9[a]	Ref. 18	This work SCF[a]	This work CI
N state rotational barrier[c] (kcal)	83	—	83	—	67.3	—
N → T vertical excitation energy[d] (eV)	4.5	4.2	4.5	4.26	4.24	4.34
N-T energy difference ($\theta = 90°$)[c] (kcal)	8.1	—	1.6	—	8.26	1.4
N-V vertical excitation energy[d] (eV)	13.2	9.3	9.8	8.32	8.3	8.84

[a]A two configuration wavefunction was used for the N state.

[b]A Hartree-Fock wavefunction was used for the N state.

[c]Energy given in kcal/mole.

[d]Energy given in eV.

TABLE V. N, T, V State energies as a function of wagging angle.

State	Wagging Angle[a] 0°	15°	22.5°	30°
N	-77.85299	-77.85186	b	-77.84868
T	-77.85556	-77.85474	b	-77.85154
V	-77.73080	-77.3108	-77.73134	-77.73155

[a]One CH_2 group was rotated by the angle given.

[b]Not calculated.

TABLE VI. Energies from CI calculations.

State	Twist Angle 0°[a]	30°[b]	60°[b]	90°[b]
N	-77.9852	-77.9646	-77.9154	d
	0.0 eV[c]	0.56	1.80	
T	-77.8259	-77.8532	-77.8700	d
	4.34	3.59	3.13	
V	-77.6602	-77.68110	-77.7039	-77.7334
	8.84	8.28	7.66	6.85
R (3pCH)	d	-77.6619	-77.6479	d
		8.56	9.18	

[a]C-C distance of 1.35 Å.

[b]C-C distance of 1.41 Å.

[c]The lower numbers are the energy in eV relative to the N state energy from the CI calculation at 0°.

[d]Not calculated.

TABLE VII. Expectation values for CI wavefunctions.

State	$\langle x^2 \rangle$ [a]	$\langle y^2 \rangle$	$\langle z^2 \rangle$
N	7.04	2.82	5.85
T	8.69	2.96	6.28
V (CI)	24.42	8.24	22.12
V (no σ-π correlation)[b]	38.27	12.87	36.01

[a]This is the expectation value for the four electron CI wavefunction. No nuclear contribution is included. Atomic units are used.

[b]Only Type I and II terms were included.

TABLE VIII. Transition moments for C_2H_4 transitions.

State[a]	Twist Angle[b] 0°	30°	60°	90°
V	1.01	1.05	0.75	0.0[c]
V (no σ-π terms)	0.76	d	d	0.0[c]
R (3pCH)	0.0[c]	0.05	0.21	d

[a]For transitions from the N state. CI wavefunctions used. Atomic units were used in calculating the dipole length transition moment. The oscillator strength f is related to the dipole length transition moment $\vec{R}_{NV}$ by the equation

$$f = \frac{2}{3}\Delta E|\vec{R}_{NV}|^2,$$

where ΔE is the excitation energy. The transition moment at 0° should be used.

[b]C-C bond distances from Table VI.

[c]These values are known to be zero from symmetry arguments.

[d] Not calculated.

FIGURE CAPTIONS

Fig. 1 — The π, π^* and 3pCH orbitals or C_2H_4 twist angles of 30° and 60° are shown. All figures cover the range from -10 bohr to +10 bohr in each direction.

Fig. 2 — Potential curves for bond stretching. The amplitudes of the vibrational wavefunction are plotted on the corresponding energy level.

Fig. 3 — Potential curves for internal rotation. The amplitudes of the vibrational wavefunction are plotted on the corresponding energy level.

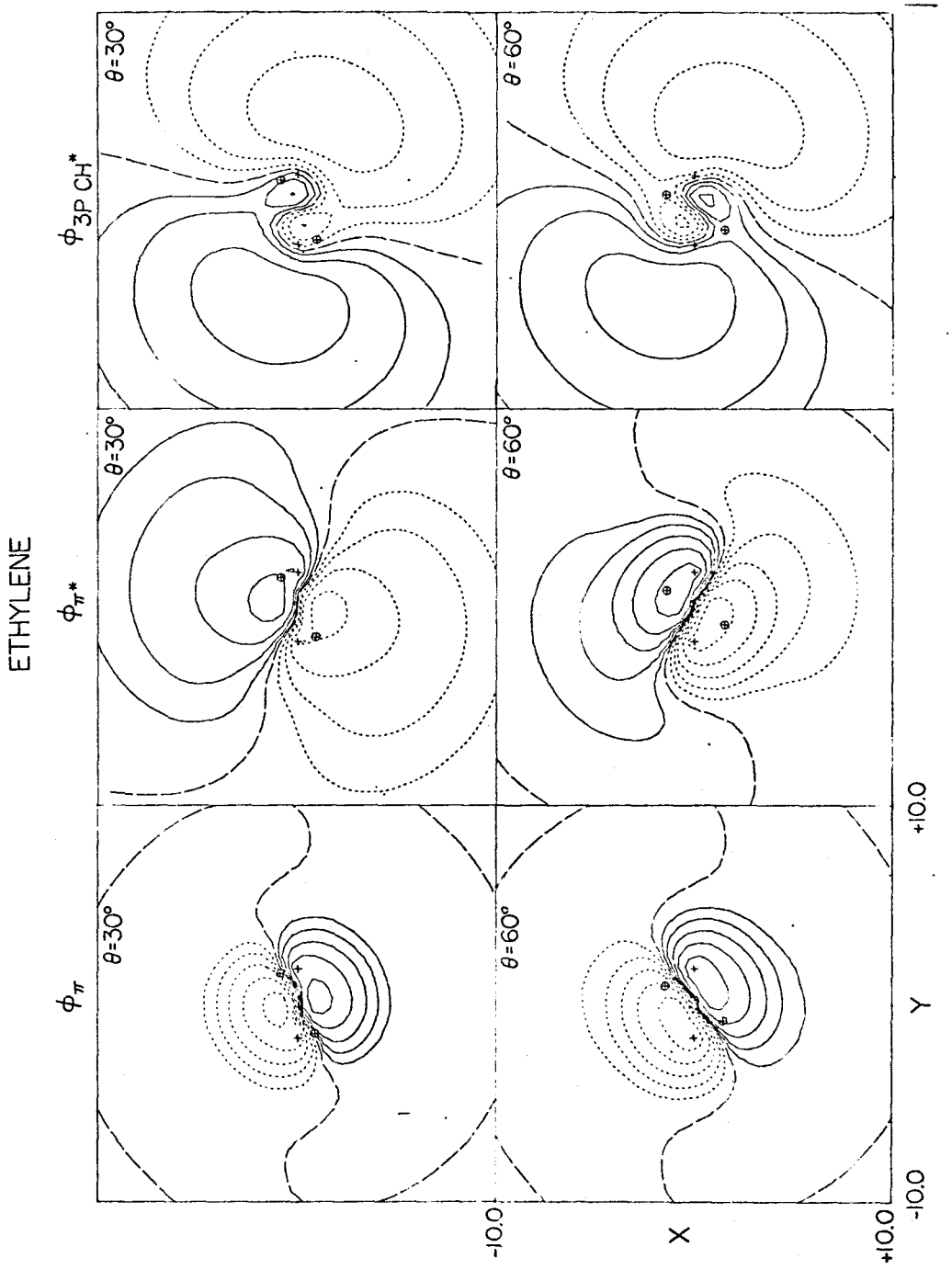
ETHYLENE
ϕ_π
ϕ_{π^*}
$\phi_{3P\ CH^*}$
θ=30°
θ=60°
-10.0
+10.0
X
Y

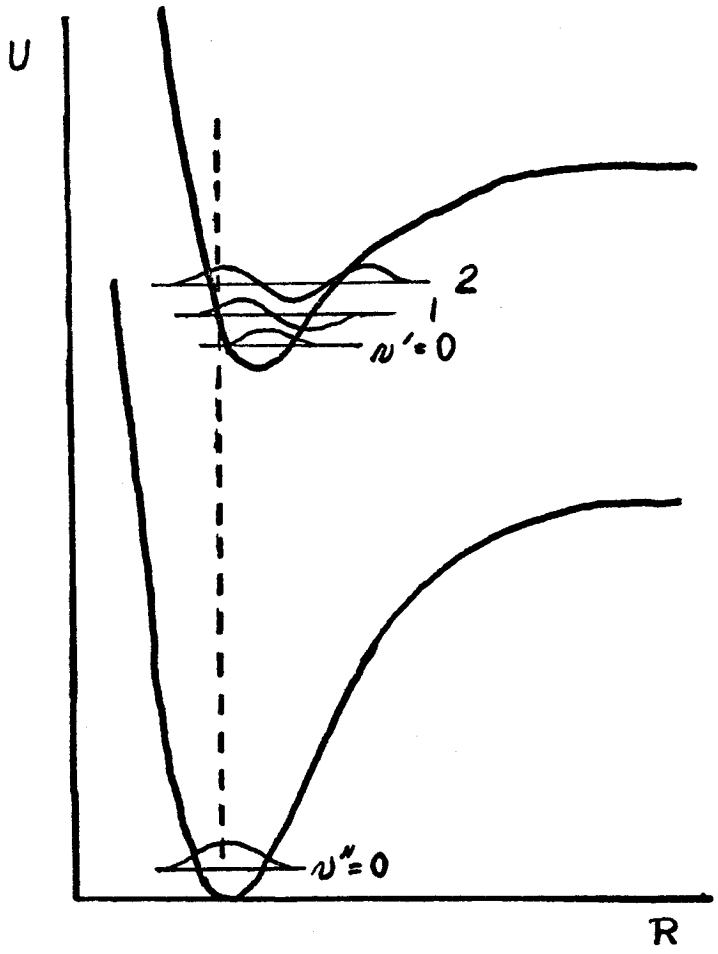
U
2
1
v' = 0
v'' = 0
R

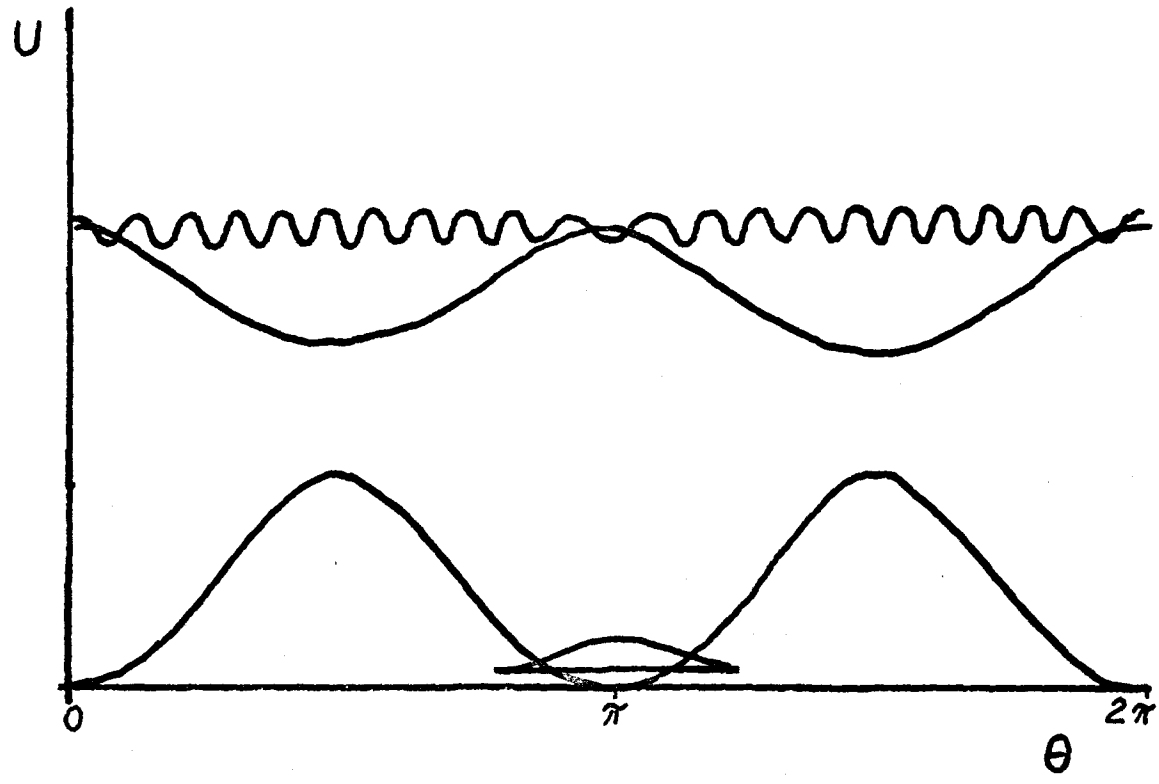
U
0
π
2π
θ

PART III

DEVELOPMENT AND USE OF A GENERALIZED VALENCE BOND METHOD FOR ATOMIC AND MOLECULAR WAVEFUNCTIONS

CHAPTER 3.1 The GVB Method

Self-Consistent Procedures for Generalized Valence Bond Wavefunctions and Applications H_3, BH, H_2O, C_2H_6 and O_2.**

W. J. HUNT,† P. J. HAY,‡ AND W. A. GODDARD III

Arthur Amos Noyes Laboratory of Chemical Physics*
California Institute of Technology
Pasadena, California 91109

Methods of efficiently optimizing the orbitals of Generalized Valence Bond (GVB) Wavefunctions are discussed, and applied to LiH, BH, H_3, H_2O, C_6H_6, and O_2. The strong orthogonality and perfect pairing restrictions are tested for the $X\ ^1\Sigma^+$ state of LiH, the $X\ ^1\Sigma^+$, a $^3\Pi$, and $A\ ^1\Pi$ states of BH, and the $H_2 + D \rightleftharpoons H + HD$ exchange reaction. The orbitals of H_2O and C_2H_6 naturally localize into OH, CH, and CC bonding pairs. The nonbonding orbitals of H_2O are approximately tetrahedral but this description is only 2 kcal lower than the optimum description in terms of symmetry functions. The calculated rotational barrier for C_2H_6 is 3.1 kcal, in good agreement with the experimental value.

---

* Contribution No.

** Partially supported by a grant (GP-15423) from the National Science Foundation.

† National Defense Education Act predoctoral fellow.

‡ National Science Foundation predoctoral fellow.

The description of the O_2 molecule in the GVB approach is presented and the results of carrying out CI calculations using the GVB orbitals is discussed. The GVB orbitals are found to be a good basis set for configuration interaction calculations. The general features of GVB orbitals in other molecules are summarized.

I. INTRODUCTION

The electronic structure of molecules is usually described in terms of either the molecular orbital (MO) or valence bond (VB) models. In particular, the single-configuration MO (or Hartree-Fock) wavefunction has proved extremely useful in computing properties of ground and excited state molecules. Configuration interaction studies have shown that for typical molecules near the equilibrium geometry the Hartree-Fock wavefunction is by far the most important configuration in the "exact" wavefunction. Conceptually, such advances as Walsh diagrams[1] for predicting molecular geometries and the Woodward Hoffmann rules[2] for predicting chemical reactions have their origins in molecular orbital theory.

There are, however, at least two serious drawbacks to the Hartree-Fock model:

1. Molecular orbitals do not usually dissociate correctly, so that one cannot describe bond-breaking processes within this model.

2. Molecular orbitals have the full symmetry of the molecule and bear little resemblance to the expected shapes of bond orbitals and lone pair orbitals.[3]

Our objective here is to discuss an improved SCF method which is tractable and yet removes these serious deficiencies of MO theory. The emphasis will not be on getting 100% of the correlation energy. Rather the aim will be to obtain a generally useful orbital representation for describing molecular bonding and chemical reactions.

II. THE WAVEFUNCTIONS

A. Basic Approach

The Hartree-Fock (HF) wavefunction for (a closed shell) singlet state has the form

$$\mathcal{A}[\phi_1\alpha\phi_1\beta\phi_2\alpha\phi_2\beta\cdots\phi_n\alpha\phi_n\beta] \qquad (1)$$

with each orbital appearing twice (doubly occupied). This double occupation of the orbitals leads to some of the deficiencies of the HF procedure, and several approaches (SOGI,[4a] SO-SCF,[4b] and BRNO[4c]) have been proposed in which the pair

$$\phi_i\alpha\phi_i\beta$$

is replaced by

$$\phi_{ia}\alpha\phi_{ib}\beta$$

to yield the wavefunction

$$\mathcal{A}[\phi_{1a}\phi_{1b}\phi_{2a}\phi_{2b}\cdots\chi], \qquad (2)$$

where χ is allowed to be a general N-electron spinfunction and where χ and the orbitals ϕ_i are solved for self-consistently. This approach leads to the proper description of bond breaking[5] and leads directly to localized bonding and nonbonding orbitals (vide infra).

One reason for the simplicity of Hartree-Fock calculations is that the orbitals of (1) can be taken as orthogonal. Unfortunately this is not the case for wavefunctions of the form (2) (where χ is a general N-electron spinfunction). This lack of orthogonality leads to significant computational problems for large systems and greatly restricts the usefulness of such approaches. We would like to retain the conceptual usefulness of wavefunctions of the form (2) and yet simplify the calculations so that reasonably large molecules can be considered. Most of the basic restrictions and approaches to be used have been suggested elsewhere,[6,7] but are summarized here to clarify our later discussions:

(i) The spin function χ is taken to be

$$\chi_{VB} = [\alpha(1)\beta(2) - \beta(1)\alpha(2)][\alpha(3)\beta(4) - \beta(3)\alpha(4)]\cdots$$

where for a state of spin S the last 2S spins are α. This spin function is the one used in G1[8] and simple valence bond[9] wavefunctions. With restriction (1) the wavefunction (2) can be re-written as

$$\mathcal{A}[(\phi_{1a}\phi_{1b} + \phi_{1b}\phi_{1a})(\phi_{2a}\phi_{2b} + \phi_{2b}\phi_{2a})\cdots$$

$$(\phi_{na}\phi_{nb} + \phi_{nb}\phi_{na})\alpha\beta\alpha\beta\cdots\alpha\beta] \qquad (3)$$

where each term in parentheses is said to be singlet paired.

(ii) The various orbitals are required to be orthogonal to each other unless they are singlet paired, i.e.,

$$\langle \phi_{ia} | \phi_{ib} \rangle \neq 0$$

$$\langle \phi_i | \phi_j \rangle = 0 \quad \text{otherwise.}$$

This restriction has often been used for wavefunctions and is known as the strong orthogonality[10] or separated pair[11,12] restriction.

(iii) The orbitals of (3) are solved for self-consistently.

The wavefunction (3) has the form of a simple valence bond (VB) function, the difference being that in (3) the orbitals are solved for self-consistently rather than taken as (hybridized) atomic orbitals as in VB. For this reason we refer to the wavefunction (3) as the generalized valence bond (GVB) wavefunction.

Wavefunction (3) is a special case of the strongly orthogonal geminal[12] wavefunction

$$\mathcal{A}[\Omega_1(1,2), \Omega_2(3,4) \cdots \chi_{VB}] \tag{4}$$

where each geminal Ω_i can be expanded in terms of natural orbitals.[13]

$$\Omega_i(1,2) = \sum_{j=1}^{P} C_{ji}\, \phi_{ji}(1)\phi_{ji}(2). \tag{5}$$

The ideas of representing electron pairs in this form were originally formulated by Hurley, Lennard-Jones and Pople[6] (HLJP), who discussed the strong orthogonality restriction as well as the representation of pair functions in both the natural orbital (5) and generalized valence bond (3) forms.

In terms of natural orbitals, each pair function of (3) has the form

$$\phi_{ia}(1)\phi_{ib}(2) + \phi_{ib}(1)\phi_{ia}(2) = C_{1i}\phi_{1i}(1)\phi_{1i}(2) + C_{2i}\phi_{2i}(1)\phi_{2i}(2)\,, \qquad (6)$$

that is, only two natural orbitals are used for each pair function.[14] Substituting (6) into (3) we find that the expansion of (3) in terms of those natural orbitals contains only terms of closed shell form. As discussed below this leads to great simplification in the calculations.

There are many cases in which we will want to keep some pairs doubly occupied rather than allowing them to be split. In such cases we take

$$C_{1i} = 1 \text{ and } C_{2i} = 0$$

in (6). In addition, for non singlet states of spin S we will usually take the last 2S orbitals to be unpaired and with the same spin.

B. The Equations

As has been shown by HLJP and Kutzelnigg,[7] the dependence of the energy in (3) upon the orbitals of pair i has the form

$$E = E_{(i)} + f_{1i}\langle\phi_{1i}|(2h_{eff} + J_{1i})|\phi_{1i}\rangle + f_{2i}\langle\phi_{2i}|(2h_{eff} + J_{2i})|\phi_{2i}\rangle + C_{1i}C_{2i}\langle\phi_{1i}|K_{2i}|\phi_{1i}\rangle \qquad (7)$$

where $E_{(i)}$ is independent of the orbitals in pair i,

$$h_{eff} = h + \sum_{j\neq 1i,2i} f_j(2J_j - K_j)$$

and

f_k = 1 for a double occupied orbital

= $\frac{1}{2}$ for an open-shell singly occupied orbital

= C_k^2 for a natural orbital of a split pair as in (6).

Here h_{eff} is analogous to the usual Hartree-Fock one-electron Hamiltonian except that it contains no terms due to either orbital of pair i. For a nonsinglet state of spin S there will be 2S orbitals corresponding to the unpaired spins; these orbitals are referred to as open-shell orbitals ($f_k = \frac{1}{2}$). Any number of the pairs can be double occupied ($f_k = 1$).

Separating from E_i the terms involving the other pairs, we obtain the general expansion

$$E = \sum_k f_k h_k + \sum_{k,\ell} (a_{k\ell} J_{k\ell} + b_{k\ell} K_{k\ell}) \tag{8}$$

which has the form appropriate for general HF and many types of MC-SCF wavefunctions. [In (8) $h_k \equiv \langle k|h|k\rangle$ and $J_{k\ell}$ and $K_{k\ell}$ are the normal Coulomb and exchange integrals.]

Using the variational principle, one obtains the self-consistent field equations[8, 15b]

$$\hat{\bar{H}}_k \phi_k = [\hat{H}_k - \sum_{j \neq k} |j\rangle\langle j|\hat{H}_j]\phi_k = \epsilon_k \phi_k \tag{9}$$

$$k = 1, 2, \cdots, M,$$

where $H_k = f_k h + \sum_\ell a_{k\ell} J_\ell + b_{k\ell} K_{k\ell}$ and M is the number of distinct orbitals. [J and K are the usual Coulomb and exchange operators from HF theory]. In general, there are fewer than M such equations to solve, since all doubly-occupied orbitals can be taken as eigenfunctions of the same closed-shell Hamiltonian.

In the homogeneous approach normally used in solving MC-SCF equations,[16-19] one explicitly constructs each $\overline{H}_k$ for a set of trial functions $\{\phi_j^0\}$ and solves (9) for the ϕ_k to use in the next iteration. We have found this approach to be unsatisfactory and instead use the method suggested in Ref. 15c. In this method each iteration in the SCF process consists of three distinct steps:

(1) The Hamiltonian matrices $\underset{\sim}{H}_k$ are constructed using the trial functions $\{\phi_j^0\}$ and trial CI coefficients $\{C_i^0\}$ and a new set of CI coefficients is obtained by solving the 2×2 matrix equations for each pair.

(2) Each Hamiltonian matrix $\underset{\sim}{H}_k$ is diagonalized according to the OCBSE[15a] procedure. In this approach the eigensolutions of $\underset{\sim}{H}_k$ are obtained in the space orthogonal to the vectors of shells k′, where $k' \neq k$, thereby avoiding the necessity of using coupling operators in the SCF equations.

(3) Since this procedure does not permit mixing of occupied orbitals of shell k with occupied orbitals of other shells, we obtain this optimum mixing by using the set of old orbitals $\{\phi_i^0\}$ as a basis for the expansion of the new (unknown) orbitals $\{\phi_i\}$

$$\phi_i = \phi_i^0 + \sum_{v>i} \phi_v^0 \, \Delta_{vi} - \sum_{v<i} \phi_v^0 \, \Delta_{iv}$$

and optimize the mixing of occupied orbitals with each other by solving for the correction coefficients

$$\{\Delta_{vi},\ v > i,\ i = 1,\ M\}$$

as in Ref. 7. Since this procedure optimizes the mixing of natural orbitals, terms such as

$$C_{12}(\phi_{1i}\phi_{2i} + \phi_{2i}\phi_{1i})$$

need not appear in the expansion [Eq. (6)] of the GVB pair.

The above iterative procedure insures that when the SCF equations have converged, one has obtained the optimum set of orbitals. Although for step (2) the orbitals of shell k are restricted to be in a space orthogonal to the orbitals of other shells, this space changes from iteration to iteration as the occupied orbitals mix in virtual orbital components in step (2) and occupied orbital components in step (3). This differs from some previous strongly orthogonal geminal calculations[21,22,24] where each geminal was obtained in a partitioned subspace of the basis, but where the partition was imposed at the beginning of the calculation and not optimized.

C. Comparison with Other Methods

We emphasize that, with the exceptions of strongly orthogonal geminal calculations on small diatomic molecules[7,12,23] and of several multi-configuration SCF calculations,[16-19] previous calculations on wavefunctions of the form (3) have not optimized the orbitals within a given basis to a level comparable to the degree of convergence obtained in Hartree-Fock calculations.

The GVB method is related to the multi-configuration SCF approach except that the form of the GVB wavefunction is more restricted in order to lead to an orbital type wavefunction (3).

Several types of calculations have been carried out using strongly orthogonal geminals as in (4) including approximate treatments by McWeeny and Ohno[24] on the water molecule and Parks and Parr[11] on formaldehyde. Silver, Mehler, and Ruedenberg[12] obtained fully optimized SOG wavefunctions for Be, LiH, BH and NH using more than two NO's in each geminal, and Scarzafava[20] carried out similar calculations on H_2O. Ahrlichs and Kutzelnigg[7,23] also used a procedure similar to ours on Be and LiH.

Calculations by Franchini, et al.,[21] have employed the procedure of localizing the Hartree-Fock orbitals and expanding each geminal in a CI wavefunction as in (5) with a fixed partition of the basis set. In this scheme, the orbitals are not fully optimized since the space available to each geminal was arbitrarily determined before the calculation.

McWeeny and Klessinger[22,25] have carried out minimum basis self-consistent group calculations on many molecules by starting with a set of symmetrically orthogonalized hybridized atomic orbitals and carrying out a two by two CI calculation on each geminal. Since the energy was optimized as a function of only one hybridization parameter per atom, the resulting orbitals were not completely optimum. For several molecules this has resulted in very poor descriptions of the barriers to internal rotation.[22b] (e.g. ethane is calculated to have a barrier of 5.1 kcal with the eclipsed configuration lower).

Although several authors have discussed ways of relaxing orthogonality constraints,[27,28] the complications involved are excessive. Hinze[47] has developed an approach for general MC-SCF wavefunctions in which the mixings of occupied orbitals with each other is optimized through successive 2 x 2 rotations. This procedure leads to fully optimized orbitals. Hinze has applied this method to various states of LiH[47] and White, Dunning, Pitzer, and Matthews have applied Hinze's program to a series of calculations on various states of CF.[48]

Harrison and Allen[26] have used VB configurations with orbitals based on atomic HF calculations but do not solve for the optimum orbitals. Multi-configuration techniques for diatomic molecules using elliptic basis functions were discussed by Taylor and Harris.[29] VB-CI methods have also been used on LiH and BeH^+ by Miller et al.[30] and on He_2 potential curves by Klein[31] and Gupta and Matsen.[32]

III. TESTS OF STRONG ORTHOGONALITY AND "PERFECT PAIRING"

In order to test the validity of the restrictions involved in GVB calculations, we will compare the results of GVB and SOGI calculations for several systems. This forms a useful test of both the strong orthogonality and perfect pairing restrictions, since neither restriction is made in the SOGI method.

A. LiH and BH ($^1\Sigma^+$)

For a four-electron singlet system, we can write the GVB and SOGI wavefunctions as

$$\psi_{GVB} = \mathcal{A}[\phi_{1a}\phi_{1b}\phi_{2a}\phi_{2b}\chi_1]$$

$$\psi_{SOGI} = \mathcal{A}[\phi_{1a}\phi_{1b}\phi_{2a}\phi_{2b}(\cos\theta\chi_1 + \sin\theta\chi_2)]$$

where χ_1 and χ_2 are the two linearly independent spin functions

$$\chi_1 = \tfrac{1}{2}(\alpha\beta - \beta\alpha)(\alpha\beta - \beta\alpha)$$

$$\chi_2 = \frac{1}{\sqrt{3}}\,[2\alpha\alpha\beta\beta + 2\beta\beta\alpha\alpha - (\alpha\beta + \beta\alpha)(\alpha\beta + \beta\alpha)].$$

In GVB the pair $[\phi_{1a}, \phi_{1b}]$ is constrained to be orthogonal to pair $[\phi_{2a}, \phi_{2b}]$ and the second spin function χ_2 is not used.

SOGI calculations on the ground states of LiH[2,33] and BH[5] have shown that contributions from spin functions other than χ_1 are negligible. Thus comparing SOGI and GVB for these systems is primarily a test of the strong orthogonality restriction. From Table I we see that for LiH at R_e, E_{GVB} is 0.0296 h lower than E_{HF}

and only 0.0008 h higher than E_{SOGI}. Similar results were also obtained for BH at R_e where E_{GVB} was only 0.0018 h greater than E_{SOGI} while 0.045 h lower than E_{HF}. In comparing the GVB and SOGI orbitals of these systems (see Fig. 1 for BH), we find that the main effect involves orthogonality of the GVB valence orbital to the core orbitals, the GVB valence orbitals have a node in the core region. Otherwise the relative relationships between the valence orbitals are quite similar for these two methods. Thus we conclude that at least for these two systems the orbitals and energies are not greatly modified by the strong orthogonal restrictions.

We also carried out calculations in which the 1s orbitals of the LiH and BH were forced to be doubly occupied (but solved for self-consistently). Although in each case the energy is lowered about 0.012 h upon splitting the core orbitals, we find that this core splitting leads to a negligible modification in the valence orbitals. Thus, in the following calculations we will keep the 1s core orbitals paired [f_k = 1 in (10)], but we will solve them self-consistently with the valence orbitals.

B. $H_2 + D \rightarrow H + HD$

A more significant test of the GVB approach is the description of the reaction

$$H_2 + D \rightarrow H + HD$$

where SOGI calculations have shown[4a] that the spin coupling changes from having singlet-coupled electron pair on the H_2 for the reactants to a singlet-coupled electron pair on the HD for the products. Thus

in the linear transition state with $R_{HH} = R_{HD}$, Ψ_{SOGI} contains equal contributions from the two spin couplings. GVB calculations at $R_{HH} = R_{HD} = 1.8$ bohr using Ladner's[4a] basis set yielded an energy 13 kcal/mole (0.021 a.u.) higher than E_{SOGI} (see Table II). This error in the GVB result is quite significant, being as large as for Hartree-Fock. (The calculated barrier height from the SOGI calculation was 16.9 kcal/mole). However, the GVB orbitals have shapes somewhat similar to those of the SOGI orbitals as shown in Fig. 3. The GVB wavefunction has the form

$$\mathcal{A}\,[(gg' + g'g)u\alpha\beta\alpha]$$

where all orbitals have the full $D_{\infty h}$ symmetry of the molecule (g or u). An alternative description of the $^2\Sigma_u^+$ state, $\mathcal{A}[(ab + ba)u\alpha\beta\alpha]$ with a and b symmetrically related by mirror plane reflections but solved for self-consistently yielded an even higher energy.

To determine whether one can improve upon the GVB results for H_3 without a great deal of effort, we used the three GVB orbitals as a basis set and carried out a SOGI calculation. This is equivalent to a three basis function, three electron CI calculation using all configurations. We find that this accounts for 69% of the error between GVB and SOGI, leading to a barrier 4 kcal greater than the SOGI barrier.

C. BH $^1\Pi$ and $^3\Pi$ States

Recent SOGI calculations[34] have shown that the lowest $^1\Pi$ and $^3\Pi$ states of BH also involve significant changes in spin-coupling as

the internuclear distance (R) is decreased from ∞ to R_e. Thus, this system serves as another good test case of the limitations of GVB. In the ^2P state of B, Ψ_{GVB} has the form[5]

$$\mathcal{A}\{[1s^2][sz, s\bar{z}]2p_x\,\alpha\beta\alpha\beta\alpha\}$$

where sz and $s\bar{z}$ have the form

$$sz = \phi_s + \lambda\phi_{pz}$$

$$s\bar{z} = \phi_s - \lambda\phi_{pz}$$

that is, these functions are sp-like hybridized orbitals polarized along the z axis.

In contrast to the $^1\Sigma$ state, where the 1s hydrogen orbital is singlet-coupled to the px orbital, the Π states arise from breaking up the nonbonding pair to form the BH bond:[34]

$$^3\Pi: \quad \psi_{GVB} = \mathcal{A}\{[1s^2][sz, h]\, s\bar{z}\ px\ \alpha\beta\alpha\beta\alpha\alpha\}$$

$$^1\Pi: \quad \psi_{GVB} = \mathcal{A}\{[1s^2][sz, h][s\bar{z},\ pz]\,\alpha\beta\alpha\beta\alpha\beta\}$$

Here we refer to the orbitals with symbols (sz, $s\bar{z}$, px, h) to denote their basic shapes, although each orbital is solved for self-consistently. From the results at R = 2.25 and R = 4.0 in Table II, it is seen that the GVB wavefunction is higher in energy than ψ_{SOGI} by amounts ranging from 0.0046 a.u. for the $^3\Pi$ state (R = 2.25) to 0.0198 a.u. for the $^1\Pi$ (R = 2.25).

The description of the $^1\Pi$ state is rather poor and so we examined the improvements to be obtained by solving for the CI wavefunction using the four GVB orbitals as the basis. At R = 2.25 a_0 this accounted for 56% of the error between GVB and SOGI but still led to an energy 0.0088 greater than E_{SOGI}. Another difficult case occurs in the $^2\Pi$ state of CH for large R. At R = ∞ the C atom is in the ^3P state and hence two valence orbitals are coupled antisymmetrically. Coupling the H orbital symmetrically to the carbon p-orbital is thus incorrect at large R. As a result the GVB wavefunction for CH at large R is 0.35 eV above the limit of $C(^3P) + H(^2S)$. However, Bobrowicz[49] has shown that starting with the GVB orbitals and carrying out a three-basis function CI (or SOGI) calculation leads to a proper description of the wavefunction at large R.

D. Summary

From reflections on these studies we have concluded that

(1) The GVB approach should lead to an adequate description of the ground state of most molecules that can be described in terms of one covalent VB structure,

(2) this method also should lead to an adequate description of bond breaking and bond formation when spin coupling changes are not important (thus, biradicals should be well described),

(3) however, the GVB approach may be of less quantitative use in describing reactions involving extensive spin coupling changes. In such cases a simple CI calculation using the GVB natural orbitals may be satisfactory.

Further implications for CI calculations will be discussed later.

IV. THE WATER MOLECULE

The optimum GVB orbitals of the ground state of H_2O lead to a description having two equivalent bonding pairs, two equivalent non-bonding pairs, and an oxygen 1s core pair:

$$\Psi_{GVB} = \mathcal{A}\{[1s_a, 1s_b][b_{1a}, b_{1b}][b_{2a}, b_{2b}][\ell_{1a}, \ell_{1b}][\ell_{2a}, \ell_{2b}]\chi\}$$

This description is not forced upon the system by any arbitrary symmetry requirements, but rather is obtained by solving for the optimum ten GVB orbitals. The orbitals for the equilibrium geometry of the H_2O molecule were obtained using a basis set[33] of contracted Gaussian functions including 3d oxygen polarization functions. We see from Table IV that the major improvement over the Hartree-Fock wavefunction is in the description of the bonding pairs, where an energy lowering of 13 kcal/mole for each bond is obtained.

In Fig. 2 we see that each orbital of a bonding pair (ϕ_{2a} and ϕ_{2b}) is localized on a different center. The ϕ_{2a} orbital, localized on the oxygen atom, has some s character but is mainly (81.9%) p-like (corresponding to sp 4.7 bonding). Similarly, the ϕ_{2b} orbital remains essentially a hydrogenic 1s orbital, delocalized onto the oxygen atom (indicating some ionic character in the bond).

The nonbonding pairs have 59% p-character ($sp^{1.46}$) and are bent back from the oxygen in the plane perpendicular to the molecular plane. Each pair consists of two orbitals (ϕ_{4a} and ϕ_{4b} in Fig. 2) oriented in the same direction but having different radial dependencies, i.e., one being more diffuse than the other. This description is not equivalent to the case where we require the lone-pair functions to have a_1 and b_1 symmetry (i.e., symmetric and antisymmetric with the molecular plane), which in fact (see Table III) leads to an energy only 0.0031 h (2 kcal/mole) higher.

The above results generally agree with previous GVB-like calculations on H_2O by other investigators. Klessinger[22a] has carried out a group function calculation on the OH bonds in H_2O where he obtained an energy lowering of each OH bond of 0.0142 h compared with our value of 0.0209 h. The uv form of Scarzafava's separated-pair wavefunction[20] and The group functions of Franchini, Moccia and Zandomeneghi[21] are roughly equivalent in sophistication to our GVB approach, but lead to slightly worse energies because their method does not achieve full optimization. Scarzafava[20] obtained full orbital optimization and his uv wavefunction is comparable in energy to ours; he also obtained more general separated pair and CI wavefunctions for H_2O. A recent strongly orthogonal geminal calculation by Shull and coworkers[36] demonstrated the transferability of geminals from H_2O to H_2O_2.

V. THE ETHANE MOLECULE

The ethane molecule is a good test case of the GVB approach since a highly restricted wavefunction might not lead to a proper description of the small (2.9 kcal/mole) rotational barrier.

For the ethane molecule, we solved for the GVB orbitals in the STO-4G minimum basis set of contracted Gaussian functions developed by Pople.[43] We obtain six equivalent C-H bond pairs, one of which is shown in Fig. 3 (orbitals ϕ_{2a} and ϕ_{2b}). In contrast to the delocalized molecular orbital, we see that one of the GVB orbitals is an essentially unchanged hydrogen 1s orbital and the other is a hybrid orbital (68.5% p-character, hence $sp^{2.17}$) on the C oriented toward the H. Each C-H bond is lowered 0.0157 h (10 kcal) relative to the HF description. The C-C bond

orbitals (orbitals ϕ_{1a} and ϕ_{1b} in Fig. 3) have a smaller energy lowering (0.0139 h or 9 kcal) and a higher overlap than the C-H bond orbitals (0.835 vs 0.826) but dissociate continuously into the p-orbitals of two methyl radicals as the groups are pulled apart.

We find that GVB leads to a rotational barrier of 3.1 kcal (with the staggered configuration lower) in good agreement with the HF results (3.3 kcpm) and with experiment (2.9 kcpm). This constrast with the barrier of -5.1 kcal (eclipsed from lower) found by Klessinger using partially optimized orbitals.

VI. THE OXYGEN MOLECULE

The failure to predict a triplet ground state for the O_2 molecule was one of the major difficulties of valence bond theory.[37] It is therefore of interest to examine O_2 in the GVB description, which is a synthesis of the MO and VB methods. The wavefunction for the $^3\Sigma_g^-$ state is

$$\psi_{GVB} = \mathcal{A}\{[\delta_A, \delta_B][\pi_{xu}^2][\pi_{yu}^2][\pi_{xg}\pi_{yg}\chi\}$$

(where the 1 and 2 orbitals have been taken to be doubly occupied and are not shown). Little improvement in energy (0.001 h) is obtained by allowing the π_u orbitals to split or to become asymmetric. Thus ψ_{GVB} differs from ψ_{HF} by the presence of two sigma orbitals [σ_A, σ_B] that are related to the $3\sigma_g$ and $3\sigma_u$ natural orbitals.

From Table V we see that the HF and GVB results both predict the correct qualitative relation of the $^3\Sigma_g^-$, $^1\Delta_g$, and $^1\Sigma_g^+$ states.[38] In using the GVB natural orbitals as a basis set for a small configuration interaction (CI) calculation, effectively relaxes both

The strong orthogonality and the spin-coupling restrictions as well as including the correlation terms involving only valence-like orbitals. (internal correlation). The importance of these terms has been emphasized in the theory of Silverstone and Sinanoglu[40] and by the first-order wavefunction calculations of Schaefer.[41]

The calculated dissociation energy from the GVB-CI calculation is in much better agreement with the experimental results and with the more extensive calculation by Schaefer.[41a] Calculations on other states using the natural orbitals from the ground state GVB wavefunction are also reported in Table V, where the results are in general agreement with experiment.[42]

VII. GENERAL CHARACTERISTICS OF THE GVB APPROACH TO MOLECULES

The previous discussions of H_2O, C_2H_6, and O_2 illustrated some specific aspects of the GVB method; in this section we will summarize some of the results obtained for other molecules. These will be discussed more fully in future publications.

The basis sets used are MBS (minimum basis set; Pople's STO-4G basis with standard molecular exponents)[43] and POL (the [4s2p] DZ set[35] augumented by one set of d-type uncontracted Gaussian functions on each of the B, C, N, O, and F atoms).

In Table VI we see that the two orbitals making up a sigma bond have high overlap: for C-H bonds it is 0.82-0.87 and for sigma bonds involving two first-row atoms, 0.85-0.93. Thus, at ————————|

the equilibrium distance, HF should yield a relatively good description since the energy gain in the GVB method is only 0.005-0.015 a.u. for each bond. However, pi bonds are not so well described by HF, as the GVB overlap is only 0.57-0.73 and the increase in bond energy in GVB is 0.03-0.045 a.u. (0.8-1.2 eV). Thus π bonds are much closer to the dissociated bond limit than is the case for sigma bonds.

The most drastic improvement can be noted in cases where there are two molecular orbitals--one occupied and one virtual--which are nearly degenerate. Such situations arise in biradicals such as singlet CH_2, the trimethylene biradical,[44] benzenes,[45] the C_2 molecule and cases where a bond is broken. In the last case, thw two nonbonding electrons are especially poorly described by a single $2\sigma_u$ orbital as in HF [The GVB orbitals have small overlap (0.33) and the pair splitting energy is 63 kcal]. This leads to a dissociation energy for C_2 of -22.1 kcal/mole in HF as compared with 72.7 for GVB and the experimental value of 144.

We conclude that the wavefunction leads to useful wavefunctions and remove many difficulties and inconsistencies of the Hartree-Fock method.

FIGURE CAPTIONS

FIG. 1. Comparison of the SOGI and GVB orbitals for BH ($^1\Sigma^+$). ϕ_{2a} is one of the two symmetrically related nonbonding orbitals. ϕ_{3a} and ϕ_{3b} are the bonding orbitals.

FIG. 2. The GVB orbitals for the H_2O molecule. ϕ_{2a} and ϕ_{2b} represent the orbitals of one of the two equivalent lone pairs. ϕ_{4a} and ϕ_{4b} represent the orbitals of one of the two equivalent OH bonds.

FIG. 3. The GVB orbitals for the CC bond (ϕ_{1a} and ϕ_{1b}) and a CH bond (ϕ_{2a} and ϕ_{2b}) in ethane.

REFERENCES

1. One can transform the Hartree-Fock orbitals to a localized form, but the invariance of the energy under such transformations prevents a unique localization scheme.
2. R. B. Woodward and R. Hoffmann, The Conservation of Orbital Symmetry (Academic Press, New York, 1970).
3. A. D. Walsh, J. Chem. Soc., 1953, 2260.
4a. R.C. Ladner and W.A. Goddard III, J. Chem. Phys., 51, 1073 (1969).
4b. U. Kaldor and F. E. Harris, Phys. Rev., 183, 1 (1969).
4c. S. Hameed, S. S. Hui, J. I. Musher, and J. M. Schulman, J. Chem. Phys., 51, 502 (1969).
5. (a) R. J. Blint, W. A. Goddard III, R. C. Ladner, and W. E. Palke, Chem. Phys. Letters 5, 302 (1970); (b) R. J. Blint and W. A. Goddard III, J. Chem. Phys. 55, 0000 (1971); (c) W. A. Goddard III and R. C. Ladner, J.Amer.Chem.Soc., 93, 000 (1971).
6. A. C. Hurley, J. E. Lennard-Jones, and J. A. Pople, Proc. Roy. Soc. (London) A220, 446 (1953).
7. W. Kutzelnigg, J. Chem. Phys. 40, 3640 (1964).
8. W. A. Goddard III, Phys. Rev. 157, 73, 81 (1967).
9. (a) L. Pauling, J. Am. Chem. Soc. 53, 1367 (1931); L. Pauling, Proc. Natl. Acad. Sci. U.S. 14, 359 (1928); (b) J. C. Slater, Phys. Rev. 37, 481 (1931); ibid. 38, 1109 (1931).
10. T. Arai, J. Chem. Phys. 33, 95 (1960); P. O. Löwdin, ibid. 35, 78 (1961).
11. J. M. Parks and R. G. Parr, J. Chem. Phys. 28, 335 (1958); ibid. 32, 1567 (1960).
12. D. M. Silver, E. L. Mehler, and K. Ruedenberg, J. Chem. Phys. 52, 1174, 1181, 1206 (1970).
13. (a) P. O. Löwdin, Phys. Rev. 97, 1474 (1955); (b) P. O. Löwdin

and H. Shull, Phys. Rev. 101, 1730 (1956); (c) W. Kutzelnigg, Theoret. Chim. Acta 1, 327 (1963); (d) H. Shull, J. Chem. Phys. 30, 1405 (1959).

14. In Eq. (6) ϕ_{ia}, ϕ_{ib}, ϕ_{1i}, and ϕ_{2i} are all normalized so that $C_{1i}^2 + C_{2i}^2 = 1$.

15. (a) W. J. Hunt, T. H. Dunning Jr., and W. A. Goddard III, Chem. Phys. Letters 3, 606 (1969); (b) W. A. Goddard III, T. H. Dunning Jr., and W. J. Hunt, ibid. 4, 231 (1969); (c) W. J. Hunt, W. A. Goddard III, and T. H. Dunning Jr., ibid. 6, 147 (1970).

16. A. C. Wahl and G. Das, Advan. Quant. Chem. 5, 261 (1971).

17. E. Clementi and A. Veillard, J. Chem. Phys. 44, 3050 (1966).

18. J. Hinze and C.C. J. Roothaan, Progr. Theoret. Phys. (Kyoto) Suppl. 40, 37 (1967).

19. R. McWeeny, Trans. Faraday Soc. 2, 7 (1968).

20. E. Scarzafava, Ph.D. thesis, Indiana University, 1969.

21. P. F. Franchini, R. Moccia, and M. Zandomeneghi, Int. J. Quant. Chem. 4, 487 (1970).

22. (a) M. Klessinger, J. Chem. Phys. 43, S117 (1965); (b) ibid. 53, 225 (1970); (c) idem, Sym. Faraday Soc. 2, 73 (1968).

23. R. Ahrlichs and W. Kutzelnigg, J. Chem. Phys. 48, 1819 (1968).

24. R. McWeeny and K. A. Ohno, Proc. Roy. Soc. (London) A255, 367 (1960).

25. M. Klessinger and R. McWeeny, J. Chem. Phys. 42, 3343 (1965).

26. J. F. Harrison and L. C. Allen, J. Am. Chem. Soc. 91, 807 (1969).

27. V. A. Nicely and J. F. Harrison, J. Chem. Phys. 54, 4363 (1971).

28. D. M. Silver, J. Chem. Phys. 50, 5108 (1969).

29. H. S. Taylor and F. E. Harris, Mol. Phys. 6, 183 (1963).

30. J. Miller, R. H. Friedman, R. P. Hurst, and F. A. Matsen, J. Chem. Phys. 27, 1385 (1957).

31. D. J. Klein, J. Chem. Phys. 50, 5152 (1969).

32. B. K. Gupta and F. A. Matsen, J. Chem. Phys. 50, 3797 (1969).

33. C. Melius and W. A. Goddard III, J. Chem. Phys. 55, 0000 (1971).

34. R. J. Blint and W. A. Goddard III, to be published.

35. A (9s5p2d) and (4s) primitive set was contracted to a [4s, 3p, 1d] and [2s] set on the oxygen and hydrogens, respectively. (a) S. Huzinaga, J. Chem. Phys. 42, 1293 (1965); (b) T. H. Dunning, J. Chem. Phys. 53, 2823 (1970).

36. M. Levy, W. J. Stevens, H. Shull, and S. Hagstrom, J. Chem. Phys. 52, 5483 (1970).

37. See J. C. Slater, Quantum Theory of Molecules and Solids (McGraw-Hill Book Co., Inc., New York, 1963), Vol. 1, p. 121.

38. The [4s3p] contracted Gaussian basis described by Huzinaga and Dunning (Ref. 35) was used, augmented by d-type polarization functions on each center (z^2, xz, and yz only), with orbital exponents of . The experimental value[39] of R_e = 1.209Å was used.

39. G. Herzberg, Spectra of Diatomic Molecules (D. Van Nostrand-Reinhold Co., New York, 1950).

40. H. J. Silverstone and O. Sinanoglu, J. Chem. Phys. 46, 854 (1967).

41. (a) H. F. Schaefer III, J. Chem. Phys. 54, 2207 (1971); ibid. 55, 176 (1971).

42. S. Trajmar, W. Williams, and A. Kuppermann, J. Chem. Phys., in press.

43. W. J. Hehre, R. F. Stewart, and J. A. Pople, J. Chem. Phys. 51, 2657 (1969).

44. P. J. Hay, W. A. Goddard III, and W. J. Hunt, J. Amer. Chem. Soc., to be published.

45. R. Hoffmann, A. Imamura and W. J. Henre, J. Amer. Chem. Soc., 90, 1498 (1968); D. L. Wilhite and J. L. Whitten, J. Amer. Chem. Soc., 93, 2858 (1971).

46. The results here were obtained in the STO-4G basis used for C_2H_6 (see Ref. 43).

47. J. Hinze, private communication.

48. W. White, T. H. Dunning Jr., R. M. Pitzer and W. Matthews, to be published.

49. F. Bobrowicz and W. A. Goddard III, to be published.

TABLE I. Comparison of HF GVB and SOGI calculations on ground states of LiH ($R = 3.015\ a_0$) and BH ($R = 2.336\ a_0$).

	Energy (Hartree)		D_e (eV)	Energy Lowering	
	$R = R_e$	$R = \infty$		Pair	$\Delta\varepsilon_i$ (Hartree)
LiH					
HF[a]	-7.98326	-7.93123	1.42	—	—
GVB[f]					
1-pair	-8.00054	-7.93123	1.89	bond	-0.01728
2-pair	-8.01289	-7.94336	1.89	bond	-0.01710
				core	-0.01249
SOGI[bf]	-8.01369	-7.94435	1.89	—	—
Exp[c]			2.52		
BH					
HF[a]	-25.12820	-25.01790	2.73	—	—
GVB[g]					
2-pair	-25.16542	-25.04735	3.21	bond	-0.01443
				lone	-0.02279
3-pair	-25.17769	-25.0599	3.21	bond	-0.01436
				lone	-0.02276
				core	-0.01236
SOGI[dg]	-25.18014	-25.06119	3.24	—	—
Exp[e]			3.56		

TABLE I. Continued

[a] Cade and Huo [J. Chem. Phys. 47, 614 (1967)] using a more extensive basis obtain E = -7.9873 and D_e = 1.49 for LiH and E = -25.13137 and D_e = 2.77 for BH.

[b] Palke and Goddard [J. Chem. Phys. 50, 4524(1969), using a more extensive basis obtain E = -8.0173 and D_e = 1.90.

[c] G. Herzberg, Spectra of Diatomic Molecules, (D. VanNostrand Co., Princeton, N.J., 1950); R. Velasco, Can. J. Phys. 35, 1204 (1957).

[d] Blint and Goddard (Ref. 5b).

[e] P. G. Wilkinson, Astrophys. J. 138, 614 (1967).

[f] Using a double zeta plus polarization for (DZP) basis consisting of

[g] Using the DZP basis from Ref. 5b.

[h] The energy lowering due to splitting the one pair.

TABLE II. Comparison of GVB and SOGI calculations for (a) the transition state of the $H_2 + D \rightleftharpoons H + HD$ reaction at $R_{12} = R_{23} = 1.8\ a_0$ and (b) the $^3\Pi$ and $^1\Pi$ states of BH.

	Energy (Hartree)		Barrier height (kcal/mole)
	$R_{12} = R_{23} = 1.8\ a_0$	$H_2 + D$	
HF	-1.5930	-1.6335	25
GVB			
$r\ell u$[b]	-1.5936	-1.6517	36
$gg'u$[b]	-1.6035	-1.6517	30
GVB-CI (3 BF)[c]	-1.6178	-1.6517	21
SOGI[d]	-1.6240	-1.6517	17
CI[e]	-1.6521	-1.6696	11

	Energy (Hartree)	
	$R = 2.25\ a_0$	$R = 4.0\ a_0$
BH $^3\Pi$		
HF	-25.11333	-25.01847
GVB	-25.12413	-25.03240
GVB-CI (4 BF)	-25.12800	-25.03742
SOGI[f]	-25.12874	-25.04170
BH $^1\Pi$		
HF	-25.03375	-25.02459
GVB	-25.04307	-25.03987
GVB-CI (4 BF)	-25.05400	-25.04964
SOGI[f]	-25.06285	-25.05242

TABLE II. Continued

[a] Energy of saddle point ($R_{12} = R_{23} = 1.8\ a_0$) relative to H + HD.

[b] $r\ell u$ and $gg'u$ refer to the two possible orbital configurations; see text for further discussion.

[c] Complete CI using the GVB orthogonal orbitals.

[d] Ladner and Goddard (Ref. 4a).

[e] I. Shavitt, R. M. Stevens, F. L. Minn and M. Karplus, J. Chem. Phys. 48, 2700 (1968).

[f] Blint and Goddard (Ref. 34).

TABLE III. Calculations on the ground state of the water molecule[a]

Method	Energy	Pair Information: Pair	Pair Information: $\Delta\Sigma$ Energy, Lowering
This work			
HF	-76.0377	—	—
GVB 4 pairs ($\sigma\pi$)	-76.0988	bond(2)	-0.0207
		lone-σ	-0.0086
		lone-π	-0.0118
GVB 4 pairs (lobes)	-76.1019	bond(2)	-0.0209
		lone(2)	-0.0115
GVB 5 pairs (lobes)	-76.1118	bond(2)	-0.0209
		lone(2)	-0.0114
		core(1)	-0.0100
Scarzafava (Ref. 20)			
HF	-76.038		
Separated pair (uv form) - 5 pairs	-76.1100		
Klessinger (Ref. 22c)			
HF	-75.6807		
Group function - 2 pairs	-75.7139		
Franchini, et al. (Ref. 21)			
HF	-76.0374		
Group function - 4 pairs	-76.0997		

TABLE III. Continued

Method	Energy	Pair Information: Pair	Pair Information: ΔΣ
Other calculations			
HF[b]	-76.059		
HF[e]	-76.0630		
CI[c]	-76.1422		
CI[d]	-76.2205		

[a] The geometry is that used by Dunning (Ref. 35b).

[b] D. Neuman and J. W. Moskowitz, J. Chem. Phys. 49, 2056 (1968).

[c] R. P. Hosteny, R. R. Gilman, T. H. Dunning, A. Pipano and I. Shavitt, Chem. Phys. Letters 7, 325 (1970).

[d] C. Bender and H. F. Schaeffer, to be published.

[e] T. H. Dunning and R. N. Pitzer, to be published.

TABLE IV. Comparison of calculations on the ethane molecule.

	Energy (Hartree)		Barrier (kcal/mole)	Pair Information				
					Energy Lowering		Orbital Overlap	
	Staggered	Eclipsed		Pair	Staggered	Eclipsed	Staggered	Eclipsed
This work								
HF	-78.8608	-78.8555	+3.3					
GVB	-78.9691	-78.9641	+3.1	CC bond	-0.0139	-0.0139	0.835	0.836
				CH bond	-0.0157	-0.0158	0.826	0.826
Klessinger[b]								
HF	-78.9562	-78.9510	+3.3					
SCGF	-78.9641	-79.0188	-5.1					
Exper[c]			2.93					

[a] The geometry used was taken to be that used by R. M. Pitzer and W. N Lipscomb, J. Chem. Phys., 39, 1995 (1963).

[b] Ref.

[c] S. Weiss and G. Leroi, J. Chem. Phys., 48, 962 (1968).

TABLE V. Oxygen Molecule (R = 2.282 a_0)

	$^3\Sigma_g^-$ state	
	E	D_e
HF	-149.6331	0.95
GVB (one pair)	-149.6595	1.68
GVB-CI	-149.7315	3.64
CI[a]	-149.7944	4.72
Exp[b]	—	5.21

State	Excitation Energies			
	HF	GVB	GVB-CI	Exp
$^3\Sigma_g^-$	—	—	—	—
$^1\Delta_g$	1.43	1.28	0.91	0.98
$^1\Sigma_g^+$	2.37	2.23	1.69	1.63
$^1\Sigma_u^-$	—	—	5.91	6.1[c]
$^3\Delta_u$	—	—	6.16	6.1[c]
$^3\Sigma_u^+$	—	—	6.31	6.1[c]

[a] H. F. Schaeffer III,

[b] Reference 39.

[c] Broad unresolved feature, Reference 42.

TABLE VI. Characteristics of GVB electron pairs in bonds

Pair Type	System-State	Basis	Pair Information		
			Pair	Overlap	Energy Lowering Relative to HF (Hartrees)
Sigma bond	CH $^2\Pi$	POL		0.8264	0.0173
	CH $^4\Sigma^-$	POL		0.8640	0.0104
	CH_4	POL		0.8342	0.0153
	C_2H_2 $^1\Sigma_g^+$	MBS	CH	0.8413	0.0138
			CC	0.9289	0.0045
	C_2H_4 $^1A_{1g}$	MBS	CH	0.8388	0.0142
			CC	0.8930	0.0078
	C_2H_6 $^1A_1$	MBS	CH	0.8259	0.0157
			CC	0.8354	0.0139
	BeO $^1\Sigma^+$	MBS		0.8618	0.0085
	BeO $^3\Pi$	MBS		0.9117	0.0046
	H_2O $^1A_1$	POL	OH	0.8247	0.0209
Pi bond	C_2H_2 $^1\Sigma_g^+$	MBS		0.6639	0.0329
	C_2H_4 $^1A_{1g}$	MBS		0.5782	0.0462
	CO $^1\Sigma^+$	MBS		0.7366	0.0308
	BeO $^1\Sigma^+$	MBS		0.6662	0.0313
Lone Pair	H_2O $^1A_1$	POL		0.0115	0.0115
	CH_2 $^1A_1$	POL		0.6827	0.0214
	C_2 $^1\Sigma_g^+$	MBS		0.3313	0.1013

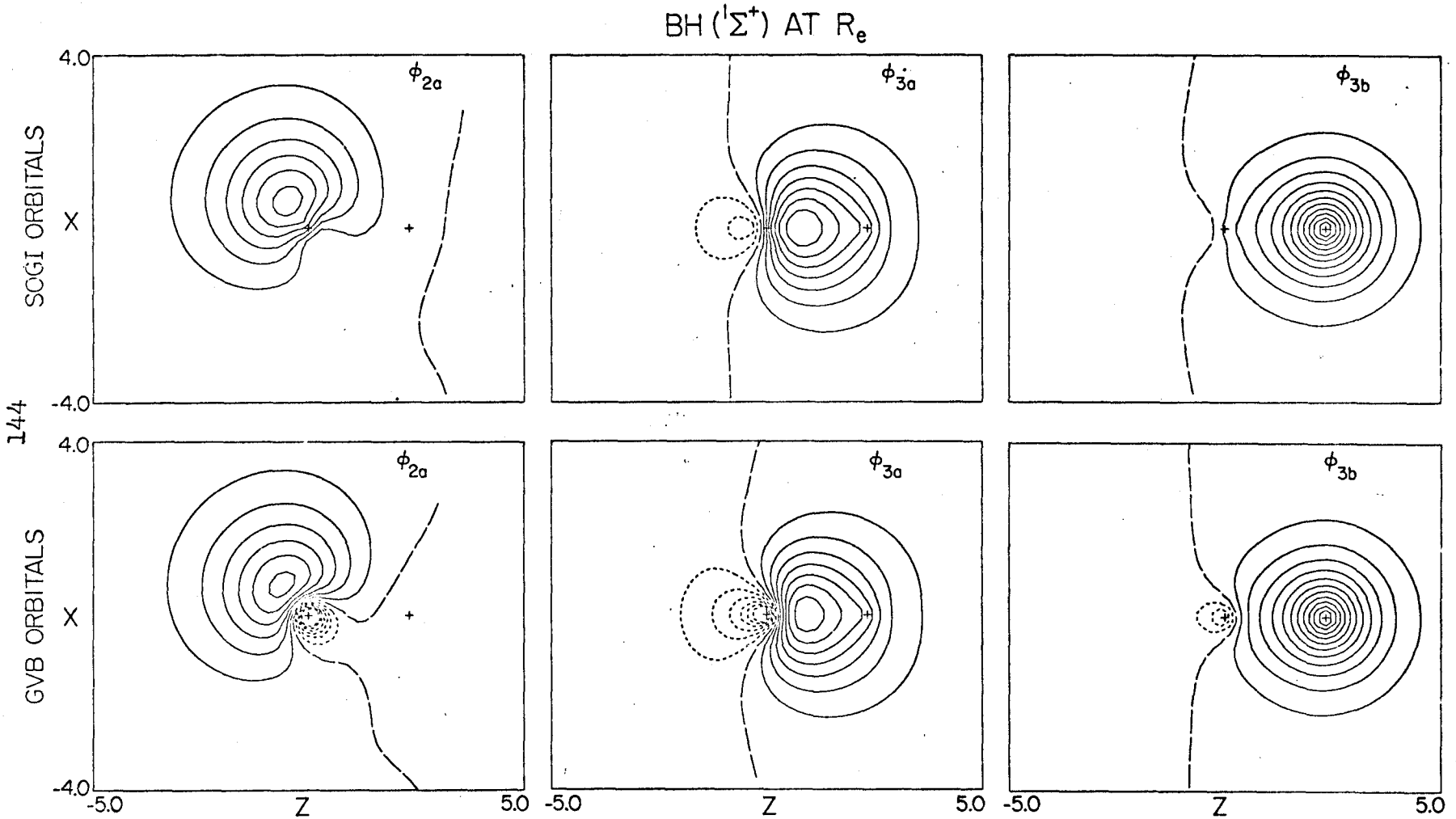
BH ($^1\Sigma^+$) AT R_e
SCGI ORBITALS
GVB ORBITALS
ϕ_{2a}
ϕ_{3a}
ϕ_{3b}
4.0
-4.0
X
-5.0
5.0
Z

WATER MOLECULE

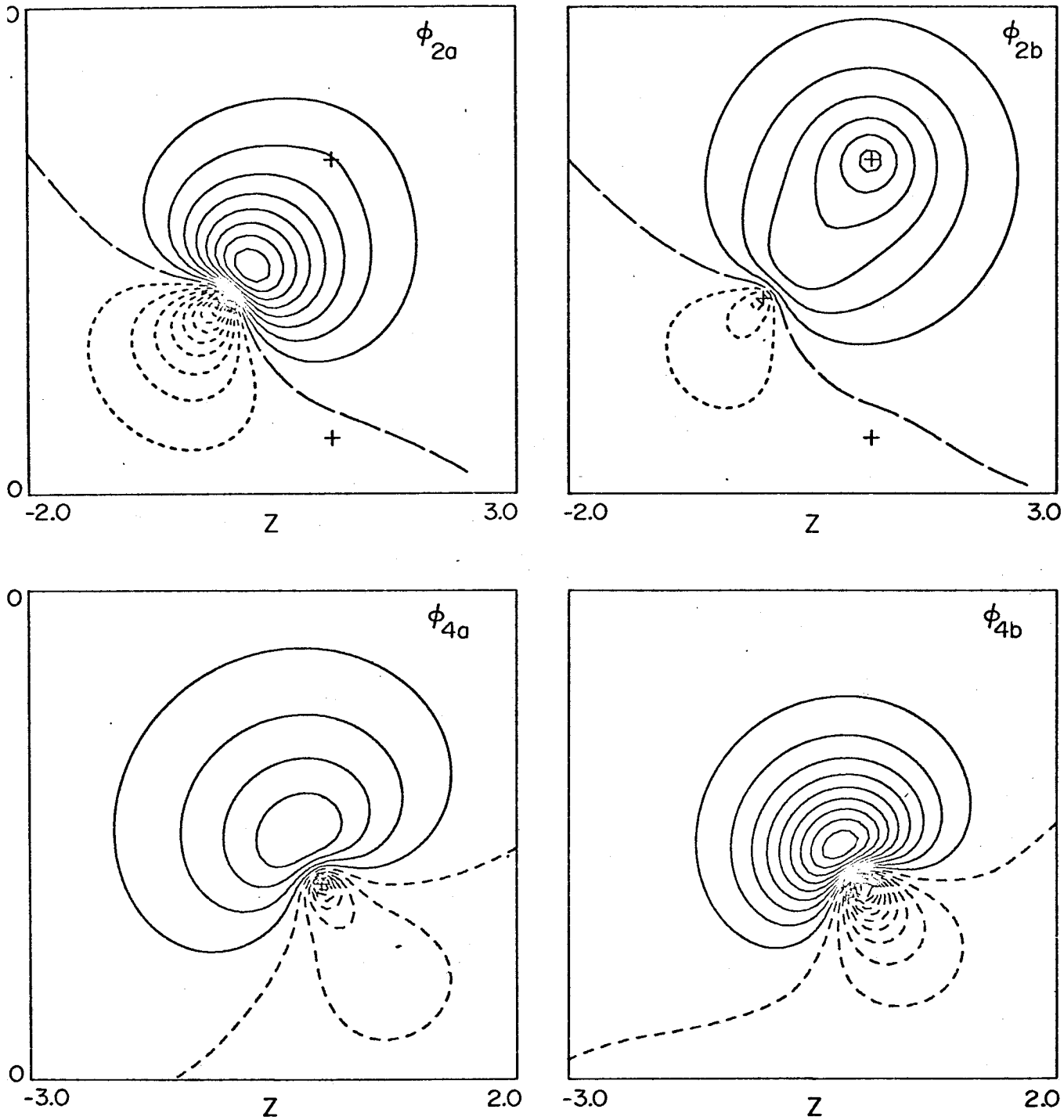

ETHANE (STAGGERED)

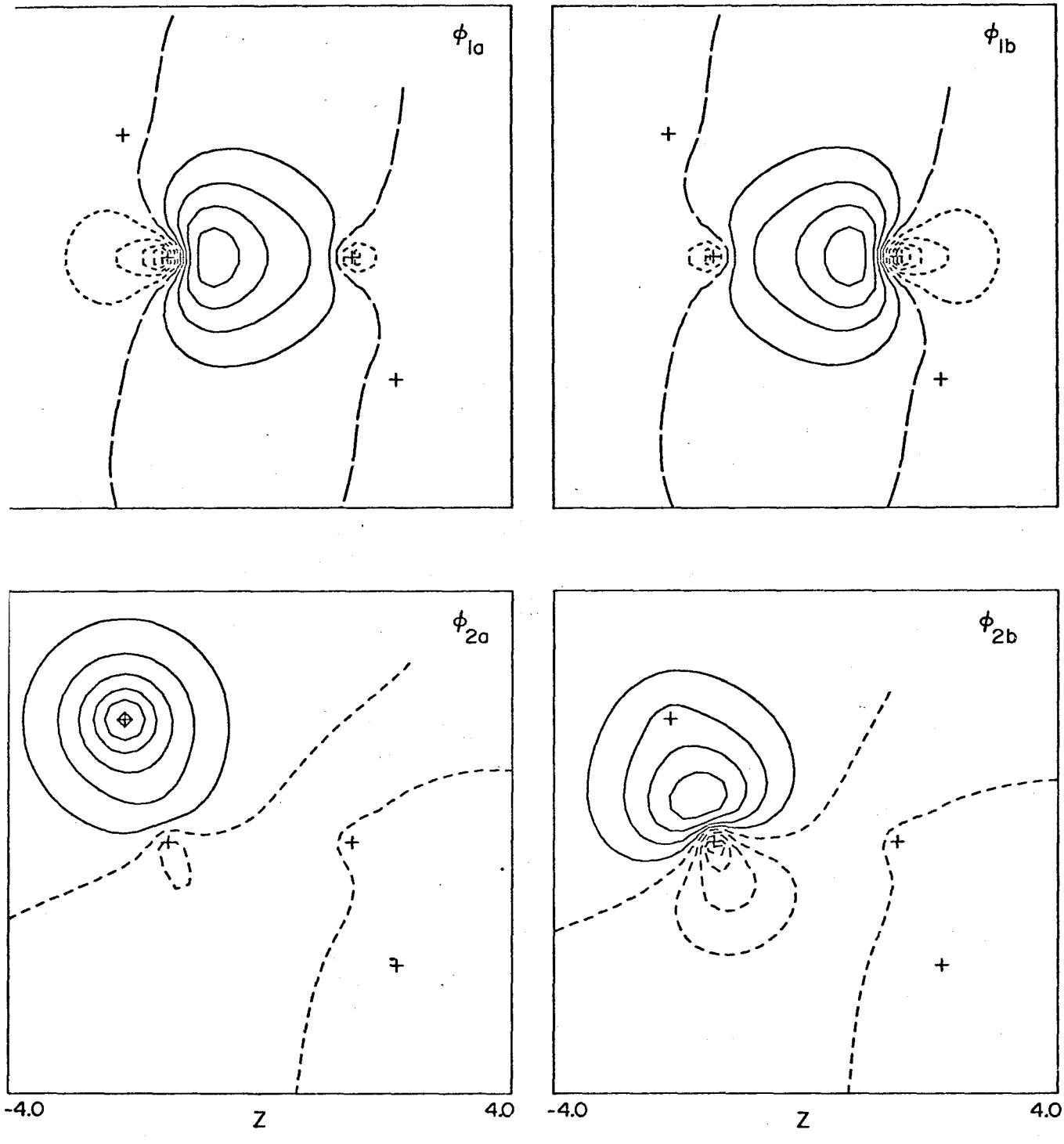

CHAPTER 3.2 The Application of the GVB Method to Ring Opening of Cyclopropane

The Orbital Description of the Ring Opening of Cyclopropane

P. J. Hay,* W. J. Hunt,‡ AND W. A. GODDARD III,†

Arthur Amos Noyes Laboratory of Chemical Physics,[1]
California Institute of Technology, Pasadena, California 91109

Summary

A theoretical study or the ring opening of cyclopropane through use of the ab initio generalized valence bond method is reported, including plots of the self-consistent GVB orbitals for several configurations. As first discovered by Jean and Salem, we find that face-to-face trimethylene is significantly stabilized by allowing the terminal groups to cant toward each other.

---

* National Science Foundation Predoctoral Fellow.

† Alfred P. Sloan Foundation Fellow.

‡ NDEA Fellow.

Only recently[2-4] have theoretical calculations been reported on the simplest diradical, trimethylene

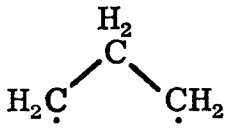

(1)

The major reason for the lack of theoretical treatments of such biradicals is the inadequacy of the molecular orbital (or Hartree-Fock) model in treating the breaking of a bond. In order to avoid this difficulty, we use the ab initio generalized valence bond (GVB) method[5] in which a doubly-occupied pair $\phi_{ia}(1)\phi_{ib}(2) + \phi_{1b}(1)\phi_{ia}(2)$ and then all orbitals (for all 24 electrons) are solved for self consistently, allowing each orbital to use all functions in the basis.

For equilateral cyclopropane ($\theta = 60°$) we carried out minimum basis set[6] GVB calculations allowing either one C-C pair or all three C-C pairs to be split. These calculations led to essentially equivalent descriptions of the C-C bonding pairs, one of which is shown in Figure 1a. We see that this bond is quite aptly described as a bent bond (the hybridization in each orbital is found to be 82% p-character), in good qualitative agreement with the VB results of Coulson and Hurley.[7]

Similar calculations (with one pair split) were performed for several configurations of face-to-face trimethylene[8] (the terminal CH_2 groups perpendicular to the CCC plane, just as in cyclopropane). As shown in Figure 2a, the energy increases monotonically as θ (the CCC angle) is increased from 60° to 130°. As reported by Salem[4] for large θ the terminal groups are not planar but are canted in such a way that

the terminal CH bonds are staggered with respect to the bonds of the central C. The energy curves for the symmetrical canting of the terminal groups are shown in Figure 2b. For $\theta = 110°$, the optimum angle (η) is about 30° for the singlet state and the energy drops 5.1 kcal over that for planar terminal groups (for the triplet state $\eta \sim 24°$ and the energy grop is about 1.2 kcal). For $\theta = 120°$, the energy drop is 4.0 kcal (1.1 kcal for the triplet state) and for $\theta = 130°$, the optimum η for the singlet state is about 25°. The nonbonded interactions normally favoring staggering of neighboring groups lead to 0.5 kcal energy lowering (with respect to a planar terminal group) in ethyl radical[9] and should lead to about 1 kcal energy lowering in trimethylene. This is about the energy lowering observed in the triplet state at $\theta = 110°$ and 120°; however, the singlet states drop several times as much.

The orbitals for the "broken bond" of trimethylene ($\theta = 110°$) are shown in Figure 1bc for the cases of $\eta = 0°$ and $\eta = 30°$. Here we see that the canting of terminal groups towards each other leads the orbitals to rehybridize such as to point away from each other (the hybridizations for the orbital pairs in Figure 1abc of these orbitals are 82%p, 100%p, and 91% p, respectively). As indicated by the dotted lines aa′ and bb′, the canting also leads to a rotation of the orbital axes towards each other (15° between aa′ and bb′). For $\theta = 110°$ and $\eta = -15°$, 0°, 15°, 30°, and 45°, the orbital overlaps are 0.108, 0.140, 0.164, 0.178, and 0.192, respectively (the orbitals have an overlap of 0.790 at $\theta = 60°$ and an overlap of 0.073 for $\theta = 130°$ and $\eta = 30°$).

REFERENCES

1. Contribution No. 4318.
2. R. Hoffmann, J. Amer. Chem. Soc., 1968, 90, 1475.
3. A. K. Q. Siu, W. M. St. John III, and E. F. Hayes, J. Amer. Chem. Soc., 1970, 92, 7249.
4. Y. Jean and L. Salem, Chem. Comm., 1971, 382. These calculations are open-shell Hartree-Fock using symmetry and equivalence restrictions and an adjusted coefficient for the exchange integral between the open shell orbitals. For singlet states, such procedures lead to only approximate total energies; however, the relative energies may be adequate for comparing various geometries.
5. The original suggestions for calculations of this type were made by Hurley, Lennard-Jones, and Pople [Proc. Roy. Soc., Ser. A., 1953, 220, 446] and have been carried out for BH, NH, and other systems by Ruedenberg and others (J. Chem. Phys., 1968, 48, 3414; ibid., 1970, 52, 1811). Such wavefunctions are also special cases of G1 wavefunctions (W. A. Goddard III, Phys. Rev., 1967, 157, 81) but are best obtained by multiconfiguration self-consistent field procedures (see W. Kutzelnigg, J. Chem. Phys., 1964, 40, 3640; W. J. Hunt, W. A. Goddard III, and T. H. Dunning Jr., Chem. Phys. Lett., 1970, 6, 147); and J. Hinze, to be published).
6. The STO-4G basis (W. J. Hehre, R. F. Stewart, and J. A. Pople, J. Chem. Phys., 1969, 51, 2667) was used.

7. (a) C. A. Coulson and W. E. Moffitt, Phil. Mag., 1949, 40, 1; (b) The usual MO description (A. D. Walsh, Trans. Faraday Soc., 1949, 45, 179) is quite different, but these MO's can be localized to lead to a description (N. D. Newton, E. Switkes, and W. N. Lipscomb, J. Chem. Phys., 1970, 53, 2645), similar to the present one.

8. Standard C-C and C-H bond distances of 1.54 Å and 1.08 Å were used.

9. W. A. Latham, W. J. Hehre, and J. A. Pople, J. Amer. Chem. Soc., 1971, 93.

FIGURE CAPTIONS

Figure 1. The GVB orbitals of (a) one C-C bonding pair of cyclopropane; (b) the pair or orbitals describing the broken bond of trimethylene for $\theta = 110°$ but planar terminal groups; (c) the same as (b) except that the terminal groups are canted inward by 30°. The location of each carbon nucleus is indicated by +. The nodal line is indicated by long dashes and the contour intervals are 0.1 (in atomic units).

Figure 2. (a) The energy curve for the ring opening of cyclopropane. (90, 90) indicates that the terminal groups are taken as planar ($\eta = 0°$) for $\theta \geq 100°$. (90_c, 90_c) indicates that the terminal groups have been canted ($\eta = 30°$) for $\theta \geq 100°$. (b) The energy curve for the symmetrical canting of the terminal groups in trimethylene.

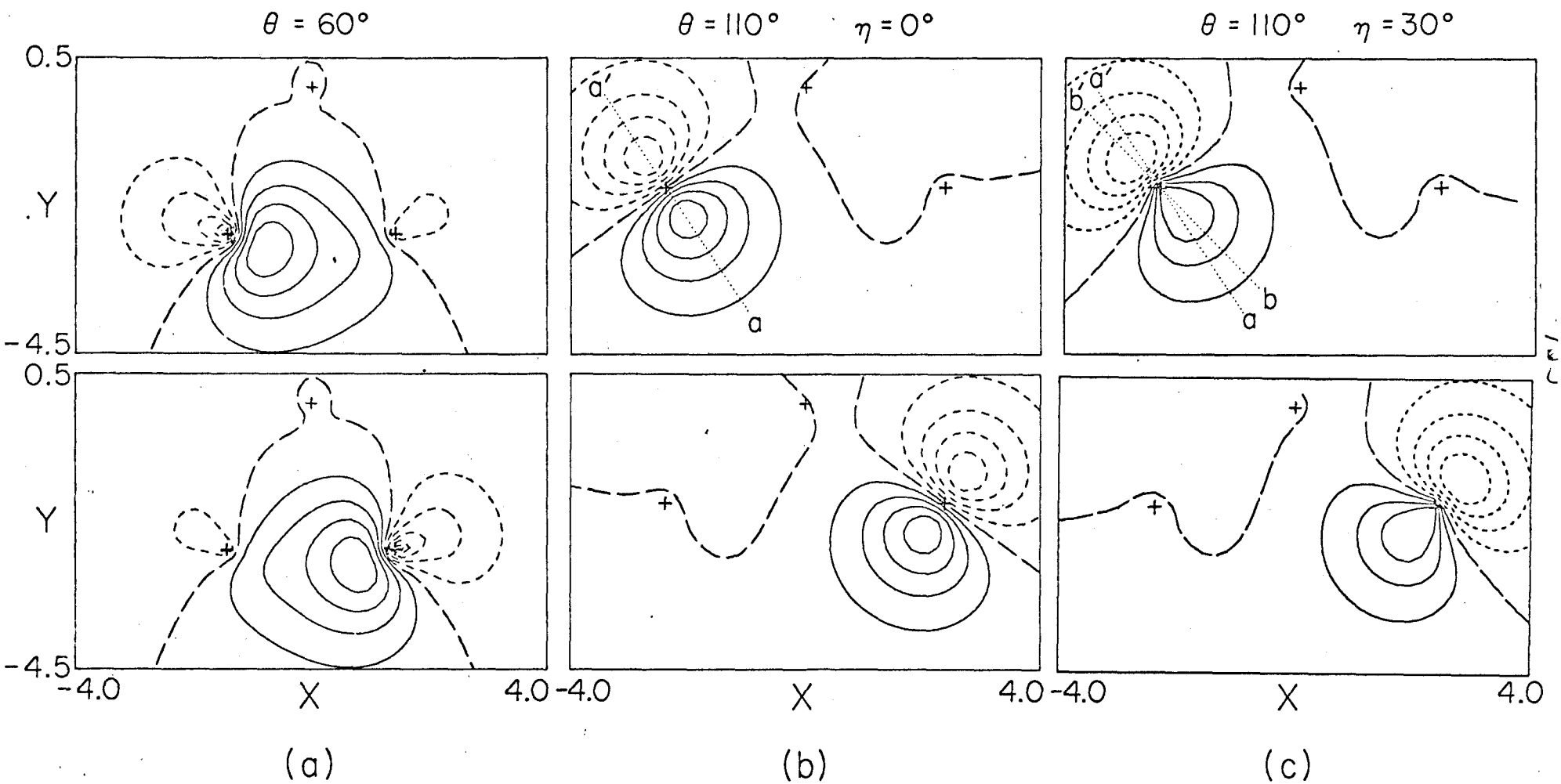
θ = 60°
θ = 110°
η = 0°
θ = 110°
η = 30°
0.5
Y
-4.5
a
b
-4.0
X
4.0
(a)
(b)
(c)

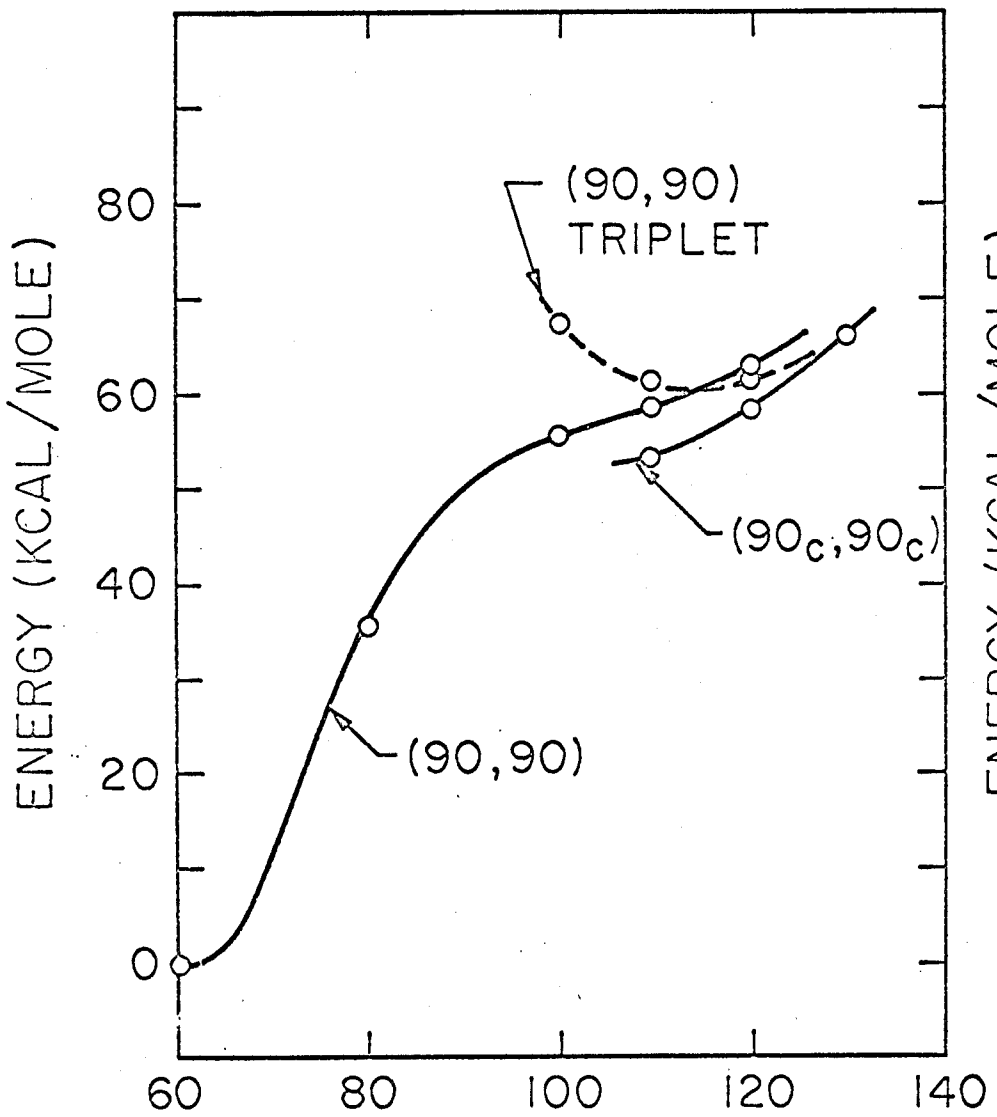
ENERGY (KCAL/MOLE)
0
20
40
60
80
(90,90)
TRIPLET
(90c,90c)
(90,90)
60
80
100
120
140
CCC ANGLE (DEGREES)

(a)

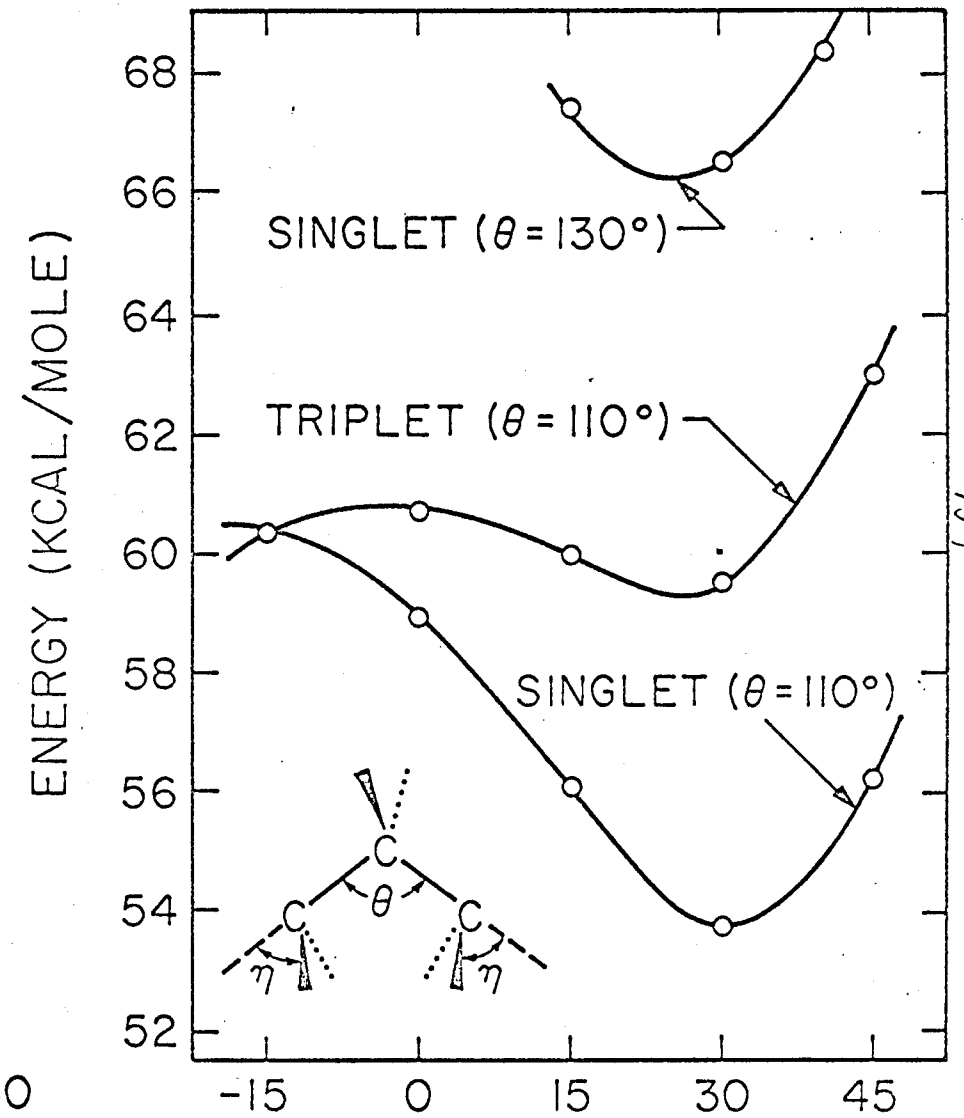
ENERGY (KCAL/MOLE)
52
54
56
58
60
62
64
66
68
SINGLET (θ = 130°)
TRIPLET (θ = 110°)
SINGLET (θ = 110°)
C
θ
C
C
η
η
-15
0
15
30
45
CANTING ANGLE η (DEGREES)

(b)

CHAPTER 3.3 A GVB Study of Low-Lying States of Methylene

GENERALIZED VALENCE BOND CALCULATIONS ON THE STATES OF METHYLENE

P. JEFFREY HAY,[†] WILLIAM J. HUNT,[††] W. A. GODDARD III*

Arthur Amos Noyes Laboratory of Chemical Physics

California Institute of Technology, Pasadena, California 91109 U.S.A.

Received:

Generalized valence bond (GVB) calculations are reported for the $^3B_1$, $^1A_1$ and $^1B_1$ states of the CH_2 molecule. The GVB method is discussed and compared with other multi-configuration and separated pair methods. The 0-0 $^3B_1 \rightarrow {}^1A_1$ and $^1A_1 \rightarrow {}^1B_1$ transitions are found to occur at 0.50 and 1.40 eV, respectively.

---

† NSF Predoctoral Fellow

†† National Defense Education Act

* Alfred P. Sloan Foundation Fellow.

We report here the results of Generalized Valence Bond (GVB) calculations on the $^1A_1$, $^3B_1$ and $^1B_1$ states of the CH_2 molecule. In Section I we discuss the procedures involved in the GVB method, which is an extension of the Hartree-Fock molecular orbital approach. In Section II we present the results for CH_2.

1. METHOD

In the GVB approach[1] we replace the orbitals ϕ_i which are doubly occupied in the Hartree-Fock (HF) wavefunction:

$$\psi_{HF} = A[\phi_1\alpha\phi_1\beta\phi_2\alpha\phi_2\beta\cdots\phi_n\alpha\phi_n\beta] \qquad (1)$$

by singlet coupled pairs of orbitals:

$$\psi_{GVB} = A[(\phi_{1a}\phi_{1b} + \phi_{1b}\phi_{1a})(\phi_{2a}\phi_{2b} + \phi_{2b}\phi_{2a}) \qquad (2)$$

$$\cdots(\phi_{na}\phi_{nb} + \phi_{nb}\phi_{na})\ \alpha\beta\alpha\beta\cdots\alpha\beta]$$

For a state of spin S the last 2S orbitals are singly occupied with open α as in HF. The wavefunction (2) has the form of a simple valence bond (VB) function,[2] the difference being that in (2) the orbitals are solved self-consistently rather than taken as atomic orbitals in VB. In addition to giving an energy lower than HF the GVB approach leads to proper treatment of the breaking of bonds and offers the conceptual advantage of leading to localized orbitals in close correspondence to the qualitative ideas of bonding and non-bonding pairs of molecules.

As was originally shown by Hurley, Lennard-Jones, and Pople,[3] each pair in (2) can be represented in terms of two natural orbitals (NO's).

$$\phi_{ia}^{(1)}\phi_{ib}^{(2)} + \phi_{ib}^{(1)}\phi_{ia}^{(2)} = C_{1i}\phi_{1i}^{(1)}\phi_{1i}^{(2)} + C_{2i}\phi_{2i}^{(1)}\phi_{2i}^{(2)} \qquad (3)$$

Coulson and Fischer[4] had also discussed GVB-like descriptions for H_2. In this representation GVB is seen to be a special case of the separated pair,[5-7] strongly orthogonal geminal,[8-10] self-consistent group,[11] and multi-configuration SCF[13-16] wavefunctions where, in general more than 2 NO's are used.[17]

In GVB as in these other methods the strong orthogonality constraint[18] is imposed, i.e., the NO's of pair i are taken to be orthogonal to each other as well as to the NO's of the other pairs. This means that the GVB orbitals satisfy the relations

$$\begin{aligned} &\langle \phi_{ia} | \phi_{ib} \rangle \neq 0 \\ &\langle \phi_i | \phi_j \rangle = 0 \qquad \text{otherwise.} \end{aligned} \qquad (4)$$

Relaxation of the orthogonality constraints makes GVB equivalent to the G1 method.[19]

As has been shown by Kutzelnigg[7] and Silver, Mehler and Ruedenberg,[6] the total electronic energy has the form

$$E = \sum_k f_k h_k + \sum_{k,\ell} A_{k\ell} J_{k\ell} + b_{k\ell} K_{k\ell} \qquad (5)$$

where $h_k = \langle k|h|k\rangle$, $J_{k\ell}$ and $K_{k\ell}$ are the usual Coulomb and exchange integrals, and f_k is the occupation number. [f_k will be 2 for

doubly occupied orbitals, 1 for singly occupied open shell orbitals, and C_i^2 for GVB NO's.]

Using the variational principle, one obtains the self-consistent field equations

$$[H_k - \sum_{j\neq k} |j\rangle\langle j|H_j]\,\phi_k = \epsilon_k\phi_k \qquad (6)$$

$$k = 1,\ 2,\ \cdots,\ N$$

where N is the number of distinct orbitals. With the exceptions of a few strongly orthogonal geminal calculations on small diatomic molecules and several multi-configuration SCF calculations, previous calculations have not fully optimized the orbitals since each function was obtained within a fixed partition of the basis. As discussed by Hunt, Dunning and Goddard,[20] the method used here leads to correct mixing of all occupied orbitals with each other and with the virtual orbitals.

In particular, lack of full optimization has led to poor descriptions of rotational barriers in self-consistent group function calculations, [e.g.; the rotational barrier in ethane was calculated to be -5.1 kcal (the eclipsed form lower)],[12] whereas good descriptions are obtained in HF and GVB [in ethane we found the eclipsed form to be higher by 3.1 kcpm in good agreement with HF and experiment (3.3 and 2.9 kcpm, respectively)].

2. THE METHYLENE MOLECULE

Several recent experimental[21, 22] and theoretical[23-26] studies on the electronic structure of CH_2, the methylene molecule, have examined various aspects of the $^3B_1$ ground state and the low-lying $^1A_1$ and $^1B_1$ excited states. Because of the important implications for singlet and triplet carbene chemistry,[7] it is surprising that little quantitative information is known about these states. Spectroscopic evidence indicated that the triplet ground state was linear and that the $^1A_1$ and $^1B_1$ band angles were 104.2° and ~ 140°, respectively. Although the ab-initio calculations predicted correct geometries for the singlet states, they all showed a relatively flat potential curve with a minimum at a bond angle of ~ 135° for the triplet state. Recent experimental data[28-30] have since confirmed a bent geometry in agreement with the theoretical predictions.

The 0-0 $^1B_1 \leftarrow {}^1A_1$ transition, while not observed directly, has been extrapolated to occur at about 0.88 eV (the lowest observed transition length at 1.34eV) and an upper limit of 1.0 eV has been assigned to the 0-0 $^1A_1 \leftarrow {}^3B_1$ transition.[21, 22]

To date the best theoretical values for these transitions, 0.97 and 0.96 eV, respectively, have been obtained by O'Neil, Schaeffer and Bender (OSB)[26] from electronic configuration interaction calculations.

The GVB function for these states has the form

$$^1A_1: \psi = A\phi_{1s}\bar{\phi}_{1s}(\phi_{1a}\bar{\phi}_{1b} + \phi_{1b}\bar{\phi}_{1a})(\phi_{2a}\bar{\phi}_{2b} + \phi_{2b}\bar{\phi}_{2a})(\phi_{3a}\bar{\phi}_{3b} + \phi_{3b}\bar{\phi}_{3a})$$

$$^{1,3}B_1: \psi = A\phi_{1s}\bar{\phi}_{1s}(\phi_{1a}\bar{\phi}_{1b} + \phi_{1b}\bar{\phi}_{1a})(\phi_{2a}\bar{\phi}_{2b} + \phi_{2b}\bar{\phi}_{2a})(\phi_{3a}\bar{\phi}_{3b} \pm \phi_{3b}\bar{\phi}_{3a})$$

where the orbitals are all optimized for the three states subject to the strong orthogonality constraints between pairs.

The calculations were performed at four HCH angles (90, 105, 135 and 180 degrees), each with a CH bond distance of 2.1 a_0. A bond angle of 105° nearly corresponds to the minimum of the $^1A_1$ potential curve, and a bond angle of 135° corresponds to the approximate minimum for the $^3B_1$ and $^1B_1$ curves. The basis sets employed were a double zeta contracted gaussian basis[31, 32] and the same set augmented by a set of uncontracted d functions on the carbon atom with an exponent of 0.532.

As shown in Fig. 1, the bonding pairs $[\phi_{1a}, \phi_{1b}]$ and $[\phi_{2a}\phi_{2b}]$ GVB pairs are qualitatively similar for all states in that each pair consists of a hybridized orbital on the carbon oriented towards one of the hydrogen and an essentially hydrogenic orbital delocalized somewhat onto the carbon. For the B_1 states the $[\phi_{3a}, \phi_{3b}]$ orbitals may be taken to be a_1 and b_1 symmetry orbitals without restriction. For the $^1A_1$ state we obtain a pair of sp hybridized lobe type orbitals pointed above and below the molecular plane and bent back from the hydrogen. The splitting in this latter pair results in a significant lowering of the energy (.0214 a.u.) relative to the Hartree-Fock description. As has been pointed out, the poor description of this pair by HF arises from the near degeneracy of the $3a_1$ and $1b_1$ orbitals.

In Table I we compare the energies of the GVB wavefunctions at the lowest calculated points for each state [in the GVB 1-pair calculation, the $^1B_1$ and $^3B_1$ states were treated as in open-shell Hartree-Fock theory and the $^1A_1$ was treated by splitting only the sp pair]. We note that the 1-pair GVB description is a reasonably consistent description for all states in that each state dropped approximately the same amount (.0221, .0227, and .0274 a.u.) in energy when the CH bonding pairs were split. The two configuration wavefunctions of OSB in the table are equivalent to the 1-pair GVB calculation although we used a larger basis set.

We also performed a configuration interaction calculation (doubled as GVB-CI) at each point using the six orthogonal GVB natural orbitals as a basis (keeping the 1s pair doubly occupied). As indicated in Table I this led to an improvement in energy of .0115, .0052, and .0080 a.u. for the respective $^3B_1$, $^1A_1$ and $^1B_1$ states. OSB obtain a much larger improvement in energy in their CI calculations (see Table I) as they also include excitations not involving valence orbitals (semi-external correlation).

As shown in Fig. 2, the $^3B_1$ state remains the ground state for all $\theta < 180°$ until θ reaches approximately 100°, where the curve crosses the $^1A_1$ state (θ is the HCH angle). The $^3B_1$ and $^1B_1$ states exhibit shallow minima at approximately $\theta = 135°$ with energies 0.39eV and 0.28eV below the energies of the respective $^3\Sigma_\delta^-$ and $^1\Delta g$ linear configurations.

From the GVB-CI results we predict the 0-0 $^3B_1 \rightarrow {}^1A_1$ transition (see Table II) to occur at 0.50 eV and the 0-0 $^1A_1 \rightarrow {}^1B_1$ transition to occur at 1.40 eV. This is in conflict with both the CI calculations of OSB and the experimental estimates for these quantities. However, the CI calculations did not use any 3d polarization functions which we find to be important for the $^1A_1$ state. Indeed when we repeated the calculations using essentially the same basis as OSB, we obtain 0.97 and 1.11 eV in good agreement with the values of 0.96 and 0.97 eV from the more extensive CI calculation for the respective 0-0 transitions. Inasmuch as the lowest observed $^1A_1$ - $^1B_1$ transactions was observed by Herzberg and Johns[22] to be at 1.34. If we assume this b to the 0-0 transition inverting for zero point energies we calculate an experimental energy of 1.41 eVin good agreement with the theoretical value. Instead, Herzberg and Johns estimated that the transition was (000)→(060) and extrapolated a value of 0.88 eV for 0-0. We find the $^3B_1$ - $^1B_1$ splitting to be 1.88 eV at 135° and 1.77eV at 180°. This splitting is essentially twice the exchange integral of the σ and π compared σ and π orbitals and would be expected to be comparable in size to the splittings in C where the ^3P - ^1O splitting is 1.26 eV. (In C the unpaired orbitals are both p orbitals).

REFERENCES

[1] W. J. Hunt, P. J. Hay and W. A. Goddard, to be published.

[2] L. Pauling, J. Amer. Chem. Soc., 53, 1367 (1931); J. C. Slater, Phys. Rev., 37, 481 (1931), 38, 1109 (1931).

[3] A. C. Hurley, J. E. Lennard-Jones and J. A. Pople, Proc. Roy Soc (London), A220, 446 (1963).

[4] C. A. Coulson and I. Fischer, Phil Mag., 40, 386 (1949).

[5] J. M. Parks and R. G. Parr, J. Chem. Phys., 28, 335, (1958); 32, 1567 (1960).

[6] D. M. Silver, E. L Mehler and K. Ruedenberg, J. Chem. Phys., 52, 1174, 1181, 1206 (1970).

[7] W. Kutzelnigg, J. Chem. Phys., 40, 3640 (1964); R. Ahrlichs and W. Kutzelnigg, J. Chem. Phys., 48, 1819 (1968).

[8] R. McWeeny and K. A. Ohno, Proc. Roy Soc., (London), A255, 367 (1960).

[9] M. Klessinger and R. McWeeny, J. Chem. Phys., 42, 3343 (1965).

[10] M. Levy, W. J. Stevens, H. Schull and S. Hagstron, J. Chem. Phys., 52, 5483 (1970).

[11] M. Klessinger, J. Chem. Phys., 43, 5117 (1965);

[12] M. Klessinger, J. Chem. Phys., 53, 225 (1970);

[13] A. C. Wahl and G. Das, Adv. Quant. Chem., 5, 261 (1971).

[14] E. Clementi and A. Veillard, J. Chem. Phys., 44, 3050 (1966).

[15] J. Hinzle and C. C. C. J. Roothaan, Prog. Theor. Physics Supp., 40, 37 (1967).

[16] R. McWeeny, Sym. Trans. Far. Soc., 2, 7 (1968).

[17] (a) P. O. Löwdin, Phys. Rev., 97, 1474 (1955);
(b) P. O. Löwdin and H. Schull, Phys, Rev., 101, 1730 (1956).

[18] T. Arai, J. Chem. Phys., 33, 95 (1960); P. O. Löwdin, J. Chem. Phys., 35, 78 (1961).

[19] W. A. Goddard III, Phys. Rev., 157, 73, 81 (1967).

[20] (a) W. J. Hunt, T. H. Dunning Jr., and W. A. Goddard III, Chem. Phys. Lett., 3, 606 (1969).
(b)W. A. Goddard III, T. H. Dunning Jr., and W. J. Hunt, Chem. Phys. Lett., 4, 231 (1969).
(c) W. J. Hunt, W. A. Goddard III, and T. H. Dunning, Jr., Chem. Phys. Lett., 6, 147 (1970).

[21] G. Herzberg, Proc. Roy. Soc (London), A262, 291 (1961).

[22] G. Herzberg and J. W. C. Johns, Proc. Roy. Soc. (London), A295, 107 (1966).

[23] J. M. Foster and S. F. Boys, Rev. Mod. Phys., 32, 305 (1960).

[24] C. Salez and A. Veillard, Theoret. Chim. Acta., 11, 441 (1968).

[25] J. F. Harrison and L. C. Allen, J. Amer. Chem. Soc., 91, 807 (1969)

[26] S. V. O'Neil, H. F. Schaeffer III, and C. F. Bender, J. Chem. Phys., 55, 162 (1971).

[27] P. P. Gaspar and G. S. Hammond, Carbene Chemistry, (Ed. W. Kirmse (Academic, New York, 1964).

[28] R. A. Bernheim, H. W. Bernard, P. S. Wang, L. S. Wood, and P. S. Skell, J. Chem. Phys., 53, 1280 (1970).

[29] E. Wassermann, W. A. Yager and V. Kuck, J. Amer. Chem. Soc., 92, 7491 (1970).

[30] G. Herzberg, J. Chem. Phys., (1971).

[31] S. Huzinager, J. Chem. Phys., 42, 1293 (1965).

[32] T H. Dunning Jr., J. Chem. Phys., 53, 2823 (1970).

Table 1

GVB Energies for the States of CH_2[a]

Reference	Method	Energy (a.u.)		
		$^3B_1(135°)$	$^1A_1(105°)$	$^1B_1(135°)$
This work	HF	-38.9202	-38.8821	-38.8544
	GVB-1 pair	-38.9202	-38.9035	.8544
	GVB-3 pair	-38.9483	-38.9362	.8818
	GVB-CI	-38.9598	-38.9414	.8898
O'Neil, Bender & Schaeffer(Ref. 26)	HF	-38.9136	-38.8620	.8452
	1 pair		-38.8772	
	CI	-38.9826	-38.9472	.9114
Harrison and Allen Ref. 25)	HF	-38.893	-38.843	.822
	VB-CI	-38.915	-38.864	.833
Foster and Boys Ref. 23)				

[a] The energies reported from Refs. 23, 25 and 26 are the calculated minima for each state.

Table 2

CH_2 Excitation Energies (eV)

References	Method	$^3B_1 \rightarrow {}^1A_1$ (0-0)	$^1A_1 \rightarrow {}^1B_1$ (0-0)	$^1A_1 \rightarrow {}^1B_1$ (vert)
This work	GVB 1 pair	0.45	1.34	1.91
		( )	( )	
	GVB 3 pair	0.32	1.49	2.06
		( )		
	GVB-CI[a]	0.50	1.40	1.88
		(0.97)	(1.11)	(1.69)
O'Neill, Bender, Schaeffer (Ref. 26)	CI	0.96	0.97	1.56
Harrison and Allen (Ref. 25)	VB-CI	1.39	0.84	1.52
Foster and Boys (Ref. 23)		1.06	1.55	
Experimental (extrapolated) (Ref. 22)	<1.0	0.88		

[a] The quantities in parentheses were obtained by using a DZ basis essentially identical to that used in Ref. 26.

FIGURE CAPTIONS

Fig. 1 GVB orbitals for CH_2 in the $^1A_1$ state. (four pages)

Fig. 2 Potential energy curves for the $^3B_1$, $^1B_1$, and $^1A_1$ states. The GVB curves are in solid lines; the CI curves are in dashed lines.

CH2 SINGLET A1 BOND ORBITAL A

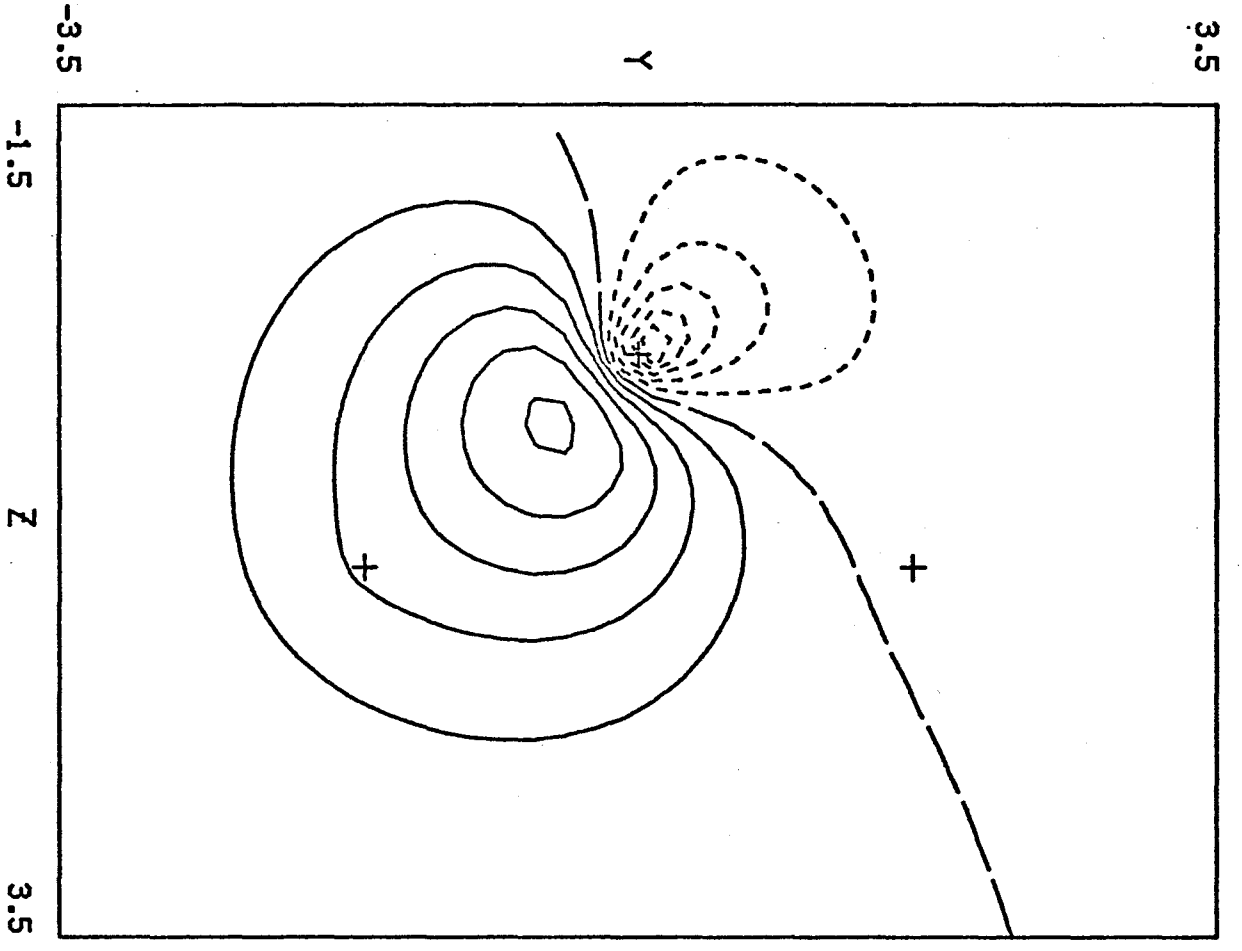

CH2 SINGLET A1 BOND ORBITAL B

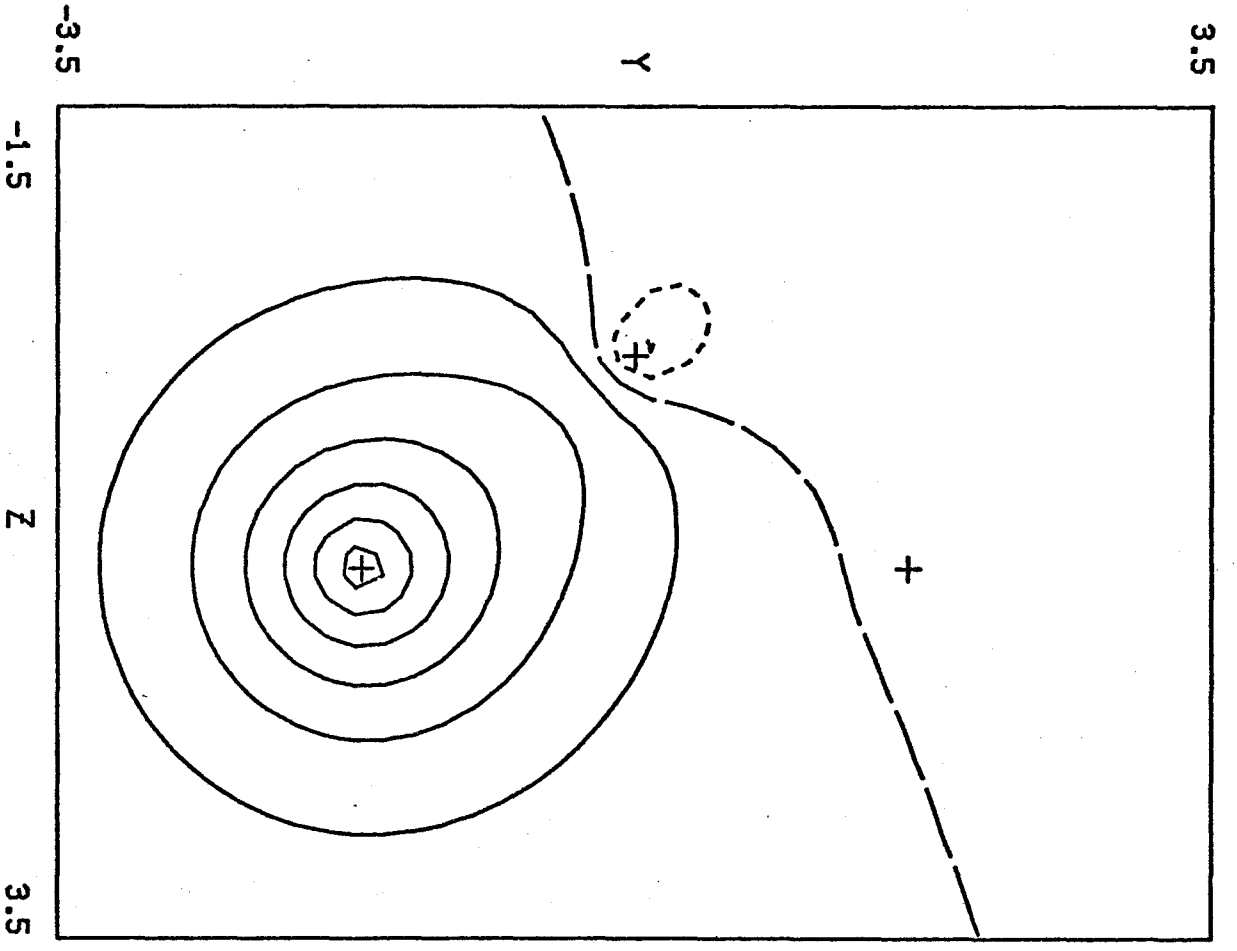

CH2 SINGLET A1 LONE ORBITAL A

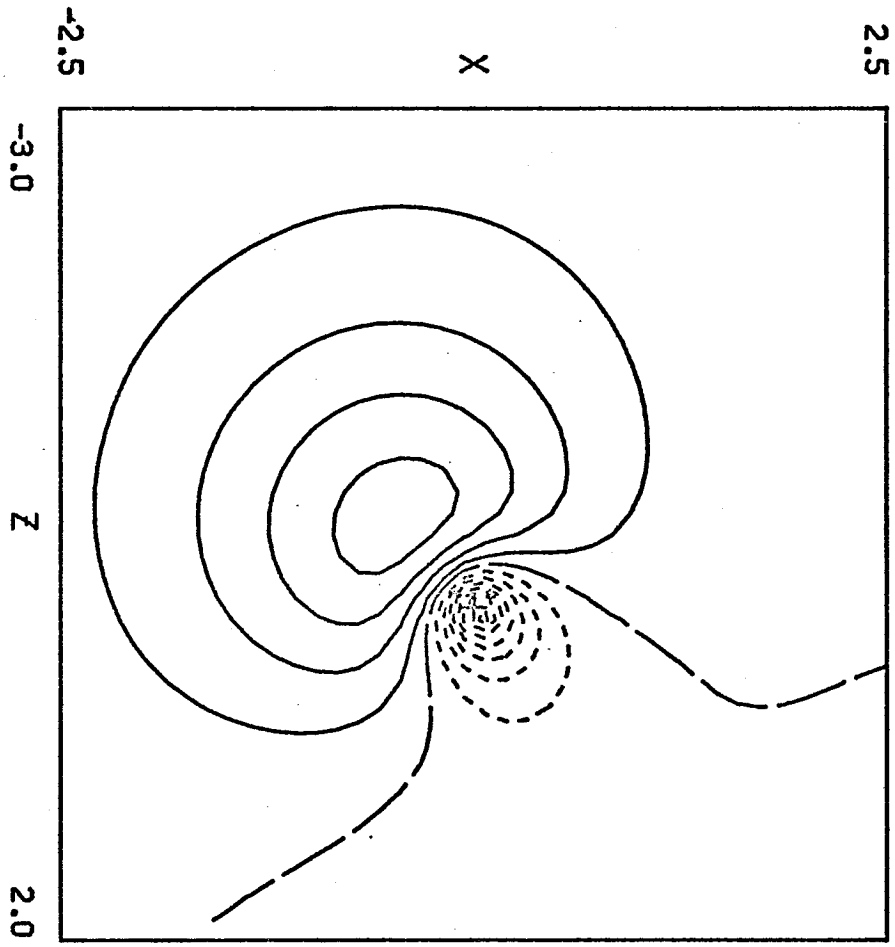

CH2 SINGLET A1 LONE ORBITAL B

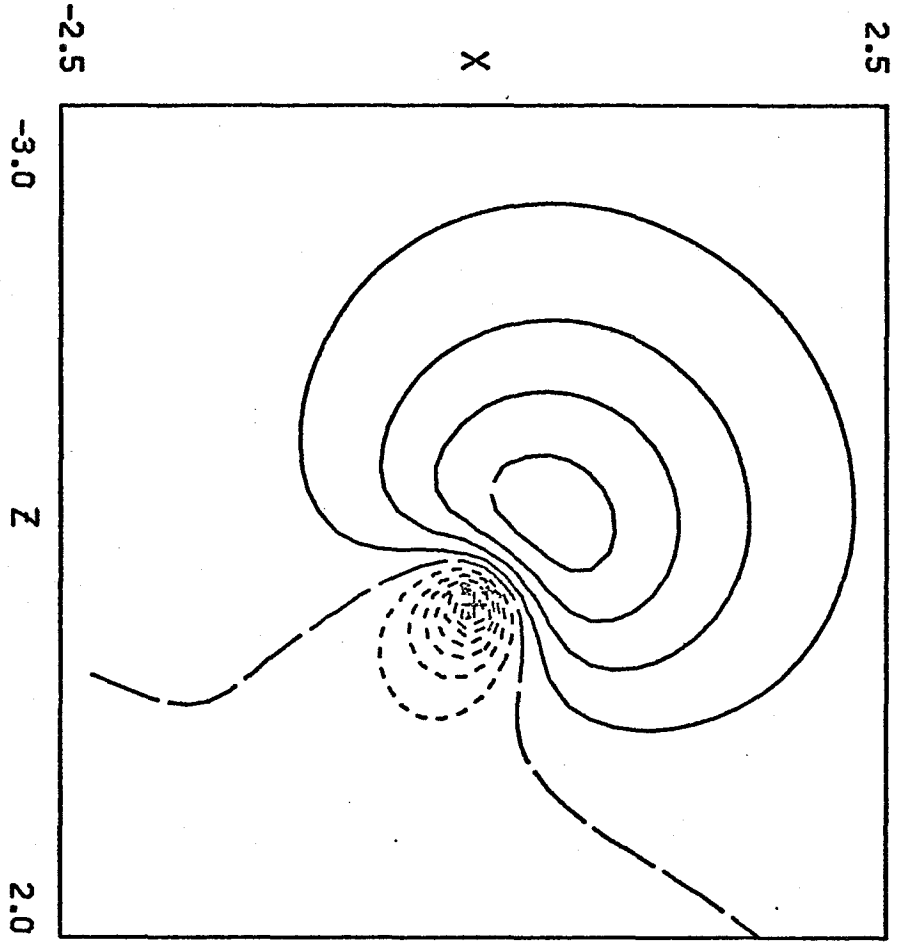

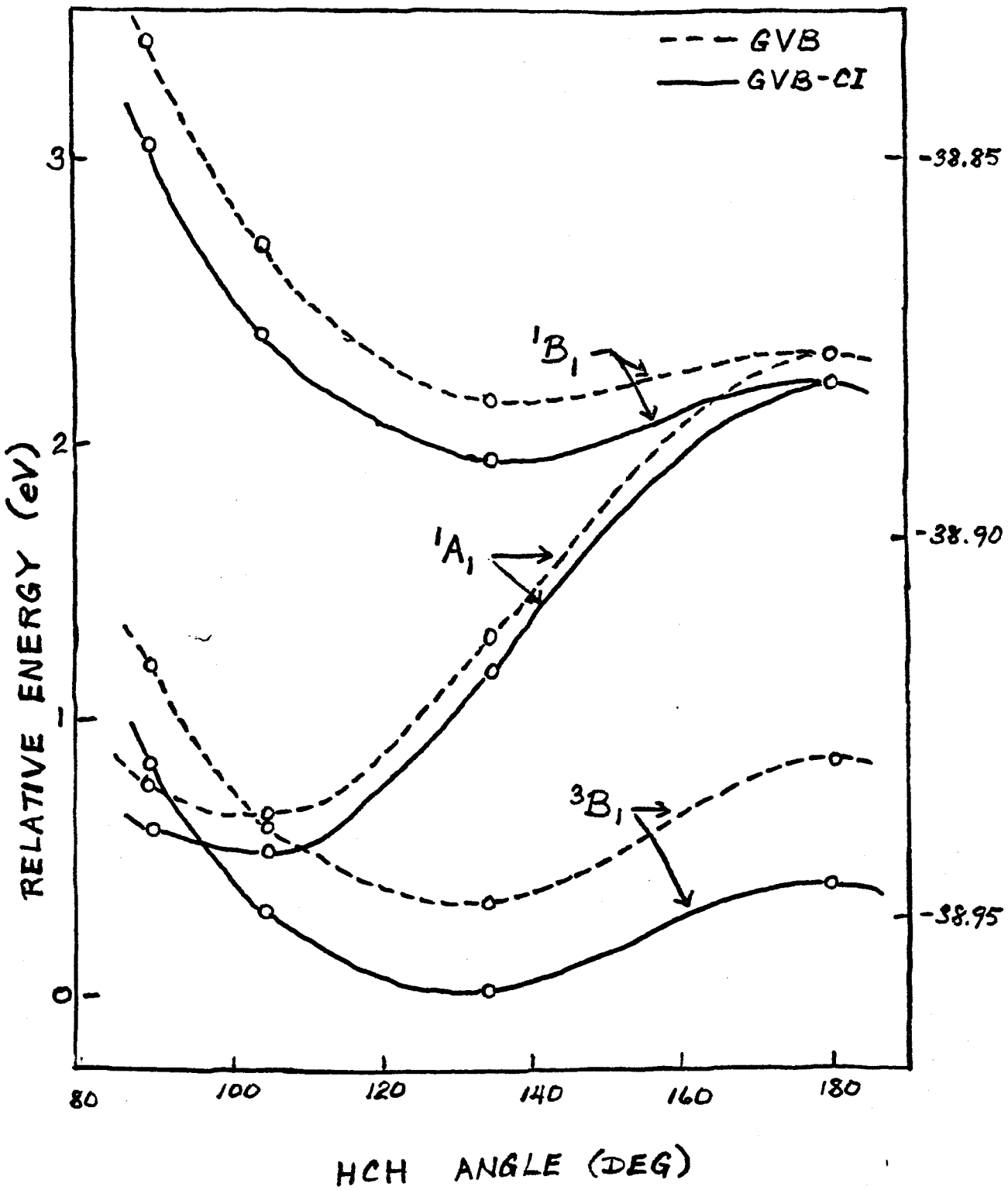
GVB
GVB-CI
$^1B_1$
$^1A_1$
$^3B_1$
RELATIVE ENERGY (eV)
3
2
1
0
-38.85
-38.90
-38.95
80
100
120
140
160
180
HCH ANGLE (DEG)

CHAPTER 3.4 Diatomic Hydrides and Fluorides — A GVB View

I. INTRODUCTION

One of the goals of quantum chemistry has been quantitative prediction of chemical phenomena. Success in this goal is being achieved slowly.[1] Unfortunately, the expense of the calculations necessary for quantitative prediction will probably prevent their use on any but the smallest chemical systems. The more important goal, however, is to provide a theoretical framework for interpreting experimental information. The valence bond (VB) theory has been a fertile source of concepts about bonds and lone pairs in molecules.[4]

In the molecular orbital (MO) theory, symmetry has played a major part in predicting the equilibrium geometries of molecules[5] and the courses of chemical reactions.[6] One of the early successes of the MO theory was the construction and use of orbital correlation diagrams for diatomic molecules.[7,8] The concept of an aufbau principle using bonding and antibonding orbitals allows a large number of experimental observations to be rationalized.[9] The straightforward prediction of the ground state of the O_2 molecule as a triplet state illustrated the power of the correlation diagram.[11] Of course the MO theory has well-known limitations as a qualitative model. The most serious of these faults is its inability to describe bond breaking as a

continuous process.[12] Thus the MO correlation diagram provides little information about the dissociation limits for molecular states.

In earlier papers of this series, we developed the generalized valence bond (GVB) method and applied it to several problems. Since the GVB method is a generalization of both the MO and VB theories, it offers a new and improved perspective for a qualitative study of diatomic molecules. In this paper we examine the hydrides and fluorides of first row atoms. Although the results of calculations are presented, the emphasis will be placed on new concepts based on the GVB method.

II. THE GVB METHOD

In the VB theory[12] each bond is described by a two-electron wavefunction of the form

$$\phi_A(1)\phi_B(2)[\alpha(1)\beta(2) - \beta(1)\alpha(2)] \qquad (1)$$

where ϕ_A and ϕ_B are atomic orbitals from atoms A and B, and α and β are the usual spin functions. Since ϕ_A and ϕ_B are not variationally optimized, several problems arise. The choice of atomic orbitals is not always clear. For example in methane the choice of sp^3 hybrid orbitals would be clear, but in CH_3F the choice would not be obvious. The form (1) given above is appropriate for a covalent bond. We might also have used ionic terms of the form $\phi_A\phi_A$ and $\phi_B\phi_B$.

A more general VB calculation would include these terms in addition to (1). The advantage of the VB approach is that a correct description of bond breaking is built into the wavefunction. The weakness of this approach is that it forms the wavefunction for a molecule in an arbitrary fashion; the quality of the resulting description is strongly dependent on the intuition of the user of the method.

The MO theory[12] represents a bond by a function of the form

$$\phi_{MO}(1)\phi_{MO}(2)[\alpha(1)\beta(2) - \beta(2)\alpha(1)]$$

The orbital ϕ_{MO} has the form

$$\phi_{MO} = C_A\phi_A + C_B\phi_B$$

where the coefficients C_A and C_B are optimized. Since only one orbital is used, the bond breaking process cannot be described correctly. The MO theory uses a simple form which is variationally optimized. This makes it useful for molecules near their equilibrium geometry.

Considering the molecule as a whole, we emphasize that the VB theory requires an arbitrary assignment of the atomic functions ϕ_A and ϕ_B to each bond while MO theory optimizes the entire choice of the orbitals ϕ_{MO}. Thus the VB approach is not as well defined a procedure as MO theory. An obvious improvement on the two methods would be to use the VB form (1) but optimize the orbitals ϕ_A and ϕ_B.[14] The result

would be a well-defined theory combining the advantages of both older methods. In order to facilitate calculations, we require the orbitals describing different electron pairs to be orthogonal. In practice we usually find this restriction to be unimportant.[15, 16]

Most of the states we will discuss have unpaired electrons. We may include these in a manner basically like that of open shell Hartree-Fock theory. These open shell orbitals are required to be orthogonal to each other and to all other orbitals.

III. CALCULATIONS

All calculations in this study used the STO-4G basis described by Pople[17] with the standard molecular exponents he recommends. This basis set has been shown to be an efficient method of carrying out minimum basis set calculations for polyatomic molecules. Integral evaluation was accomplished with the Polyatom program as modified by Basch et al.[18] SCF calculations used programs written by the author.[19]

Nuclear geometries used were those determined experimentally[10,20] for the ground states of the molecules considered. A listing of these values appears in Table I.

IV. THE GVB DESCRIPTION OF ATOMS

We discussed the relation of VB, MO, and GVB methods in the description of bonds, but any doubly occupied molecular orbital may be "split" to give two GVB orbitals. In atoms we find one very important splitting. The Hartree-Fock description of the beryllium atom in the 1s ground state has the electron configuration[21]

$$(1s)^2(2s)^2.$$

The 1s orbital of first row atoms plays no active role in the process of molecule formation. We will omit this orbital from further discussion; in the GVB calculation it remains a doubly occupied Hartree-Fock orbital. But the description of the two valence electrons is quite different in a GVB picture.[22] The two electrons in the 2s orbital have too much repulsion between them. The energy of the wavefunction is substantially lowered if the orbitals polarize in opposite directions.[23] The two GVB orbitals become

$$\phi_A = \phi_{2s} - \lambda\phi_{2pz}$$
$$\phi_B = \phi_{2s} + \lambda\phi_{2pz}$$

These hybridized orbitals still have high overlap with each other (about 0.69), but they now have directional character. We represent one of these orbitals as

where the two lines connect points with equal amplitude. The two lobes have opposite sign. The Be atom is drawn as

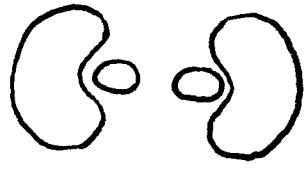

$[sp\bar{z}, spz]$

where we displace the two orbitals for clarity. The box indicates that the two orbitals are coupled together to give a singlet state. We refer to the two hybridized orbitals as $sp\bar{z}$ and spz.

To form the boron atom in the 2p state, we add a p_y orbital. The resulting picture is

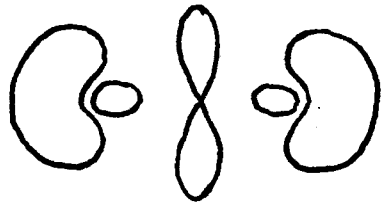

$[sp\bar{z}, spz], p_y$

where the p orbital is along the y-axis.

The carbon atom in the 3p state becomes

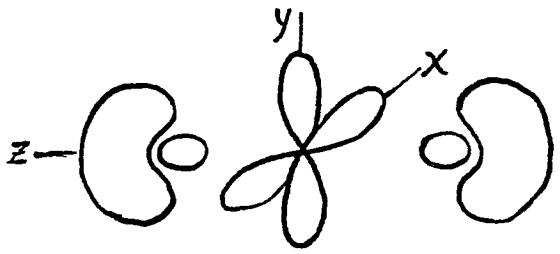

$[sp\bar{z}, spz], p_x, p_y$

where the p orbitals point along the x and y axes.

For the nitrogen atom in the 4s state, the Hartree-Fock configuration is

$$\cdots (2s)^2(2p_x)(2p_y)(2p_z).$$

Since all three p orbitals are already occupied, no empty direction exists in which the $(2s)^2$ electron pair may split. Thus for the ground states of nitrogen, oxygen, and fluorine, the GVB description is qualitatively equivalent to the Hartree-Fock picture.

The effect we described in the GVB method has been emphasized earlier by Sinanoglu[24] and by Schaefer.[25] In a more mathematical view this effect is caused by strong mixing of a configuration

$$\cdots (2s)^0(2p)^N$$

with the Hartree-Fock configuration

$$\cdots (2s)^2(2p)^{N-2}.$$

The quantitative effect of this second configuration on energy differences between states of the atom[24] and on

one-electron properties[25] has been the primary concern previously. Our interest here is in the new qualitative picture the GVB method suggests for bond formation.

V. GVB WAVEFUNCTIONS FOR BeH AND BeF

Starting with the GVB description for the Be atom, we can easily understand the $^2\Sigma^+$ ground state of the BeH molecule. At $R = \infty$, the two Be orbitals of the 1s state are singlet coupled. At $R = R_e$, we represent the wavefunction as

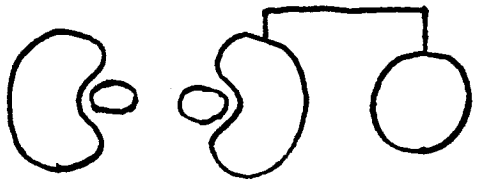

$$[spz, H], sp\bar{z}$$

The line connecting spz and H indicates singlet coupling. Now the wavefunction clearly must change form between $R = \infty$ and $R = R_e$. A similar change in form must occur in reactions[29] such as the exchange process

$$H_2 + D \rightarrow HD + H.$$

In such reactions potential energy barriers exist along the reaction path. By analogy we would expect a potential energy maximum to occur at some distance greater than R_e. Although configuration interaction calculations by Chan and Davidson[26] did not find such a barrier between R_e and 5.0 bohr, a recent multiconfiguration self consistent field (MC-SCF) calculation[28] by Dunning[28] shows that a potential

maximum does exist near 5.75 bohr. These potential energy humps are expected[30] for many molecular states whose formation involves spin recoupling.

We may also get a low-lying state of $^2\pi$ symmetry using the ^{3}p state of the Be atom. Both the GVB and Hartree-Fock descriptions for this state have the configuration $(2s)^1(2p)^1$. To get a $^2\pi$ state, we use the $2p_y$ orbital and get the following description.

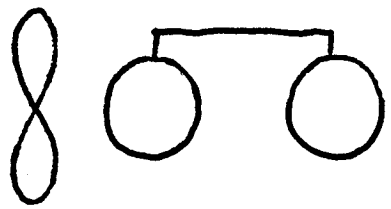

$[s,H],p_y$

Since bond formation in this state involves previously unpaired orbitals, we expect no hump in the potential curve. Another consequence is that the excitation energy for the $A^2\pi \leftarrow X^2\Sigma^+$ transition should be slightly lower than the corresponding excitation energy for the $^3p \leftarrow {}^1s$ transition in the Be atom. The experimental values of 2.5[10,30] and 2.7[31] eV support this argument. The approximate calculations carried out with the GVB method also show this result. Since the calculations allow only one spin coupling, the identity of the paired orbitals for the $^2\Sigma^+$ state must change as a function of **R**. The application of the variational principle minimizes the effects of the restriction, however.

For fluorides we expect an ionic single bond to be formed. To achieve this, we point the singly occupied fluorine orbital toward the Be atom. The $^2\Sigma^+$ state of BeF is pictured

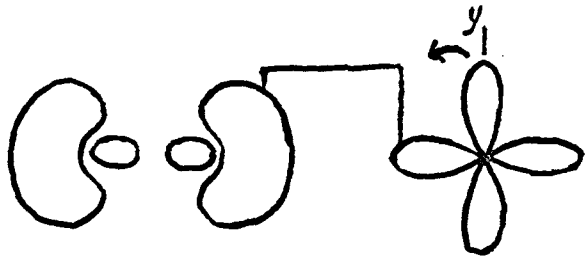

$[spz, p_zF], sp\bar{z}$

The arrow from the doubly occupied F orbital p_y indicates that it and the p_x orbital (not shown in the figure for clarity) delocalize into the empty p_y and p_x orbitals on the Be atom. As expected, the sigma bond is shown by calculations to be quite ionic. The fluorine-centered orbital is nearly unchanged from the atom, while the Be-centered orbital has transferred a large part of its amplitude to the F atom. In the $^2\pi$ state the presence of a π orbital on the Be atom should hamper delocalization of the F π orbitals. Because of this the $^2\pi$ state of BeF is 4.1 eV above the $^2\Sigma^+$ ground state.[10] The delocalization of the F π orbitals is a weak form of π-bonding. We would expect that the Be orbital would be an antibonding orbital and the F π orbitals bonding orbitals. Since the π-bonding is weaker in the excited $^2\pi$ state, the R_e value should be longer in the ground state as shown in Table II. Similarly, the force constant for the excited state is smaller than for the $^2\Sigma^+$ state, as expected.

The experimental and theoretical information necessary for these comparisons is given in Table II. The calculated values for dipole moments are clearly not useful for absolute values of dipole moments. The way in which they are useful is to show the differences between states of the same molecule. For example, the dipole moments of the $^2\Sigma^+$ states of BeH and BeF are quite small. But the $^2\pi$ states both have sizable moments in the direction B^+X^-. One electron has been transferred from the $sp\bar{z}$ orbital centered 1.14 bohr behind the Be atom to the Be p_y orbital centered 0.16 bohr toward the F atom. Thus a large amount of experimental and calculated information is understood in terms of the GVB picture. To use this picture, we did not need to carry out calculations. The overall description of BeH and BeF could be predicted from knowledge of the atomic wavefunctions. The purpose of the calculations was to provide additional information and to test the ideas predicted by the atomic wavefunctions.

VI. BH and BF

In forming BH, we have a choice between pairing the hydrogen orbital with a p orbital or an spz orbital. To get the $^1\Sigma^+$ ground state of BH, we point the boron p orbital at the H orbital as shown below.

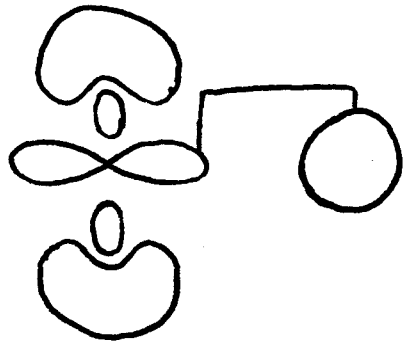

The arrows indicate that the sp orbitals bend back away from the bond.

In the $^3\pi$ state the spz orbital points toward the H atom. Bonding requires a change in the spin coupling. As for the $^2\Sigma^+$ state of BeH, we expect a hump in the potential curve. However, we may couple the σ and π singly occupied orbitals to give either a $^3\pi$ or $^1\pi$ state. For the $^3\pi$ state this coupling produces an energy contribution of $-K_{\sigma\pi}$. This energy-lowering interaction will reduce the size of the potential maximum. In the $^1\pi$ state a $+K_{\sigma\pi}$ term increases the size of the hump in the energy curve.

The schematic diagram for the $^3\pi$ and $^1\pi$ states is shown below.

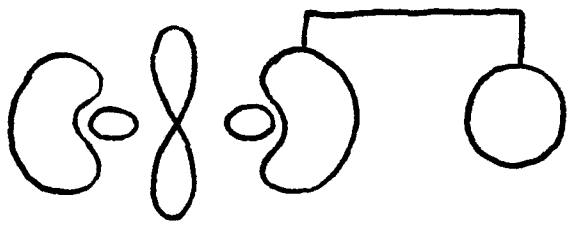

$[spz,H]$, $sp\bar{z}$, p_y

Since the transition from the $^1\Sigma^+$ state to the $^3\pi$ or $^1\pi$ state involves replacing a sigma orbital centered behind the B atom by a π orbital centered near the boron atom, we expect the dipole moment for the excited state to be changed toward B^+H^-. This trend is supported by the approximate calculations reported here and those of Harrison.[22,32] The values given in Table II indicate that the absolute values we calculate are not reliable but that the trends between states probably are valid.

For fluorides the picture is similar to that for BeF. The π orbitals on the fluorine atom delocalize in a bonding manner. In the $^3\pi$ and $^1\pi$ excited states the singly occupied B π orbital is antibonding. Thus in BF the π excited states are located much higher in energy than in BH. In addition the values of the spectroscopic constants R_e and ω_e change much more in BF for the $^{3,1}\pi \leftarrow {}^1\Sigma^+$ transition than they do for BH. The dipole moment of BF behaves similarly to that of BH. This information is tabulated in Table II.

VII. CH AND CF

Since the CH and CF molecules are the most interesting of the series considered here, we present contour plots[33] of the orbitals for several states. The diagram for the $^2\pi$ state of CH would be

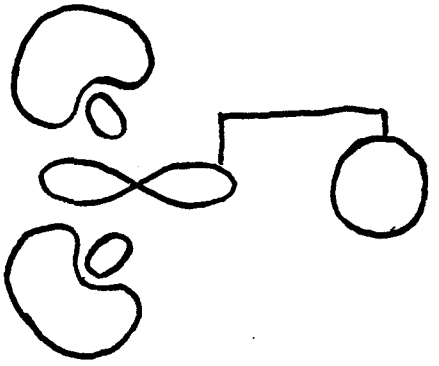

$[spy, sp\bar{y}], [p_z, H], p_x$

where we omit the singly occupied p_x orbital for clarity. In Figure 1 we show a spy orbital for CH. As we pointed out for the boron atom, in the ground state these orbitals bend back away from the bond. The bond orbitals from C and H are shown in Figures 2 and 3. We note that the hydrogen orbital is little altered by bond formation while the carbon p orbital is somewhat hybridized toward the hydrogen atom. The π_x orbital is not shown since it remains essentially an atomic-like p orbital centered on the carbon atom.

In the $^4\Sigma^-$ state the spz orbital of the carbon atom points toward H as shown below.

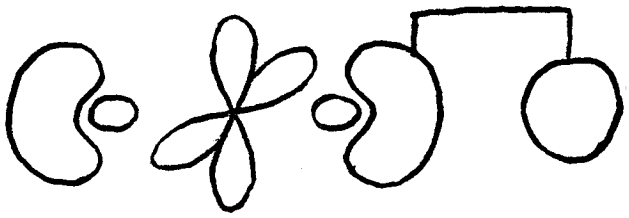

$[spz,H],sp\bar{z},p_x,p_y$

The carbon bond orbital for this state shown in Figure 4 is somewhat different from the $^2\pi$ orbital. The $sp\bar{z}$ orbital is shown in Figure 5.

The three orthogonal open shell orbitals $sp\bar{z}$, p_x, and p_y could be used to form other states of the symmetries $^2\Sigma^-$, $^2\Delta$, and $^2\Sigma^+$. We may pull these states apart to see what their dissociation limits are. In the $^2\Sigma^-$ state the p_x and p_y orbitals are triplet coupled. Thus the ^3p state of carbon is the dissociation limit of this state. Similarly the $^2\Delta(XY)$ and $^2\Delta(X^2 - Y^2)$ states dissociate to the $^1D(XY)$ and $^1D(X^2 - Y^2)$ states of carbon. Finally, the $^1\Sigma^+$ state, which is like $p_x^2 - p_y^2$, dissociates to the $^1D\ (2Z^2 - X^2 - Y^2)$ state of carbon.[34]

All these states except the ground state involve spin recoupling. Recent accurate calculations by Bobrowicz[35] indicate that in the $^4\Sigma^-$ state the exchange integrals $K_{\sigma\pi}$ which enter the energy expression with a minus sign effectively cancel the spin recoupling terms. The result is a potential curve with no hump. On the other hand, for the $^2\Sigma^-$ state these exchange integrals raise the energy and increase the size of the potential energy hump.

Herzberg and Johns[36] recently concluded that a small maximum (greater than 500 cm^{-1}) exists for the $^2\Sigma^-$ state of CH. The orbitals obtained for this state show an interesting difference from those for other states. Earlier we commented that bond formation involving spin recoupling forced the orbitals to change form as a function of R.

In Figure 6 we show the carbon spz bonding orbital. It actually has a more atomic-like form than the corresponding orbital in the $^4\Sigma^-$ state. The orbital with which it is paired, shown in Figure 7, is primarily a hydrogen s orbital with some $sp\bar{z}$ character. At larger values of R, we expect the amount of $sp\bar{z}$ character to increase until at $R = \infty$ only $sp\bar{z}$ character is left. The unpaired orbital in Figure 8 is an antisymmetric combination of $sp\bar{z}$ and H character. This keeps the orbital orthogonal to the bond orbitals. Even in calculations where all spin couplings are included and no orthogonality restriction is imposed, no orbital has a sizable overlap with more than two other orbitals.[29] The unpaired orbital is changing from a H orbital at $R = \infty$ to a $sp\bar{z}$ orbital at small R. In the $^2\Delta$ and $^2\Sigma^+$ states the $K_{\sigma\pi}$ interactions are again favorable so that the humps for these states will be small or nonexistent.

For CF we first show in Figure 9 the F bond orbital for the $^2\pi$ state. It is little changed from the atomic orbital. In contrast, the C bond orbital in Figure 10 has transferred a large amount of amplitude to the fluorine

atom. This charge transfer is counteracted by the F π orbitals in Figure 11 which are centered about 0.2 bohr from the F atom toward the C atom. The spy and spȳ carbon orbitals are forced to acquire antibonding p_y character on the F atom in order to remain orthogonal to the delocalized F π orbitals. The spy orbital is shown in Figure 12.

In the $^4\Sigma^-$ state the C bond orbital resembles those of the $^2\pi$ state since it involves a large amount of fluorine p_z character. The $^2\Sigma^-$ state[37] produces a set of sigma orbitals like those in CH. The bond orbitals and the carbon spz̄ orbital are shown in Figures 13, 14, and 15.

From Table II we see that the ground and excited states of CH all have similar values of ω_e and R_e. For CF no experimental information is available for ω_e and R_e. In addition the excitation energies for CF are much larger than for CH. This follows the trend established for Be and B. Also of interest is the grouping of dipole moments for the $^2\pi$ and $^2\Sigma^-$ states and for the $^4\Sigma^-$, $^2\Delta$, and $^2\Sigma^+$ states.

VIII. CONCLUSIONS

We have used the GVB method to discuss BeH, BeF, BH, BF, CH, and CF. A simple explanation for trends in dipole moments, equilibrium bond distances, and force constants has been offered. The straightforward way in which dissociation processes may be considered by the GVB

approach is very useful in relating the characteristics of the molecule to those of the atoms it contains. The results of the present study suggest that the GVB method will be a useful tool for investigating the chemistry of more complicated molecules such as Be_2, B_2, C_2, BN, and BeO. Calculations on these and other systems are currently in progress.

REFERENCES

1. For example, theoretical calculations in Reference 2. Suggested that the $^3B_1$ ground state of methylene, CH_2, should have a bent equilibrium geometry with an angle of 135°. Recent experimental evidence reported in Reference 3 confirms this prediction.
2. C. F. Bender and H. F. Schaefer, J. Am. Chem. Soc. 92, 4984 (1970).
3. E. Wasserman, V. J. Kuck, R. S. Hutton, and W. A. Yager, J. Am. Chem. Soc. 92, 7491 (1970).
4. L. Pauling, The Nature of the Chemical Bond (Cornell University Press, Ithaca, New York, 1960).
5. A. O. Walsh, J. Chem. Soc., 2260 (1953).
6. R. B. Woodward and R. Hoffman, The Conservation of Orbital Symmetry (Academic Press, New York, 1969).
7. J. E. Lennard-Jones, Trans. Faraday Soc. 25, 668 (1929).
8. R. S. Mulliken, Phys. Rev. 43, 279 (1933).
9. For an example of the use of MO theory in interpreting experimental information, see Reference 10.
10. G. Herzberg, Spectra of Diatomic Molecules (Van Nostrand Reinhold Company, New York, 1950).
11. R. S. Mulliken, Phys. Rev. 32, 186 (1928).
12. J. C. Slater, Quantum Theory of Molecules and Solids, Vol. I (McGraw-Hill Book Company, Inc., New York, 1963).

13. See earlier chapters of this thesis.

14. A. C. Hurley, J. E. Lennard-Jones, J. A. Pople, Proc. Roy. Soc. (London), A220, 446 (1953).

15. A small configuration interaction calculation can be used to remedy this restriction.

16. For a system with more than two electrons, several valence bond structures are often possible. We use the usual choice of the simple valence bond method. The suggestion above in Reference 15 may be used to include the other structures.

17. (a) W. J. Hehre, R. F. Stewart, and J. A. Pople, J. Chem. Phys. 51, 2667 (1969); (b) J. A. Pople, J. Amer. Chem. Soc. 92, 4786 (1970).

18. (a) "Program Set for Non-empirical Molecular Calculations, POLYATOM," Program QCPE 47.1 of the Quantum Chemistry Program Exchange (QPCE), Indiana University, Bloomington, Indiana; (b) H. Basch, M. B. Robin, and N. A. Kuebler, J. Chem. Phys. 47, 1201 (1967).

19. (a) W. J. Hunt, T. H. Dunning, and W. A. Goddard III, Chem. Phys. Lett. 3, 606 (1969); (b) W. A. Goddard III, T. H. Dunning, and W. J. Hunt, Chem. Phys. Lett. 4, (1969); (c) W. J. Hunt, W. A. Goddard III, and T. H. Dunning, Chem. Phys. Lett. 6, 147 (1970).

20. T. L. Porter, D. E. Mann, and N. Aquista, J. Mol. Spectry. 16, 228 (1965).

21. J. C. Slater, Quantum Theory of Atomic Structure, Vol. I (McGraw-Hill Book Company, Inc., New York, 1960).

22. R. J. Blint and W. A. Goddard III, J. Chem. Phys., submitted for publication; ibid., to be published; R. J. Blint, W. A. Goddard III, R. C. Ladner, and W. E. Palke, Chem. Phys. Lett. 5, 302 (1970).

23. In the calculations, spatial symmetry requirements are not enforced on the many-electron wavefunction unless necessary to produce a meaningful description.

24. H. Silverstone and O. Sinanoglu, J. Chem. Phys. 44, 1899 (1966).

25. H. F. Schaefer, Ph.D. thesis, Stanford University, April, 1969.

26. A.C.H. Chan and E. R. Davidson, J. Chem. Phys. 49, 727 (1968).

27. G. Das and A. C. Wahl, J. Chem. Phys. 44, 87 (1966).

28. T. H. Dunning, private communication.

29. (a) W. A. Goddard III and R. C. Ladner, Int. J. Quant. Chem. 35, 63 (1969); (b) W. A. Goddard III, J. Amer. Chem. Soc. 92, 7520 (1970).

30. This experimental value is the T_e number quoted in Reference 10. The excitation energy is calculated in the present work, but the discrepancy does not affect any conclusion we reach.

31. C. E. Moore, Atomic Energy Levels (Washington, 1949).

32. J. F. Harrison, Ph.D. thesis, Princeton University, 1967.

33. In the plots, positive amplitude contours have solid lines, while negative amplitude contours have dashed lines.

34. Some consideration of the symmetry of the wavefunction is necessary in this case to separate the $^1\Delta$ and $^1\Sigma^+$ states of CH.

35. F. Bobrowicz, unpublished calculations.

36. G. Herzberg and J.W.C. Johns, Astrophysical Journal 158, 399 (1969).

37. Calculations by W. P. White, T. H. Dunning, R. M. Pitzer, and W. Mathews (to be published) indicate that the potential well for this state will be shallow with a long downhill slope beyond the potential maximum.

38. W. M. Huo, J. Chem. Phys. 43, 624 (1965).

39. W. M. Huo, J. Chem. Phys. 49, 1482 (1968).

40. D. H. Phelps and F. W. Dalby, Phys. Rev. Letters 16, 3 (1966).

41. P.A.G. O'Hare and A. C. Wahl, J. Chem. Phys. 53, 666 (1971).

TABLE I. Equilibrium Geometries

Molecule	R_e[a]
BeH	2.938[b]
BeF	2.57[b]
BH	2.33[b]
BF	2.38[b]
CH	2.1[b]
CF	2.402[c]

[a]Atomic units are used.

[b]Reference 10.

[c]Reference 20.

TABLE II. Properties of Diatomic Hydrides and Fluorides

State		Excitation Energy (eV) this work	Excitation Energy (eV) other calc.	Excitation Energy (eV) exp.[a]	ω_e[a] (cm^{-1})	R_e[a] (A)	Dipole Moment[b] this work	Dipole Moment[b] other calc.	Dipole Moment[b] exp.
BeH	$^2\Sigma^+$	0.0	0.0	0.0	2058	1.343	-0.003	-0.181[c]	
	$^2\pi$	3.1		2.5	2087	1.333	-2.18		
BeF	$^2\Sigma^+$	0.0		0.0	1173	1.361	0.106		
	$^2\pi$	5.4		4.1	1266	1.394	-2.60		
BH	$^1\Sigma^+$	0.0	0.0	0.0	2366	1.232	1.02	1.61[d]	
	$^3\pi$	0.35	1.06[d]			1.201	-0.378	0.15[d]	
	$^1\pi$	3.7	2.77[d]	2.9	2344	1.226	0.47	0.704[d]	
BF	$^1\Sigma^+$	0.0		0.0	1400	1.262	1.24	1.04[e]	
	$^3\pi$	2.9					-0.402		
	$^1\pi$	6.8		6.3	1271	1.304	0.0369		
CH	$^2\pi$	0.0	0.0	0.0	2862	1.120	1.04	1.57[f]	1.46[g]
	$^4\Sigma^-$	0.12					0.023	--	
	$^2\Delta$	4.1	2.7[f]	2.9	2921	1.103	0.423	0.91[f]	
	$^2\Sigma^-$		3.3[f]	3.2	2542	1.186	1.27	1.54[f]	
	$^2\Sigma^+$		4.1[f]	4.0	2824	1.113	0.423	0.94[f]	
CF	$^2\pi$	0.0	0.0	0.0			0.463	0.48[h]	0.65[i]
	$^4\Sigma^-$	2.9	2.74[j]				-0.887		
	$^2\Delta$	6.6	6.64[j]				-0.446		
	$^2\Sigma^-$	8.5	8.96[j]				1.02		
	$^2\Sigma^+$	8.4	8.06[j]				-0.356		

a. Ref. 10

b. Negative sign means A^+H^- or A^+F^-. All values are quoted in Debyes.

c. Ref. 26.

d. Ref. 22.

e. Ref. 38.

f. Ref. 39.

g. Ref. 40.

h. Ref. 41.

i. Ref. 20.

j. Ref. 37.

FIGURE CAPTIONS

Fig. 1 An spy carbon orbital in CH for the $^2\pi$ state. The carbon atom is located at the left cross and the hydrogen atom at the right cross.

Fig. 2 A carbon p_z bond orbital for CH($^2\pi$).

Fig. 3 A hydrogen 1s orbital for CH($^2\pi$).

Fig. 4 A carbon spz bond orbital in CH($^4\Sigma^-$).

Fig. 5 A carbon $sp\bar{z}$ non-bonding orbital in CH($^4\Sigma^-$).

Fig. 6 A carbon spz bond orbital in CH($^2\Sigma^-$).

Fig. 7 The hydrogen bonding orbital in CH($^2\Sigma^-$).

Fig. 8 The carbon $sp\bar{z}$ non-bonding orbital in CH($^2\Sigma^-$).

Fig. 9 The F bond orbital in CF($^2\pi$). The left cross marks the carbon atom and the right cross marks the fluorine atom.

Fig. 10 The C bond orbital in CF($^2\pi$).

Fig. 11 The F π orbital from the $^4\Sigma^-$ state of CF. (This orbital is basically a fluorine p orbital with a small amount of carbon p character for all states of CF.)

Fig. 12 The spy orbital of carbon in CF($^2\pi$).

Fig. 13 Fluorine bond orbital in CF($^2\Sigma^-$).

Fig. 14 Carbon bond orbital in CF($^2\Sigma^-$).

Fig. 15 Carbon $sp\bar{z}$ non-bonding orbital in CF($^2\Sigma^-$).

Fig. 16 Carbon π orbital for the $^4\Sigma^-$ state of CF. Note that the orbital has a large out-of-phase component on the fluorine atom.

CH DOUBLET PI - LONE PAIR ORBITAL

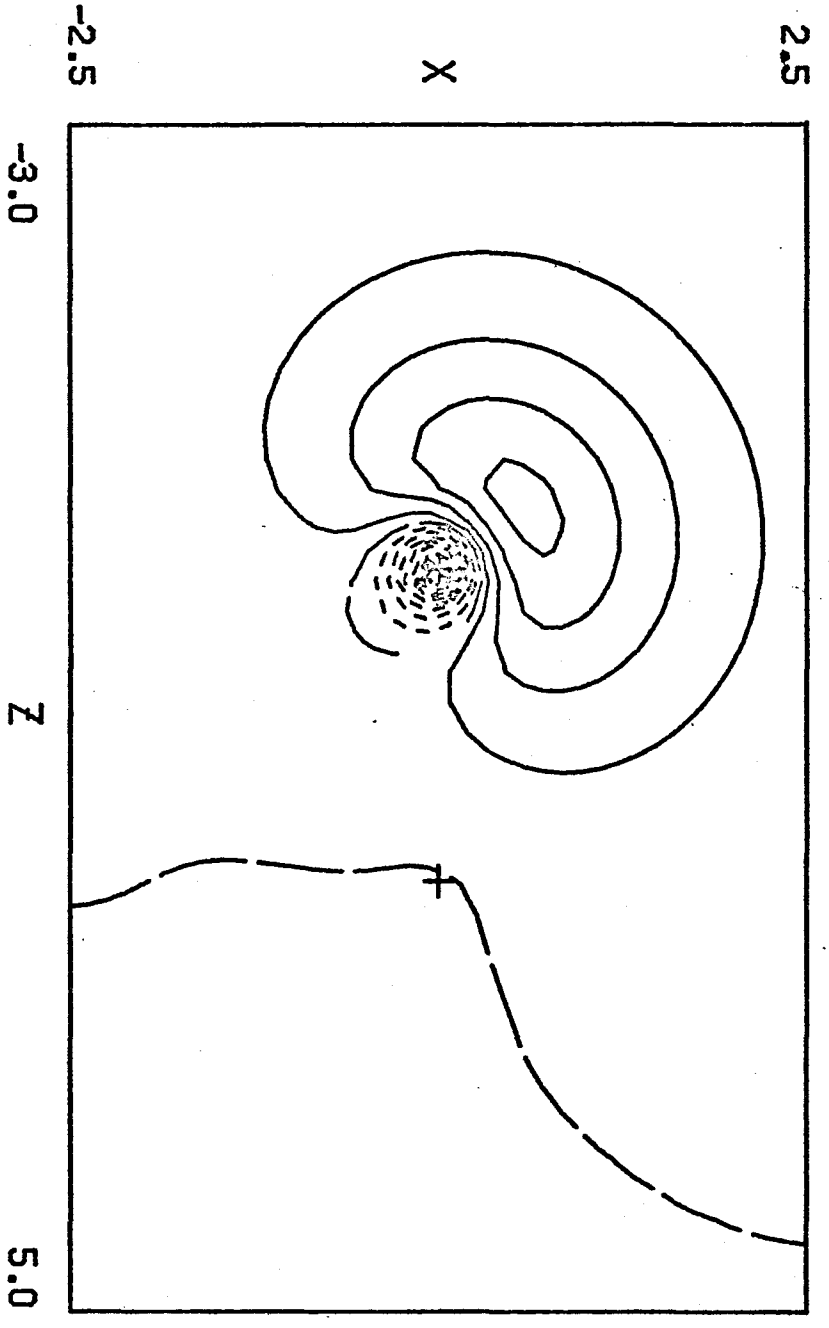

CH DOUBLET PI - C BOND ORBITAL

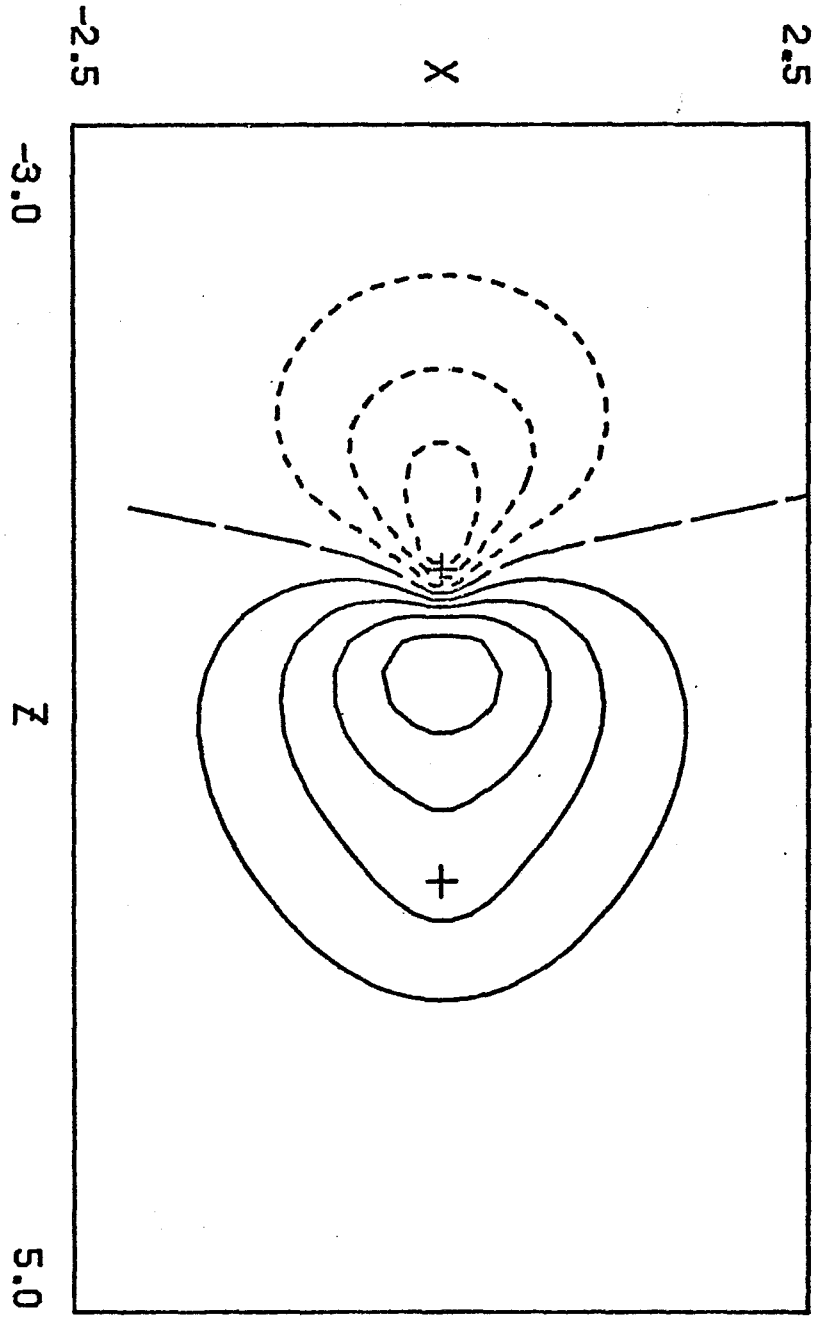

CH DØUBLET PI - H BØND ØRBITAL

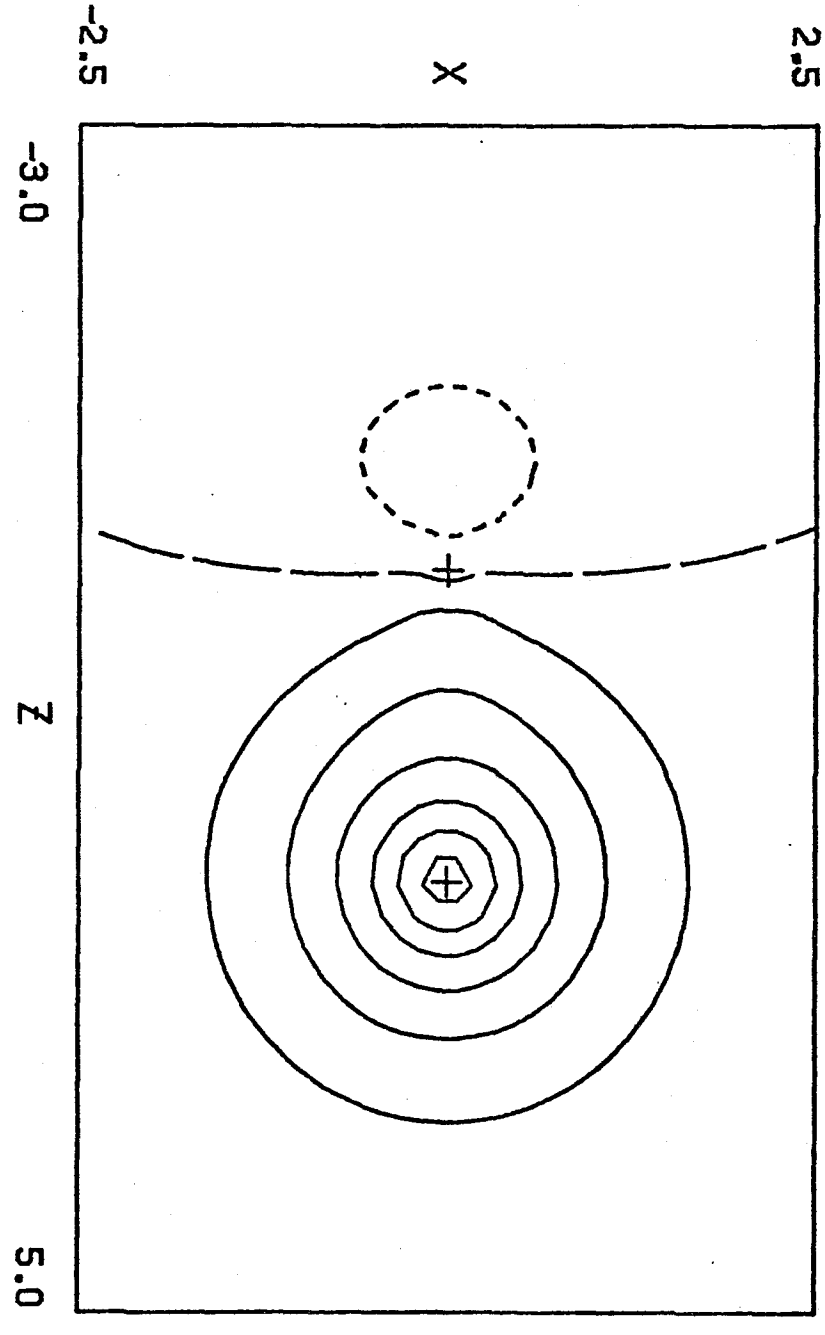

CH DOUBLET PI - H BOND ORBITAL

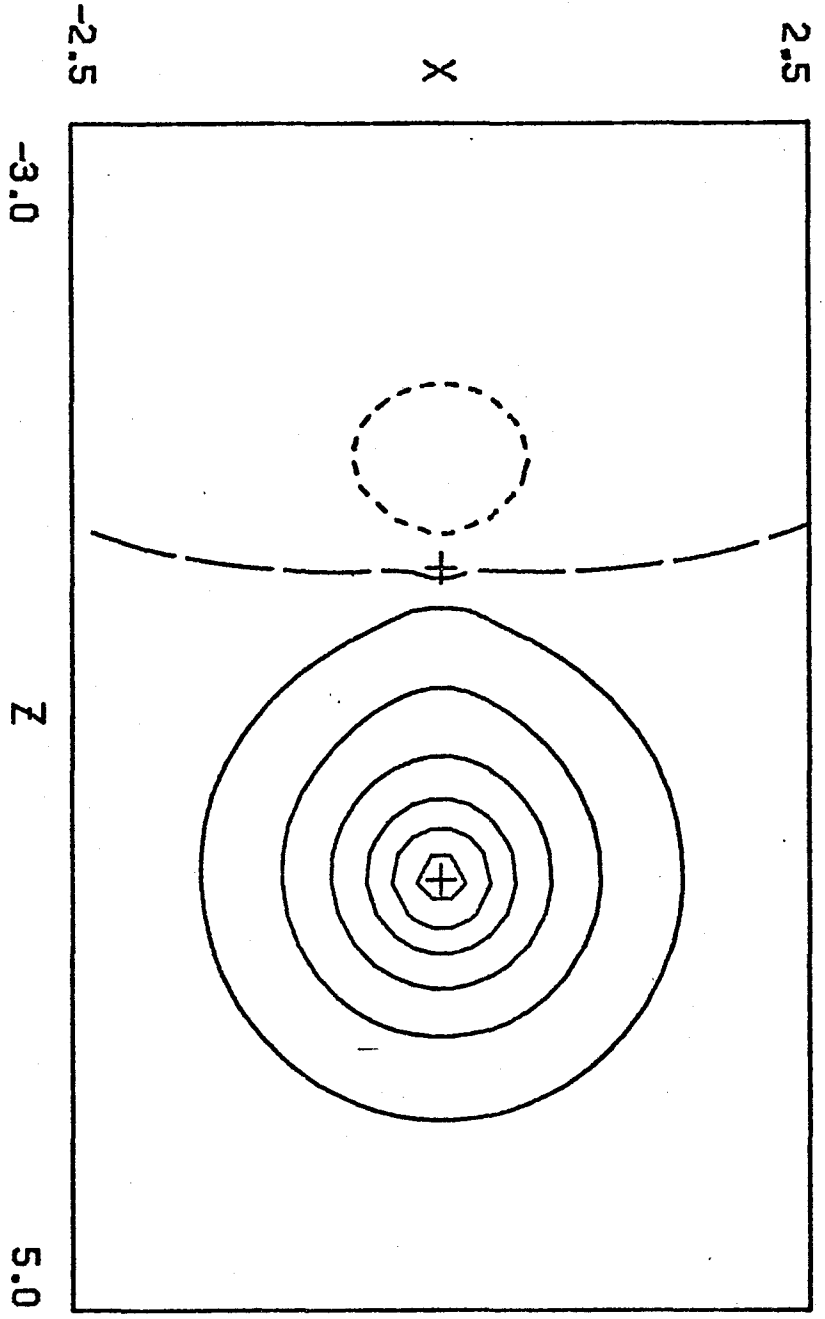

CH QUARTET SIGMA - C BOND ORBITAL

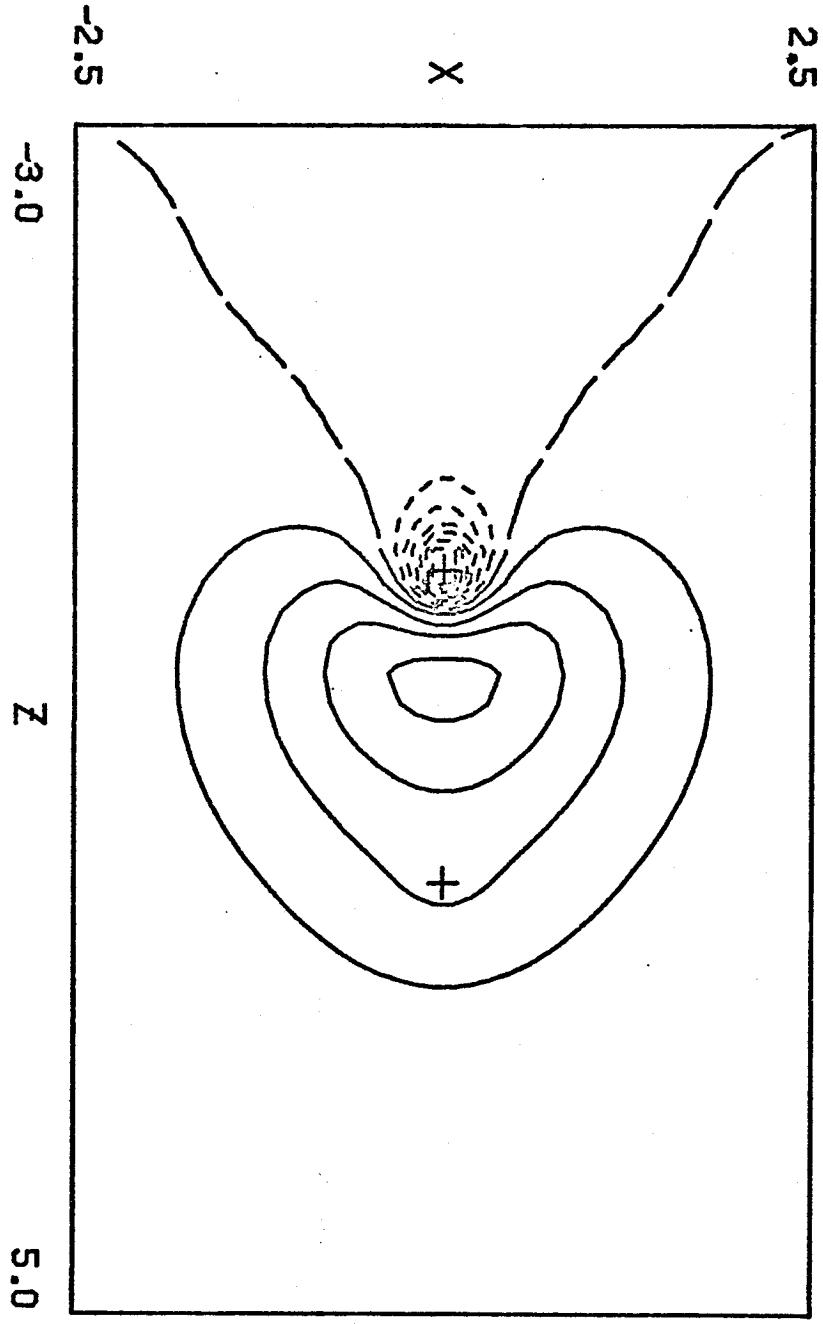

CH QUARTET SIGMA - LONE PAIR ORBITAL

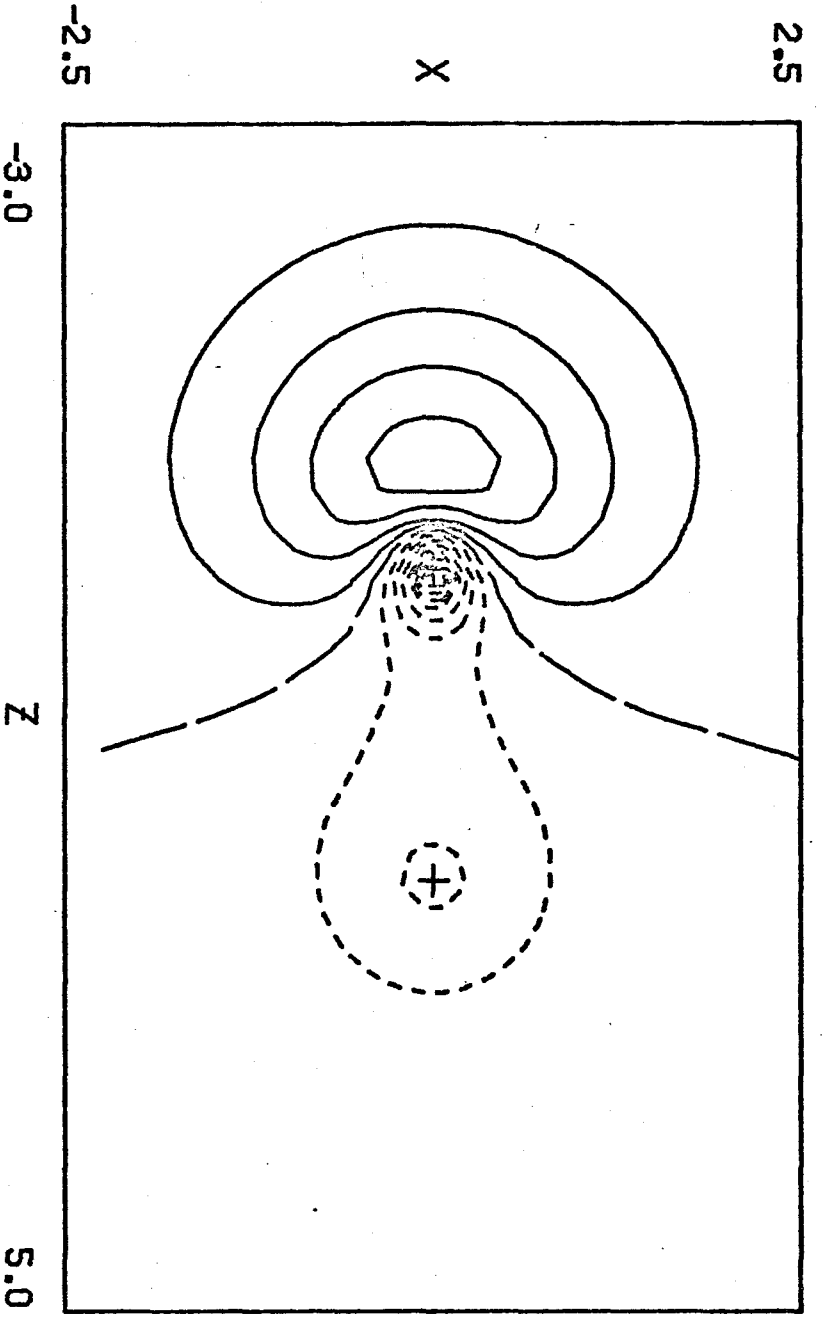

CH DOUBLET SIGMA(MINUS) -H BOND ORBITAL

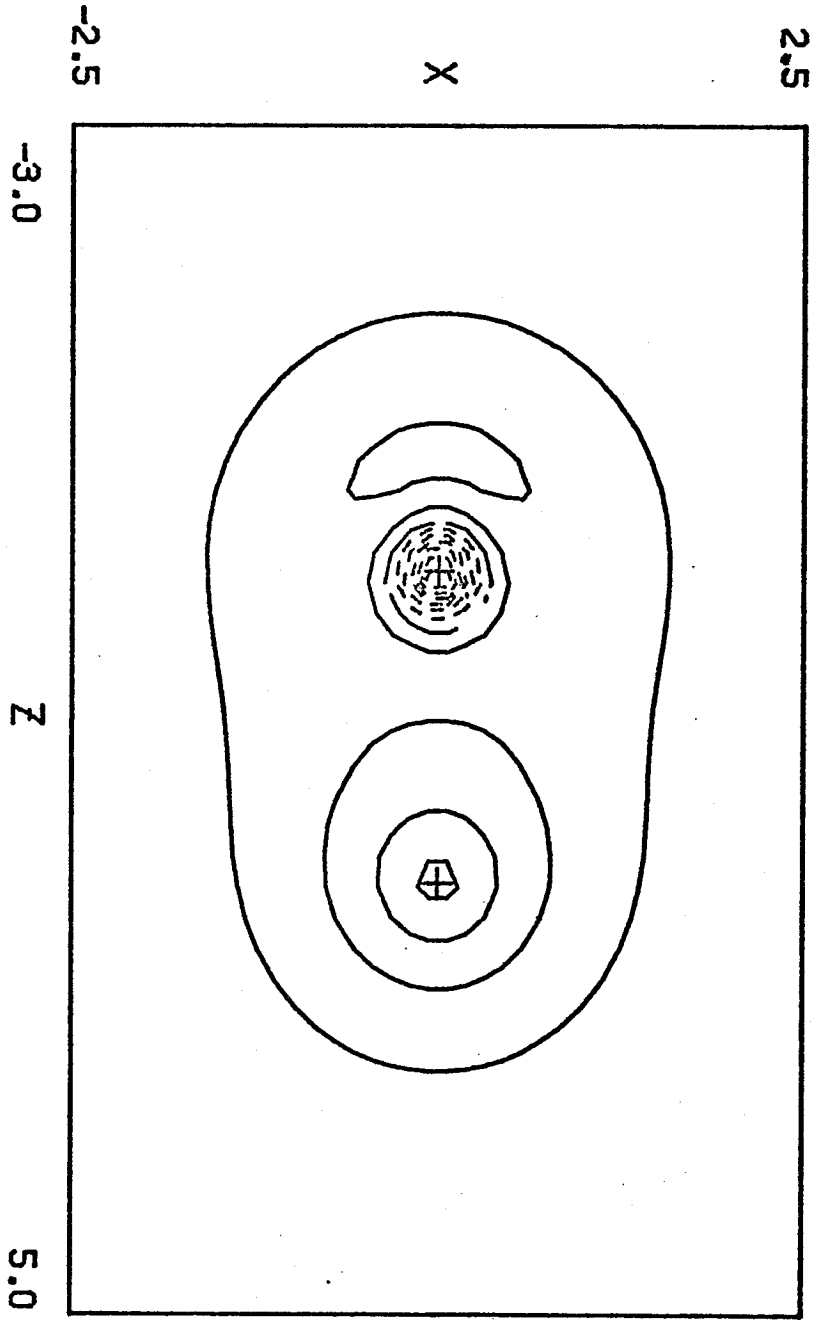

CH DØUBLET SIGMA(MINUS) -LØNE PAIR ØRBITAL

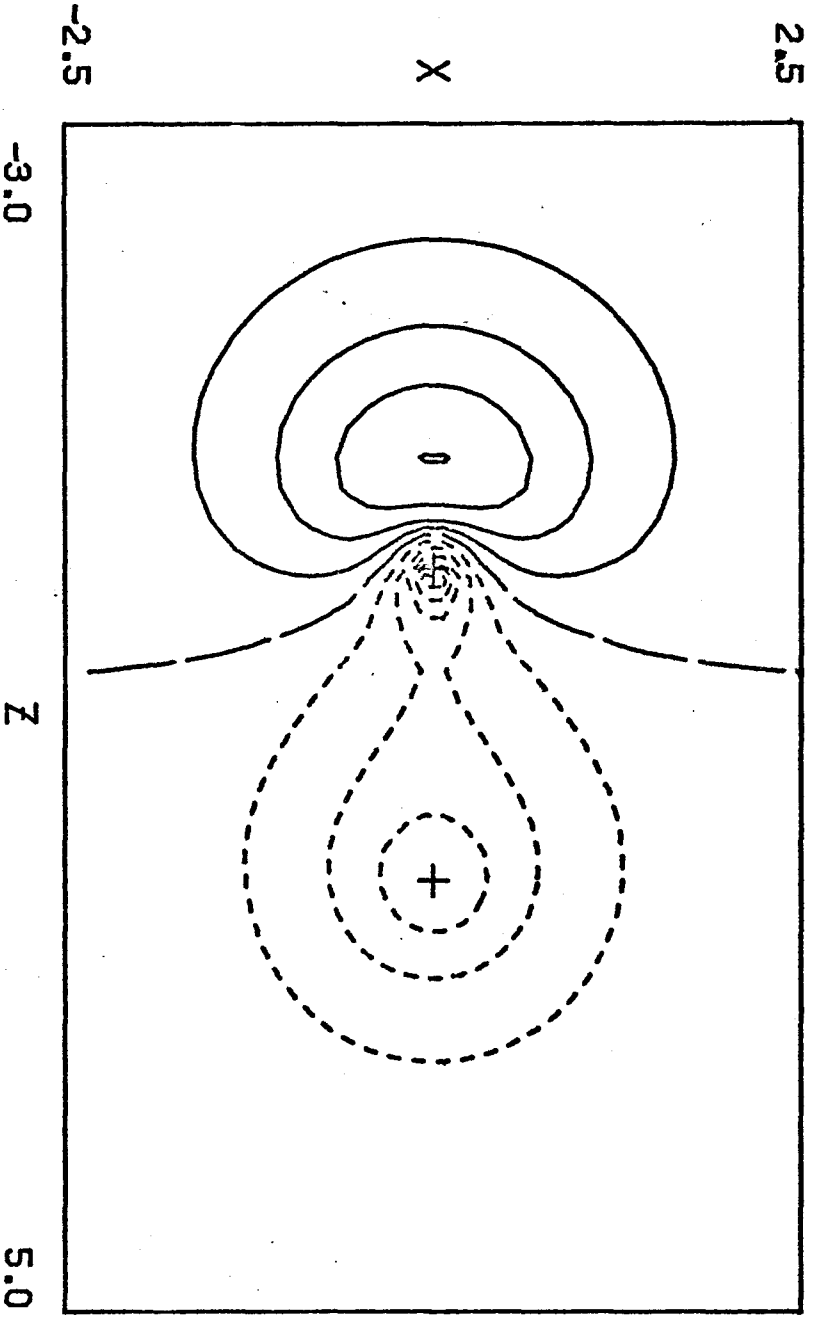

CH DOUBLET SIGMA(MINUS) -C BOND ORBITAL

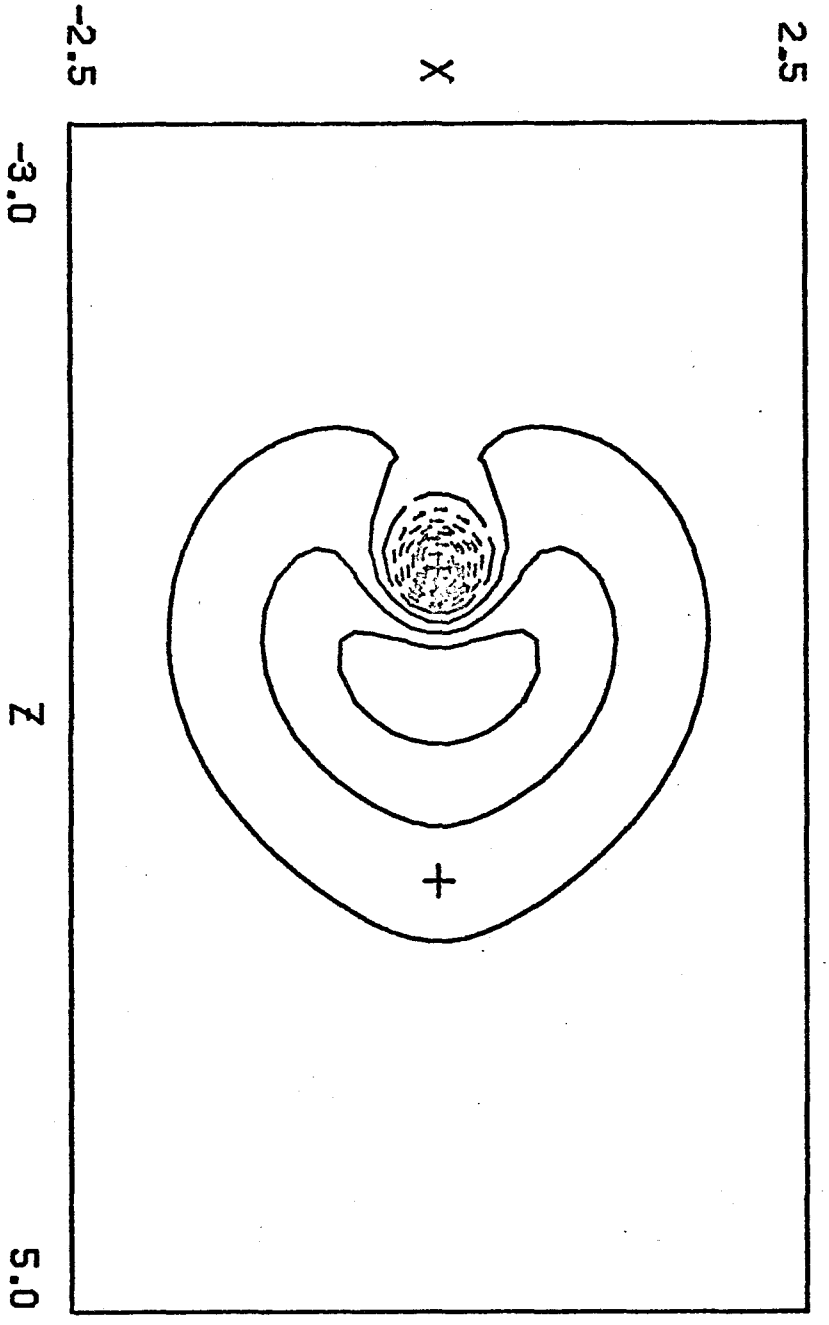

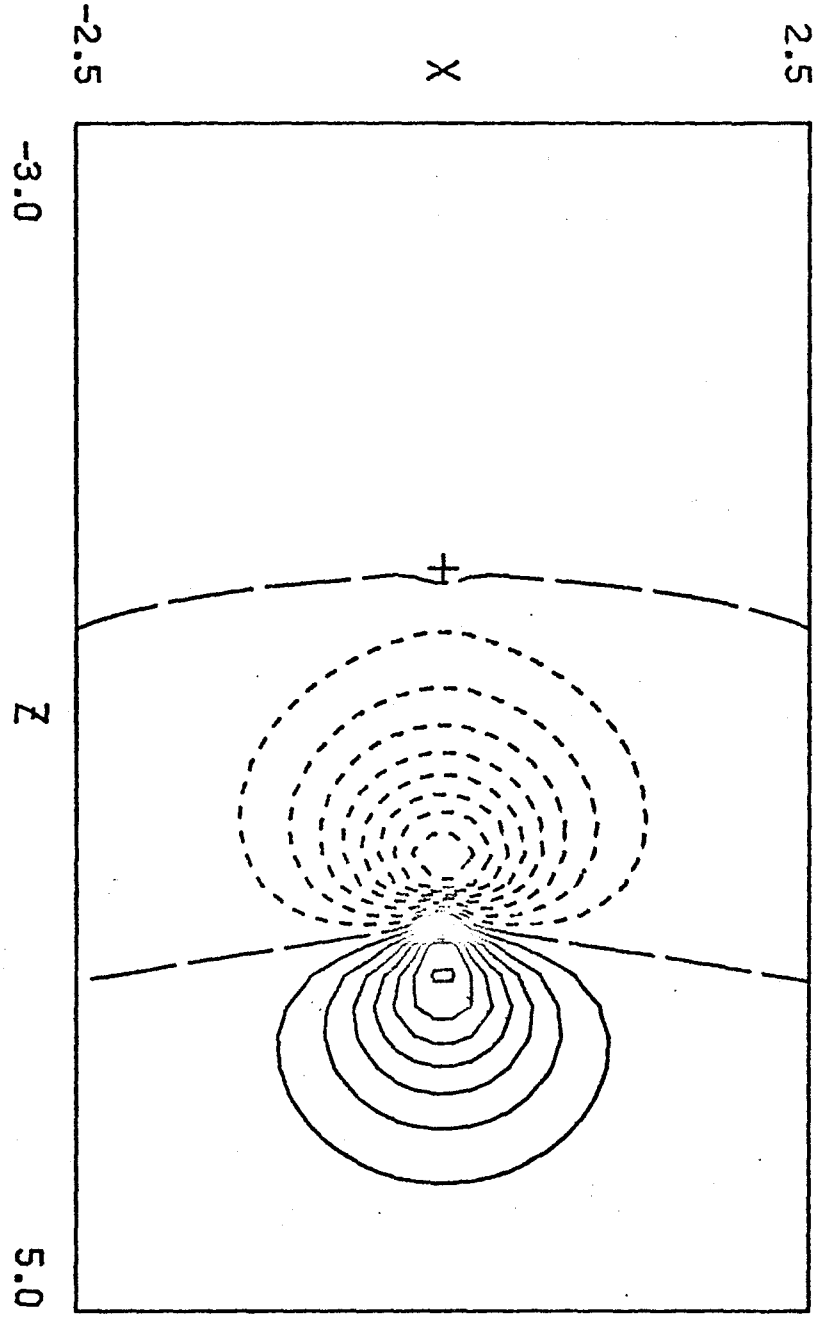

Figure 9

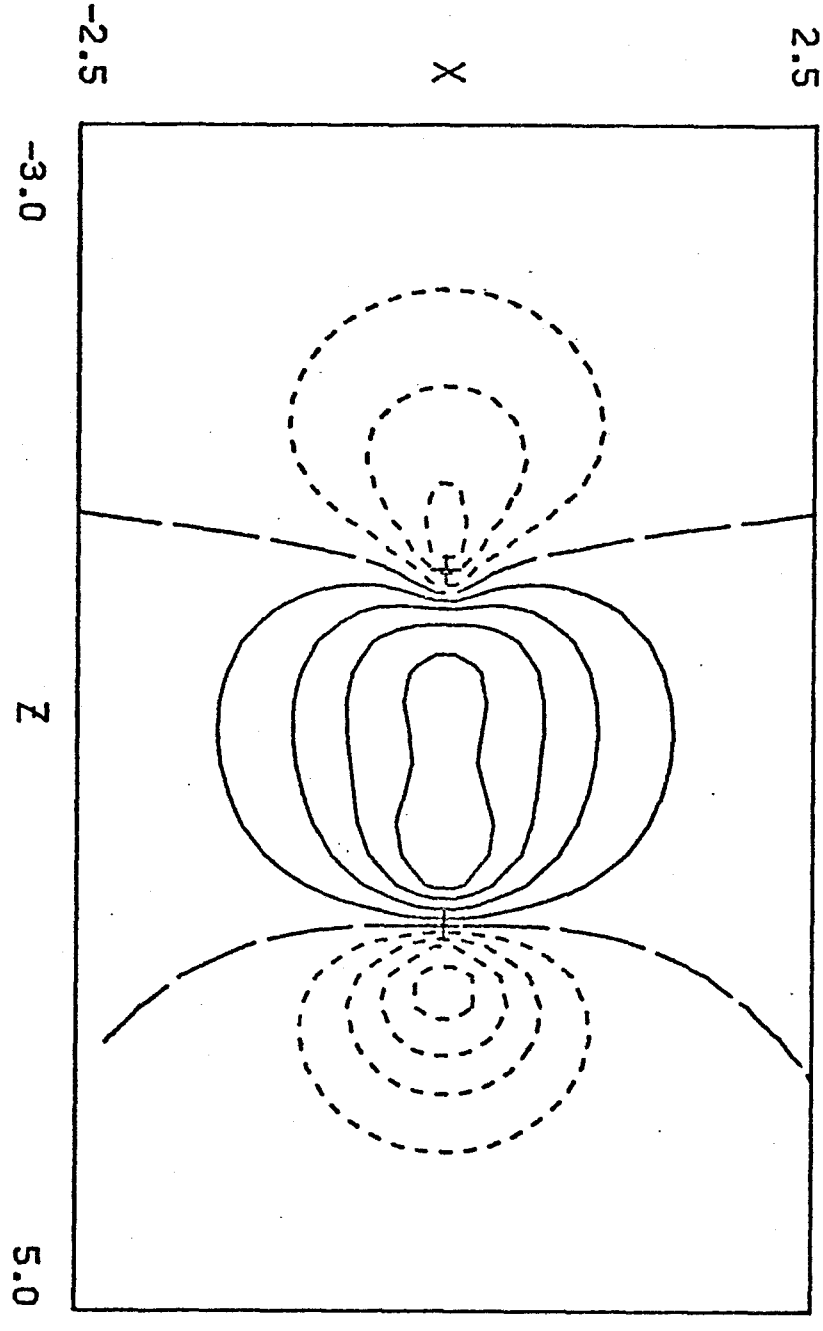

Figure 10

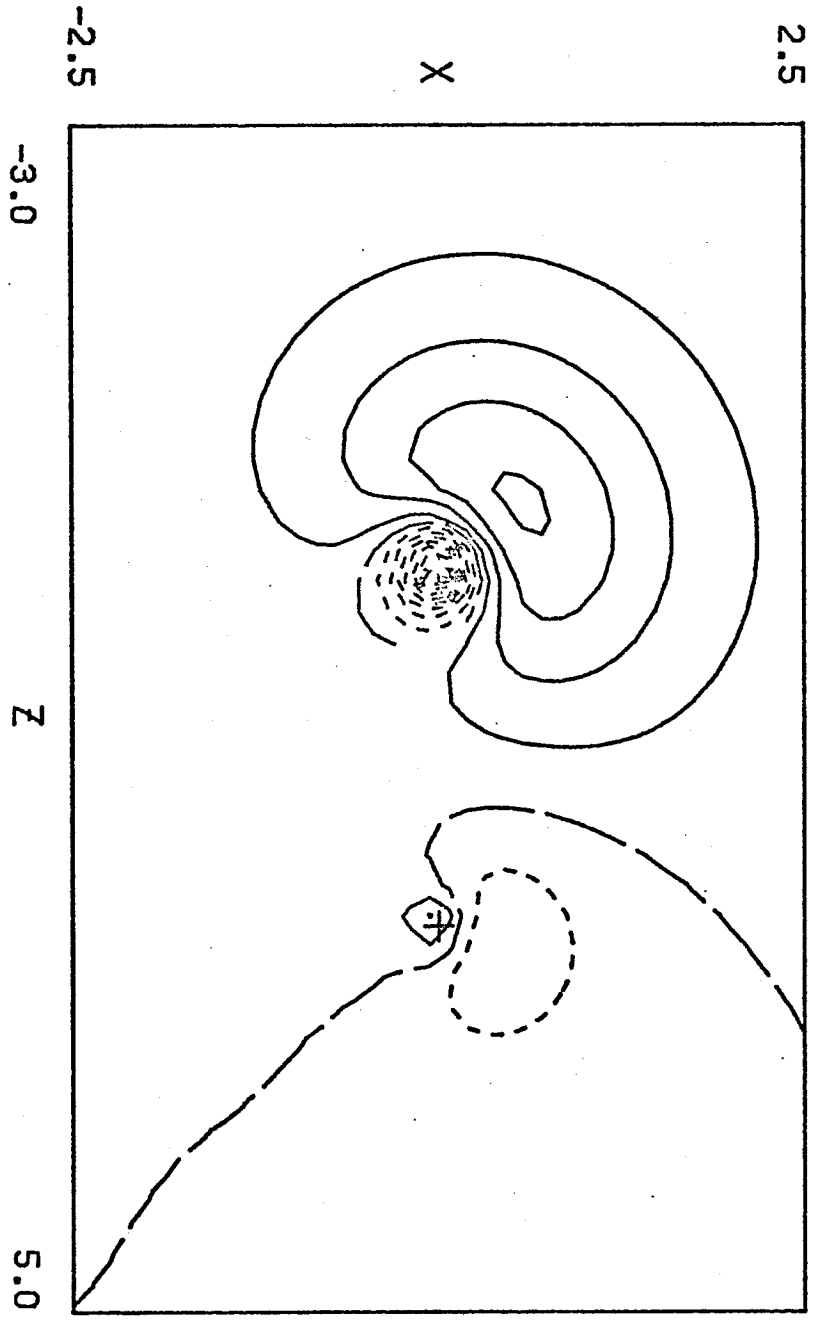

Figure 11

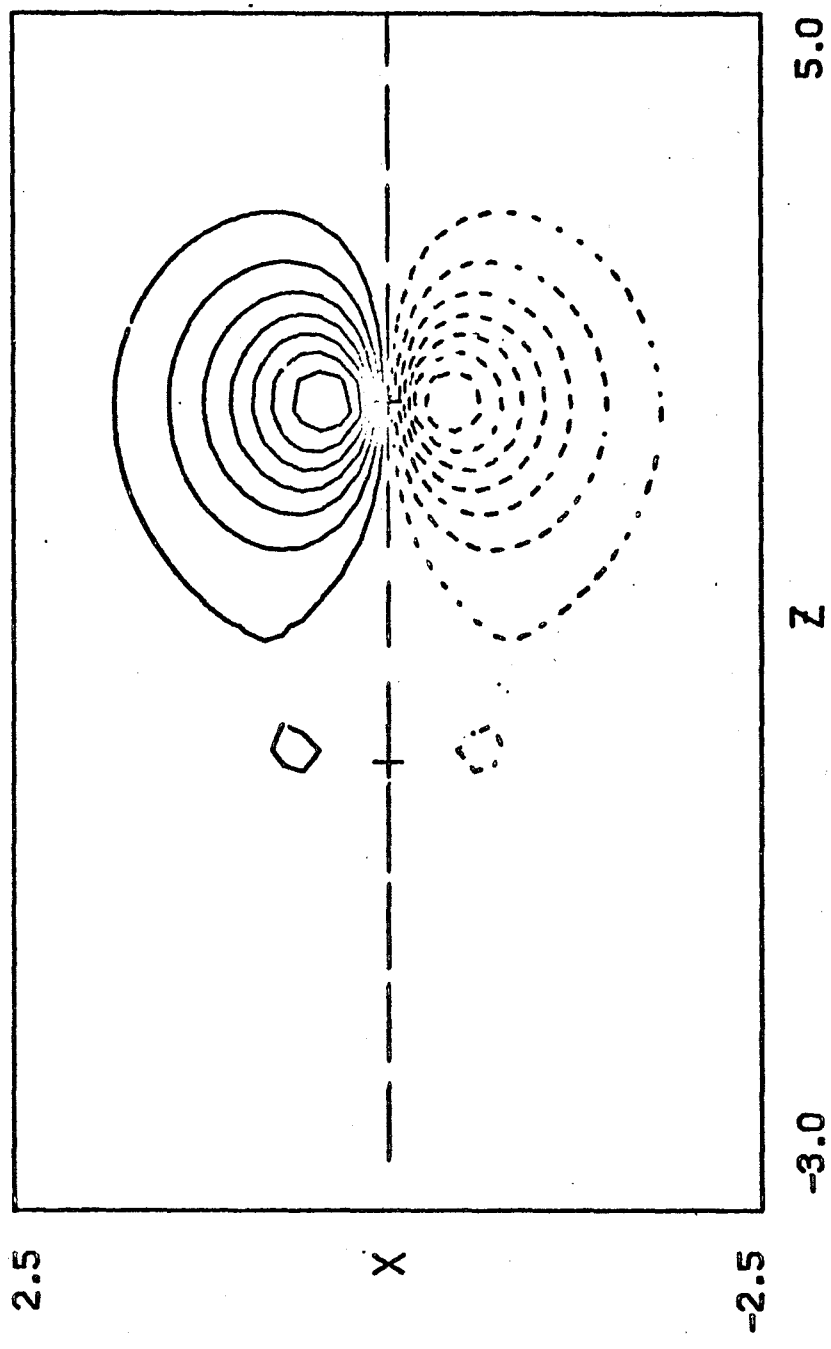

Figure 12

CF DOUBLET SIGMA(MINUS) - F BOND

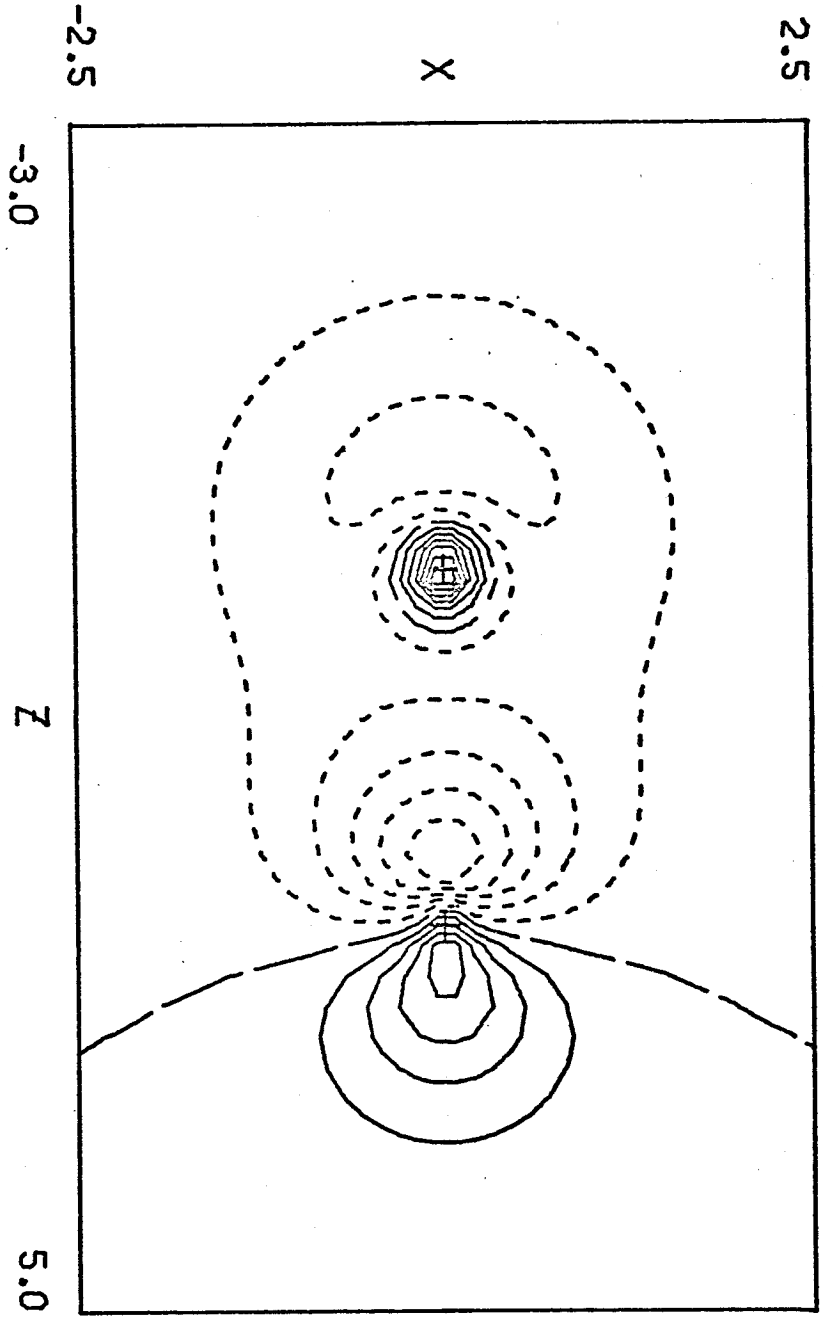

CF DOUBLET SIGMA(MINUS) - C BOND ORBITAL

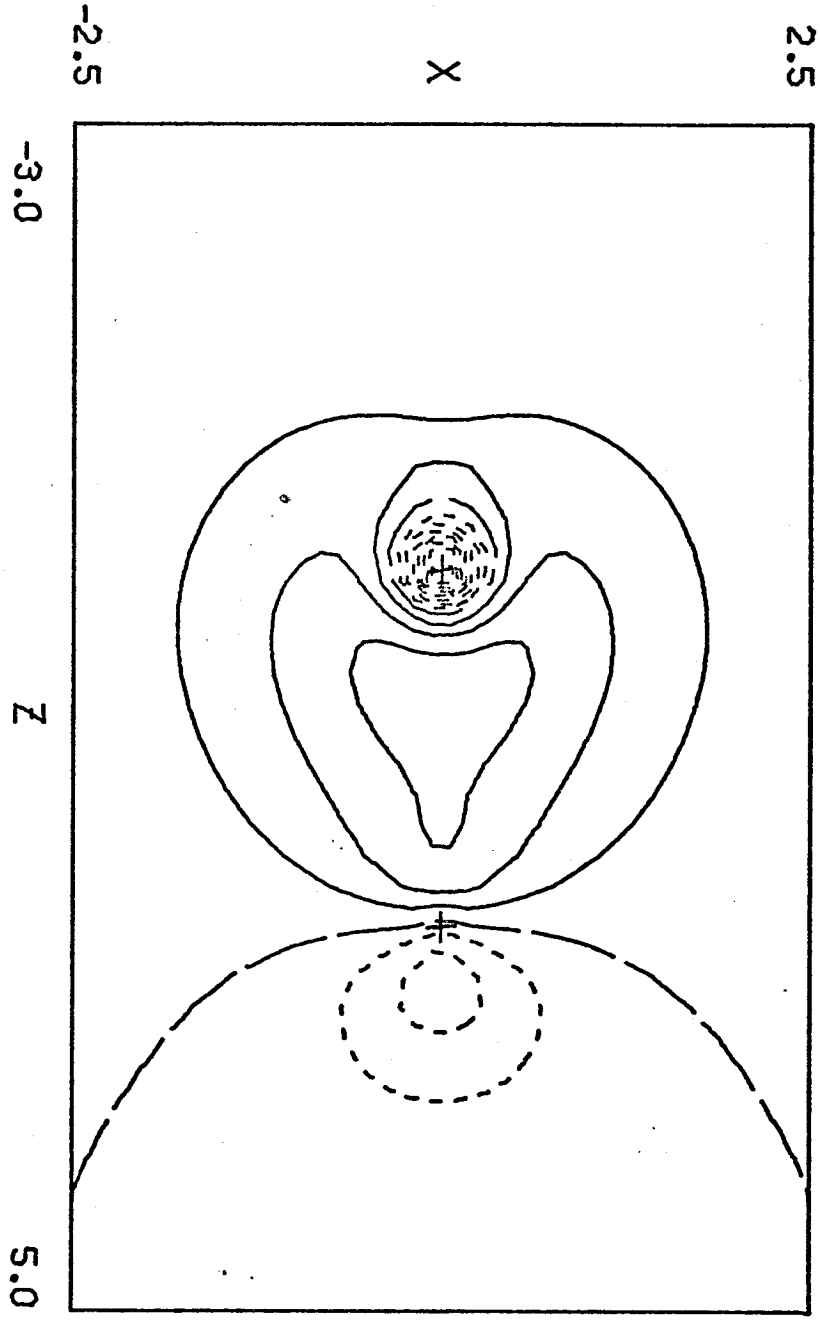

CF DOUBLET SIGMA(MINUS) - C LONE PAIR ORBIT

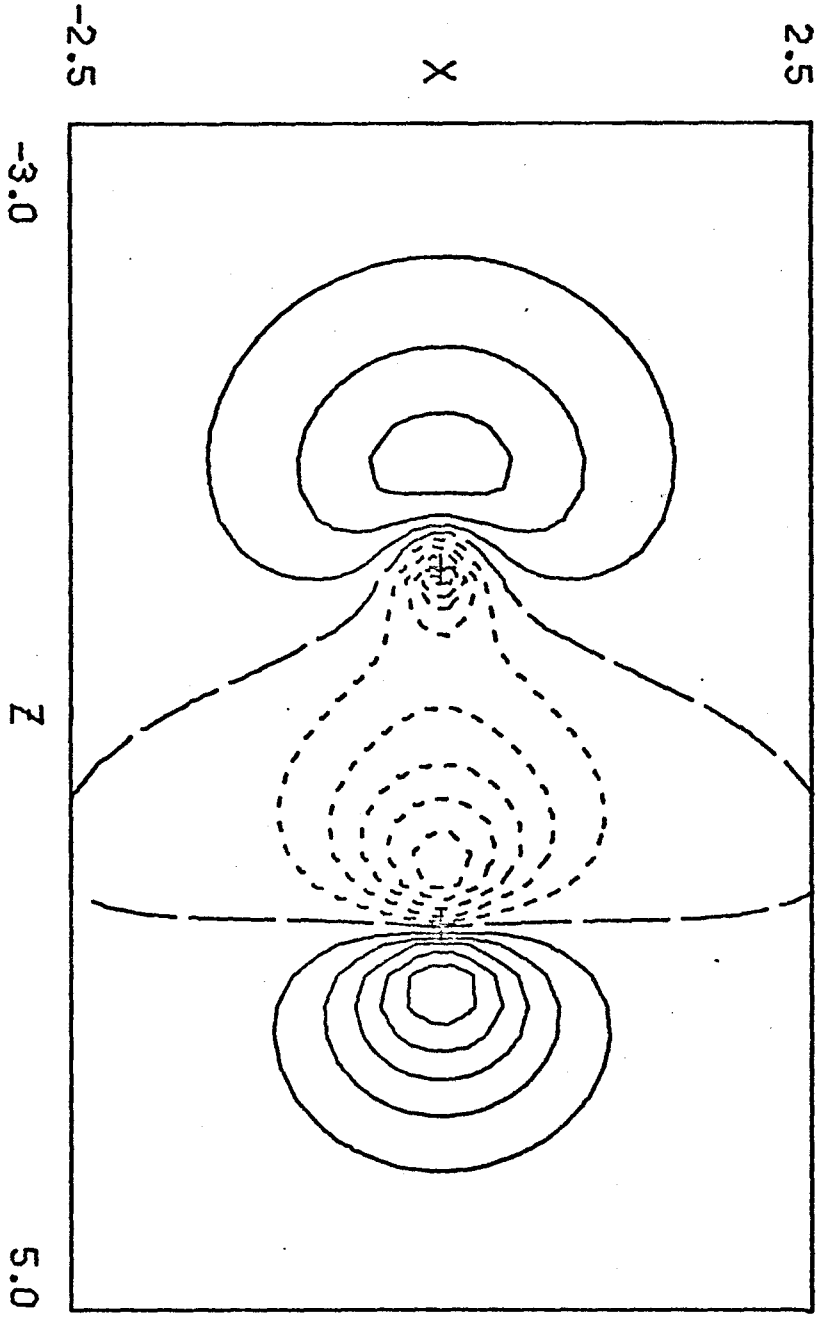

CF QUARTET SIGMA(MINUS) - C PI